CHALMERS

Installation effects of lime-cement columns

-with special focus on horizontal displacements and pore pressure changes

Master of Science Thesis in the Master's Programme Geo and Water Engineering

CHARLOTTE ANDERSSON
BRITTA KARLSTRÖM

Department of Civil and Environmental Engineering
Division of GeoEngineering
Geotechnical Engineering Research Group
CHALMERS UNIVERSITY OF TECHNOLOGY
Göteborg, Sweden 2010

Master's Thesis 2010:30

MASTER'S THESIS 2010:30

Installation effects of lime-cement columns

-with special focus on horizontal displacements and pore pressure changes

Master of Science Thesis in the Master's Programme Geo and Water Engineering

CHARLOTTE ANDERSSON

BRITTA KARLSTRÖM

Department of Civil and Environmental Engineering
Division of GeoEngineering
Geotechnical Engineering Research Group
CHALMERS UNIVERSITY OF TECHNOLOGY
Göteborg, Sweden 2010

Installation effects of lime-cement columns
-with special focus on horizontal displacements and pore pressure changes

Master of Science Thesis in the Master's Programme Geo and Water Engineering

CHARLOTTE ANDERSSON
BRITTA KARLSTRÖM

Examensarbete / Institutionen för bygg- och miljöteknik,
Chalmers tekniska högskola 2010:30

Department of Civil and Environmental Engineering
Division of GeoEngineering
Geotechnical Engineering Research Group
Chalmers University of Technology
SE-412 96 Göteborg
Sweden
Telephone: + 46 (0)31-772 1000

Cover:
Installation of lime-cement columns in Bohus. Photograph taken by Charlotte Andersson 25 May 2010.

Chalmers Reproservice
Göteborg, Sweden 2010

Installation effects of lime-cement columns
-with special focus on horizontal displacements and pore pressure changes

Master of Science Thesis in the Master's Programme Geo and Water Engineering

CHARLOTTE ANDERSSON
BRITTA KARLSTRÖM
Department of Civil and Environmental Engineering
Division of GeoEngineering
Geotechnical Engineering Research Group
Chalmers University of Technology

ABSTRACT

Year 2004 started the construction of a new double-track railway in the Göta älv valley between Göteborg and Trollhättan. Due to great clay layers in the area, lime-cement columns are used to reduce settlements and vibrations. This thesis aims to study installation effects regarding pore pressure changes and horizontal displacements caused by installation of lime-cement columns. Data from field and laboratory investigations have been evaluated and used to create a simplified soil model. To simulate the installations the FE-program Plaxis has been used and the calculated horizontal displacements and pore pressures have been compared to measured values. Methods by Rehnman and Sagaseta have also been used to calculate horizontal displacements and an analytical method for calculating the excess pore pressure have been used. A parameter analysis in Plaxis was conducted to see what impact different parameters have on the result. The results calculated in Plaxis captured the behaviour of the measured horizontal displacements well.

Key words: Horizontal displacements, pore pressure, lime-cement columns, Plaxis

Installationseffekter av kalkcementpelare
-med fokus på horisontell massundanträngning och portrycksändringar
Examensarbete inom Geo and Water Engineering
CHARLOTTE ANDERSSON
BRITTA KARLSTRÖM
Institutionen för bygg- och miljöteknik
Avdelningen för Geologi och geoteknik
Forskargrupp Geoteknik
Chalmers tekniska högskola

SAMMANFATTNING

Byggnationen av en ny dubbelspårig järnväg i Göta älvdalen mellan Göteborg och Trollhättan påbörjades 2004. På grund av mäktiga lerlager i området har kalkcementpelare använts för att minska sättningar och vibrationer. Detta examensarbete syftar till att studera effekter med avseende på portrycks ändringar och horisontell massundanträngning orsakad av kalkcementpelarinstallation. Data från fält- och laboratorieundersökningar har utvärderats och använts för att skapa en förenklad jordmodell. FE-programmet Plaxis har använts för att simulera installationen av kalkcementpelare. Beräknade värden för portryck och horisontell massundanträngning har jämförts med uppmätta värden. Metoder så som Rehnmans och Sagasetas har även använts för att beräkna horisontell massundanträngning och en analytisk metod har använts för att beräkna porövertrycket. En känslighetsanalys i Plaxis har gjorts för att se vilken påverkan olika parametrar har på resultatet. Resultaten som beräknats i Plaxis fångar beteendet hos den uppmätta horisontella massundanträngningen bra.

Nyckelord: Horisontell massundanträngning, portryck, kalkcementpelare, Plaxis.

Contents

Preface

In this thesis horizontal displacements and pore pressure changes due to installation of lime-cement columns are investigated. It aims to achieve compliance between results from the FE-program Plaxis and measured values of pore pressure changes and horizontal displacements.

The thesis has been carried out at the Division of GeoEngineering, Chalmers University of Technology during the spring of 2010. Supervisors have been Mats Olsson, Ph.D. student at the Division of GeoEngineering at Chalmers and Anders Kullingsjö, Skanska. Claes Alén, professor at the Division of GeoEngineering at Chalmers has been examiner.

First we would like to thank Mats Olsson for his help and guidance, but also for his patience and that he always has had time for us.

We would also like to thank Anders Kullingsjö for his help with calculations and computer programs.

Thanks to Anders Bergström at NCC for helping us find additional material and for his patience with all our questions.

Finally we want to thank Lars-Gunnar Holmström at Skanska for a nice and interesting visit at the construction site in Bohus.

Göteborg, June 2010

Charlotte Andersson Britta Karlström

Notations

Roman upper case letters

A_f	[-]	Skempton's pressure parameter
B_{r1}, B_{rt}	[-]	Coefficient for shearing force
D	[m]	Dimension of vane
L	[m]	Length of pile
$M_{\max}$	[Nm]	Maximum torque
OCR	[-]	Over consolidation ratio
P_j	[kPa]	Expanding pressure
R	[m]	Radial distance from centre of column
R_c	[m]	Radius of column
S_t	[-]	Sensitivity
T_Q	[kPa]	Shearing force
V	[m^3]	Volume
V_{piles}	[m^3]	Volume of driven piles
$V_{pre-coring}$	[m^3]	Volume of pre-coring
V_s	[m^3]	Volume of solid material

Roman lower case letters

b	[m]	Width of pile area
c	[Pa]	Cohesion
c'	[Pa]	Cohesion (effective stresses)
c_u	[kPa]	Undrained shear strength
d	[m]	Pile depth below ground surface
l	[m]	Length of pile area
m	[kg]	Mass
m_s	[kg]	Mass of solid material
m_w	[kg]	Mass of water
p_0	[kPa]	Initial isotropic stress

p'_0	[kPa]	Initial effective isotropic stress
$\Delta p'_c$	[kPa]	Incremental injection pressure
r	[m]	Radial distance
Δu	[kPa]	Excess pore pressure
w_n	[%]	Natural water ratio
w_L	[%]	Liquid limit

Greek letters

α	[-]	Henkel's pore pressure parameter
α_f	[-]	Henkel's pore pressure parameter at failure state
δ_r	[m]	Horizontal displacement
η	[-]	Heave factor
ϕ	[°]	Angle of internal friction
ϕ'	[°]	Angle of internal friction (effective stresses)
μ	[-]	Correction factor
ρ	[kg/m^3]	Density
ρ_s	[kg/m^3]	Density of solid material
σ'_c	[kPa]	Preconsolidation pressure
σ_f	[Pa]	Normal stress at failure
σ_n	[Pa]	Normal stress on shear plane
σ'_{V0}	[kPa]	In situ vertical stress
τ	[Pa]	Shear strength
τ_f	[Pa]	Shear strength at failure
τ_{fu}	[Pa]	Undrained shear strength
τ_k	[Pa]	Shear strength from fall cone test
τ_v	[Pa]	Shear strength from vane test

1 Introduction

Year 2004 started the project BanaVäg i Väst, which is a collaboration between Banverket and Vägverket[1]. The project aims to increase the transportation capacity between Göteborg and Trollhättan by expanding highway E45 into a four-lane road and the railway into a double-track between the two cities. The highway and the railway are located in the valley of Göta älv which stretches between Göteborg and Trollhättan.

It is well known that geotechnical difficulties can occur when constructing in the Göta älv valley due to the great clay layers and the close location to the river. So in the reconstruction of E45 and Norge/Vänerbanan, lime-cement columns are used in the construction of the road and the railway to stabilize the clay and to reduce vibrations.

In this thesis, effects of lime-cement column installation in section E32 are studied. Section E32 includes the construction of the railway between Bohus and Nödinge where NCC is the contractor.

1.1 Background

When installing lime-cement columns a very high air pressure together with rotating blades are used to distribute the lime-cement mixture in the ground. This causes a rise in pore pressure and displacement of the soil, but the magnitude of the effects is hard to predict. Since the existing railway, which is still in use, is located very close to the construction site it is important to control and minimize the horizontal displacements to avoid displacement of the railway. The installation effects could also result in a landslide, especially in areas close to Göta älv river.

1.2 Aim

The aim of this thesis is to study installation effects of lime-cement columns and try to simulate the installation process in the finite element program Plaxis. It also aims to achieve compliance between the results from Plaxis and the measurements regarding pore pressure changes and horizontal displacements available from section E32. Some analytical calculation methods for horizontal displacements and excess pore pressure are also used. The aim is also to present some recommendations about important parameters to consider when simulating installation effects of lime-cement columns.

[1] 1th of April 2010 was Trafikverket created, which is a merger between Banverket and Vägverket

1.3 Objective

The goal with this master thesis is to get a deeper knowledge about how different parameters affect the result regarding pore pressure changes and horizontal displacements when installing lime-cement columns.

1.4 Scope

Evaluation of the installation effects only consider pore pressure changes and horizontal displacements caused by lime-cement columns. Only one cross section from section E32 is studied in more detail. Göta älv river is located more than 40 m away from the investigated section and is not included in the simulations since it is considered to have no or little impact on the results.

1.5 Method

First a literature study was made to gather background information about relevant subjects for the aim and objective of this report.

Available data from field and laboratory investigations in E32 have been compiled and evaluated. The evaluated data has then been used to create a simplified soil model in the calculation program Plaxis, which is a program used to simulate displacements and stresses. The calculation model has been verified by comparing the results from Plaxis with the field measurements. Results from Plaxis have also been compared with results from Rehnmans piling theory, Sagasetas method and an analytical method for excess pore pressure.

2 Basic theory

This chapter will present background theories that are relevant for the objective of this report. The first section contains general information about lime-cement columns and then field investigations and laboratory tests are explained. Then follows a section with different empiric relations and the last section describe the calculation program that is used for the simulation.

2.1 Lime-cement columns

Lime-cement columns are used to stabilize soft soils. It is commonly used in road and railway embankments to reduce settlements and improve the stability. It also reduces vibrations that can arise from railways. Lime-cement columns can be made with two different methods; the dry-mixing method and the modified dry-mixing method. The dry mixing method is most frequently used in Sweden and is also the method used in Section E32, so only this method is described in this section. In this method no water is added, instead water in the soil is consumed for the process. Therefore this method only can be used in soils with relatively high water content, e.g. in clay and silt (Hedman & Kuokkanen 2003, p. 12).

2.1.1 Performance

When making a lime-cement column, a rotating mixing tool is driven down to desired depth, see *Figure 1*. As the tool is retracted, a mixture of lime and cement is pressed out from the bottom of the mixing tool into the borehole and then gets mixed with the soil (Carlsten 1989, p. 357). With given rotational speed and rise of the mixing tool it can be calculated that it takes about 3 minutes to construct a 10 m long column.

In Sweden, lime-cement columns usually are made to a depth of 20-25 m (Geotechnics 2009, p. 5 in Appendix A) and they can have a maximum inclination of 70˚ (SGF 1999, p. 5). Usually they are made with a diameter of 0.6-0.8 m; an increase in diameter can result in an insufficient distribution of the lime-cement mixture (Hedman & Kuokkanen 2003, p. 12).

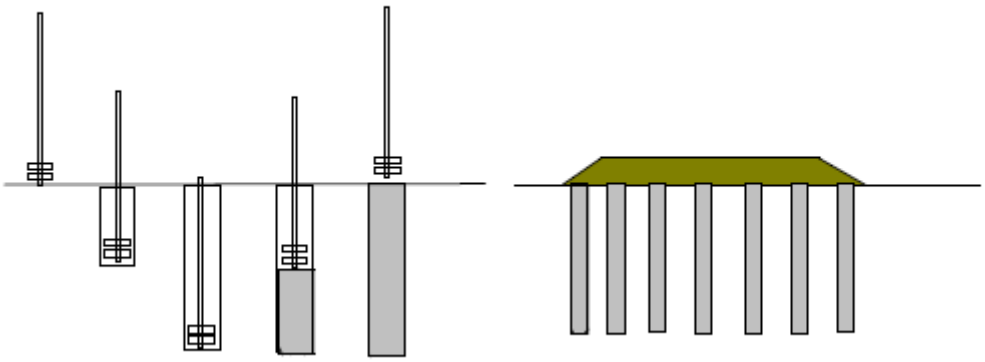

Figure 1 The procedure when installing a lime-cement column (SGF 2005).

An important factor to consider is the injection pressure. For a column with a length of 15 m the pressure is normally between 400 - 600 kPa (4 - 6 bar) (SGF 1999, p. 6). A too high pressure can cause failure in the soil, but at the same time a too low pressure can give insufficient mixing. The rotation speed of the mixing tool will also have an impact on the mixture distribution; a too high speed can cause cavities in the column while a too low speed can give inadequate mixing. The retraction speed depends on the soil type and the lime-cement mixture (SGF 1999, p. 10) and the proportion of lime and cement is chosen based on the laboratory test of the soil (Carlsten 1989, p. 360). Right after installation of a lime-cement column the compression strength starts to develop and reaches sufficient compression strength after approximately two weeks. The compression strength continues to slowly increase for several years (Honkanen & Olofsson 2001, p. 14).

2.1.2 Function

Lime-cement columns can be installed as singular columns or with overlap so that the columns interact and work as a plate (Carlsten 1989, p. 365). The columns will act together with the soil and create a stiffer and stronger material (Geotechnics 2009, p. 3 in Appendix A). A lime-cement column together with the soil can be divided into different zones. In the upper part, zone A, the columns are expected to exceed their compression strength, which leads to plastic failure of the column in this zone. Below, in zone B the columns interact with the soil as a composite material. The modulus for this zone is calculated based on the soil modulus and the columns elasticity modulus. The calculated modulus also takes into account the relation of column area compared to the unit area. The third zone C is where no stabilization of the soil has been performed, i.e. below the lime-cement columns (Geotechnics 2009, p. 12 in Appendix A). This is one way of looking at the interaction between the soil and the column.

The lime-cement columns will not be homogenous when the lime-cement slurry is mixed with the soil. Due to this, the shear strength differs in disparate directions. Since the columns are more permeable than the soil it can in some aspects be

compared to a vertical drain, which enables consolidation settlements to develop faster (Carlsten 1989, p. 355).

To make sure that the lime-cement column gets a suitable design for the intended area it is important to perform laboratory investigations of the soil properties. How the soil reacts with the lime-cement mixture is also tested in laboratory to get the right proportions of lime and cement. Test columns are installed in field and they are tested to observe possible installation problems as well as the performance of the columns (Carlsten 1989, p. 359). The tests should be conducted in such a way that problems can be discovered in time and measurements be taken (Carlsten 1989, p. 375).

2.1.3 Soil displacement

When columns are installed in the ground they will work as a ground improvement to increase the stability, but during installation the ground is affected in such a way that displacements might occur. The column itself represents a volume of material. When the column is installed in the soil there will be a volume expansion of the ground. This volume expansion will cause ground heave and lateral displacement of the soil.

2.1.3.1 Rehnman

A comparison is made between soil displacement due to installation of lime-cement columns in Plaxis and soil displacement due to installation of lime-cement columns based on Rehnmans piling theory. It is a simple analytical method used to calculate vertical and horizontal displacements due to pile driving.

Normally soil displacement occurs due to pile driving. A pile driven into the ground will result in a volume expansion, which will move the surrounding soil in both horizontal and vertical direction. The vertical displacement is called heave. The size of the heave and the direction of the horizontal displacements within and around the piling area are related to the surrounding environment. Since the soil will move in the direction where the resistance is smallest the surrounding environment will have influence on the results. This is considered in Rehnman by using different coefficients, see Section 5.2. To reduce the soil displacement pre-coring can be done. The principal is to remove the soil where the pile is going to be installed (Olsson & Holm 1993, p. 260). This technique will not be discussed further in this report.

2.1.3.2 The Sagaseta method

This is an analytical method used to calculate the horizontal and vertical displacement at the ground surface. Only horizontal displacements is considered in this thesis and it is calculated by Equation (1) (Edstam et al. 2010, p. 30).

$$\delta_r = \frac{R_c^{\,2}}{2} \cdot \frac{L}{r \cdot \sqrt{r^2 + L^2}} \qquad (1)$$

The method can also calculate the displacements at different depths, but then it becomes much more complicated and is therefore not performed in this thesis. The ground surface is assumed to be horizontal in this method. The installation of a single pile column is in this method considered as a point source where fluid is pumped out constantly in a spherical pattern around the column, see *Figure 2*.

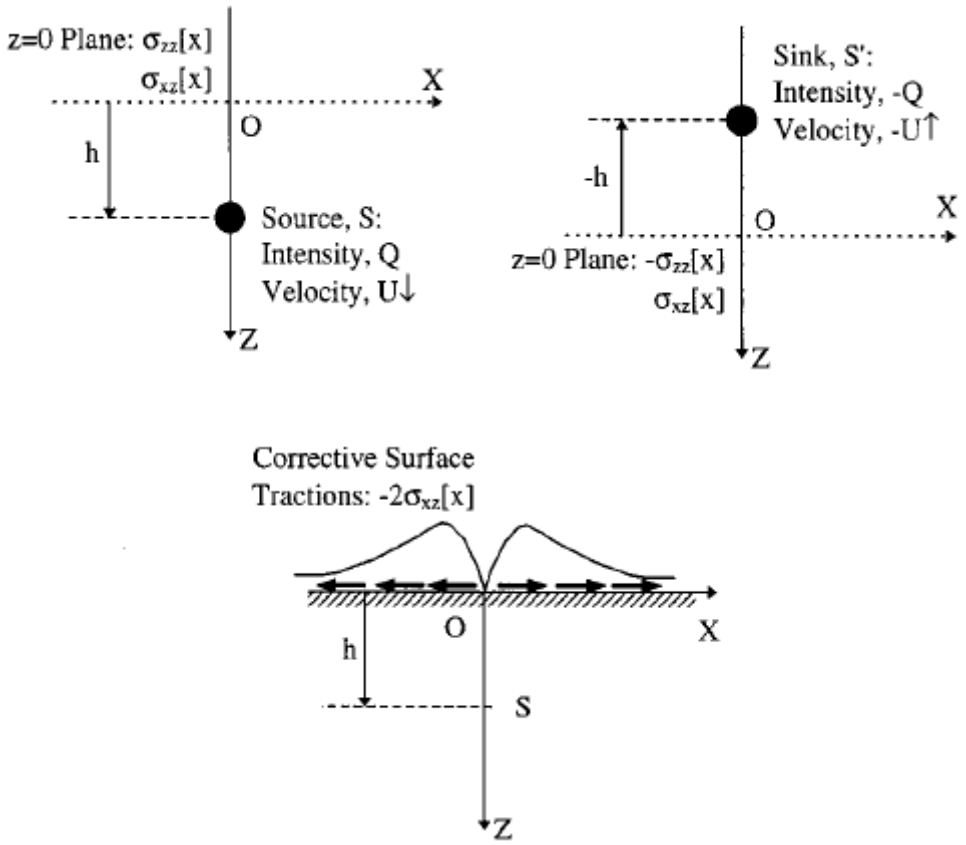

Figure 2 *Calculation model according to Sagaseta (Sagaseta et al., 1997, modified).*

The point source moves from the surface down to the lower edge of the column. A sink that moves from the surface up to a level of one pile length above the ground is used in order to simulate incompressibility. The boundary condition for the surface is that there are no normal or shear stresses, which is achieved by introducing corrected shear stresses. In order to calculate the total displacement caused by several columns the displacement from every column are added (Edstam et al. 2010, p. 29).

2.1.4 Excess pore pressure

Lime-cement columns are as mentioned before, installed through a mixture of lime-cement that are mixed with the soil through rotating blades. This will cause two different forces to act on the surrounding soil; one is the shearing force, T_Q from the rotation blades and the other is the expanding pressure, P_j caused by the injection of

the lime-cement mixture see *Figure 3*. R_p is the radius of the plastic zone and R_c is the radius of the column.

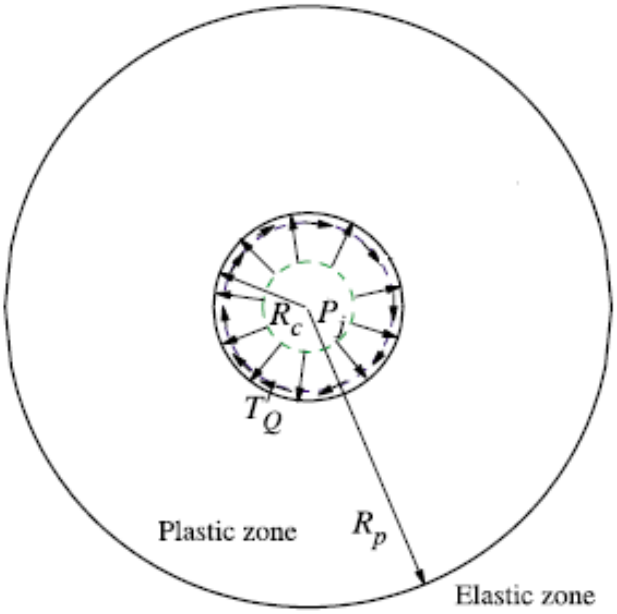

Figure 3 *Shearing force T_Q and expanding pressure P_j on the cavity wall. (Shen, et al., 2003, modified)*

The size of the injection pressure can range from 400 to 600 kPa depending on the construction method and the shearing force can have a maximum value equal to the undrained shear strength of the clay (Shen, et al. 2003, p. 295).

The assumptions for the shearing-expanding process is that it takes place in a homogeneous, isotropic, idealized elastic-perfectly plastic material defined by the Mohr-Coulomb criteria and under initially isotropic stress conditions. It is also assumed to occur under undrained conditions because the installation of the columns only takes a few minutes (Shen, et al. 2003, p. 295).

The rising pore pressure due to column installation is important to have in mind. As the pore pressure increases, the effective stresses will decrease which also reduces the shear strength. The shear strength will not be exceeded until the effective stresses have been reduced by approximately 50% (Johansson & Jendeby 1998, p.14).

2.2 Field investigations

Field investigations are performed to obtain information about soil and groundwater conditions for a specific area. In this section only investigation methods used in the project are presented. A device to measure soil displacements is also presented.

2.2.1 Cone penetration test

CPT, Cone Penetration Test, is an in situ test used to determine soil properties. A probe with a cone shaped tip, see *Figure 4,* is pressed into the soil with constant speed.

Figure 4 A type of CPT probe (School of Civil & Environmental Engineering).

The point resistance q_c can then be calculated as the total force acting on the cone, divided with the cone area. Information about how much resistance the probe was subjected to is sent to a computer. From the test you will also get the skin friction, friction ratio and the pore pressure (Bergdahl 1984, p.8).

In Sweden CPT is most commonly used to determine where different soil layers occur in the ground. The probe with its cone tip is a very fragile equipment and it cannot penetrate trough blocks without being destroyed, that is why this method is most successfully used in areas with low block ratio (SGF 1996, p.7:2). Since the CPT equipment is so sensitive it gives very detailed information about the soil layers. Except from deciding soil type, a CPT can also give some information about strength parameters and deformation properties (Sällfors 2001, p. 2.16).

2.2.2 Pressure probing

Pressure probing means that a probe with a cone shaped tip is pressed down into the soil with a constant speed. The probe is being pressed down with a force, which has to be increased with depth as the soil is being stiffer. The total resistance is calculated as the total force acting on the probe divided by the cone area. The total resistance is divided in two parts, skin resistance and point resistance. The skin resistance can be hard to determine but it is possible. The probe has a slide clutch which can be pulled apart and then pressed together again. This solution is used to determine the skin friction. When the probe is on a certain level, the shaft is being pulled back between 50-100 mm (it depends on the size of the clutch) and then pressed back to the cone

tip. The skin resistance is determined from the force that is used to press the shaft from the extended position to where it meets the cone tip again. The point resistance is therefore total resistance minus skin resistance (Bergdahl 1984, p.6).

When a very firm layer is reached and the probe cannot penetrate any further the vane is used as a drill by being rotated. To show at which levels the vane has been rotated, these areas are crosshatched in the result diagram. The rest of the results are presented as a graph, see *Figure 5*.

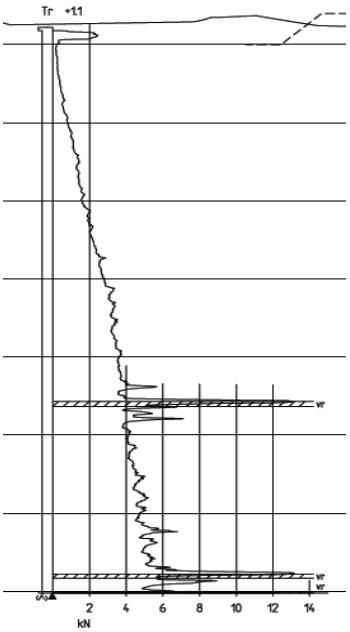

Figure 5 *Results from a pressure probing where the crosshatched area indicate where the vane has been rotated (Bygghandling, drawing: 202G0967).*

2.2.3 Vane shear test

The shear strength of a cohesion soil is usually decided from a vane shear test. This is an in situ test where a measuring instrument is pressed into the ground. At the end of the measuring instrument there are two metal plates connected perpendicular to each other, forming a cross, see *Figure 6.*

Figure 6 *A type of vane used for a vane shear test (Brookfield Viscosity Specialists)*

To be able to perform the test in different kinds of materials there are a few models that varies in size and shape.

The instrument is pressed down to a specific level; either to predefined levels or where a previous probing has indicated layers. At the right position a torque is put on the instrument so the vane starts to rotate. When the torque is equal to the shear strength the soil will fail. At the top of the measuring instrument the maximum torque ($M_{\max}$) is then registered. From that an average value of the undrained shear strength can be calculated, see Equation (2) (Bergdahl 1984, p.32).

$$\tau_{fu} = \frac{6}{7} \cdot \frac{M_{\max}}{\pi \cdot D^3} \qquad (2)$$

Values that are received from a vane shear test tend to be higher than the actual value for the clay. Therefore the values have to be reduced with a correction factor, μ that is taking the liquid limit into account. The correction factor can be calculated with Equation (3) or be taken from the diagram in *Figure 7*. The correction factor is then used in Equation (4) to calculate the shear strength (Sällfors 1993b, p.18).

$$\mu = \left(\frac{0{,}43}{w_L} \right)^{0{,}45} \geq 0{,}5 \qquad (3)$$

$$\tau_{fu} = \mu \cdot \tau_k \qquad (4)$$

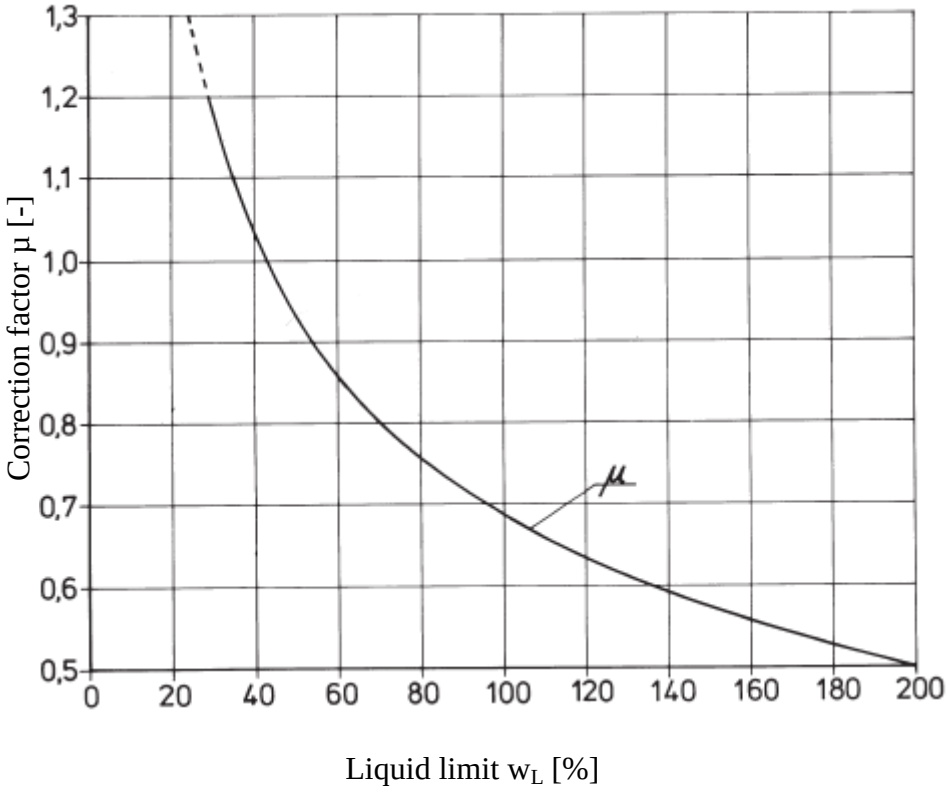

Figure 7 *Correction factor diagram for results from fall cone and vane shear test in normal consolidated or slightly over consolidated clay (Larsson et al., 2007).*

2.2.4 Soil sampling

Sample-taking of soil are necessary to be able to determine the properties of the soil layers. The samples, that are either disturbed or undisturbed, are also used to determine the soil properties in the laboratory (Sällfors 1993a, p. 20). Identification of soil type and determination of the water ratio can be made with a disturbed sample while an undisturbed sample is needed to be able to determine the strength and deformation properties of the soil (Bergdahl 1984, p. 21).

2.2.4.1 Piston sampling

Samples taken with piston sampler are undisturbed and are usually taken with a standard piston sampler of type St I or St II. Undisturbed samples can be taken mainly in cohesion soils but also in silt that contains clay or organic soil (Bergdahl 1984, p. 21).

The sampler consists of a pipe that is driven down to desired depth in the soil. When it is driven down the opening is shut by a piston inside the cylinder. When the desired depth is reached the piston is fixated on that level while the pipe is pressed down and punches out the soil sample. The speed when punching out the sample should be even and slow and one should wait a few minutes before extracting the pipe to obtain pressure relief (Bergdahl 1984, p. 22).

Inside the pipe there are three tubes that are sealed in the ends with plastic sheets and caps to prevent dehydration of the samples. The best sample is in the middle tube and upper part of the lower tube due to that the upper tube and bottom part of the lower tube are being somewhat disturbed when the piston is driven down (Sällfors 1993a, p. 23).

2.2.4.2 Auger sampling

Samples taken with auger sampler are disturbed and can be taken to a depth of about 5-10 m in cohesion soil and silt, and in sand above the groundwater level. The sampler consists of a steel rod with a spiral flange that is driven down through the soil by rotation. Soil is then attached to the flange and representative samples are packed in plastic bags to be analyzed in the laboratory where soil type, water ratio and liquid limit can be determined (Bergdahl 1984, p. 25).

2.2.4.3 Test pit

Test pits are used for shallow investigations and when other methods not are possible to perform, for example in boulder soils. An excavator is used to dig the test pit that has a depth of about 0-5 m. A test pit should be located outside the construction site to not disturb the soil around the construction (Bergdahl 1984, p. 24).

A test pit give information about the soil and its large-scale behavior, but also information about the excavatability, the groundwater table and the boulder content are notated during digging. Representative disturbed samples of the soil are taken and their positions are notated in a protocol along with the made observations. The test pit is also documented with photographs and a sketch (Bergdahl 1984, p. 24).

2.2.5 Groundwater measurement

In soil profiles that have layers with different soil types there can be several groundwater systems. Therefore should the layer sequence be determined through probing and soil sampling before the different measurement levels are chosen. The observation time should be long enough to registrate the seasonal variations. In high permeable soils the groundwater table is measured in open pipes. In piezometers that are used in low permeable soils the groundwater table is represented by the level where the pore pressure is zero (Bergdahl 1984, p. 39).

2.2.5.1 Open pipes

In high permeable soils like gravel and sand the groundwater table can be determined by using a water pipe perforated with small holes in the lower end and plugged in the bottom. The lower part is filled with for example coarse sand to function as a filter

and the pipe is driven down to the desired depth. The water level that arises in the pipe equals the pore pressure at the level of the tip (Bergdahl 1984, p. 39).

2.2.5.2 Pore pressure measurement

There are two different types of piezometers; one with an open system to be used in silty soils and tills and another with a closed system for use mainly in clay and mud (Sällfors 1993a, p. 27). The open system is similar to the open pipe; it is a steel rod perforated with big holes and with a filter consisting of a mixture of sand and plastic (Bergdahl 1984, p. 39). A small plastic hose where the water level can be measured is connected with the filter. Compared to the open pipe the open system requires a smaller amount of water to reach pressure equilibrium because the diameter of the plastic hose is smaller than the open pipe (Bergdahl 1984, p. 39).

In very dense soils like clay, peat and mud the closed system is used instead. The most commonly used piezometer in clay is the BAT type, see *Figure 8.*

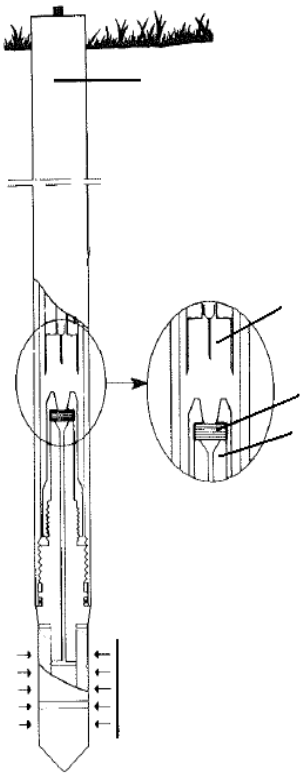

Figure 8 A commonly used piezometer in clay, type BAT (Bergdahl 1984).

In this type the measuring tip and the measuring system are separated from each other (Bergdahl 1984, p. 42). The measuring tip with an extension tube is installed on the site in a pre-bored hole. The tip consists of a plastic tip, a filter of ceramic that inside holds a water chamber that is closed in the top by a rubber membrane and a nozzle. When the pore pressure is to be measured the measuring device is lowered down in

the extension tube over the nozzle. And an injection needle on the device penetrates the rubber membrane and the pore pressure is thereby measured. The pore pressure can be read at the surface when it has stabilized (Sällfors 1993a, p. 28).

2.2.6 Inclinometer

An inclinometer is a field device used to measure horizontal movements in clay. It is installed before a construction phase is started to get a reference value for the inclination. Measurements are then performed during the whole construction period to be able to control how the ground moves (Bergdahl 1984, p.49).

A pipe is installed in the ground to a depth where no movements are expected. That is because if the pipe do not have a fix point the displacement data would be useless since the pipe would be allowed to rotate. If the pipe reaches firm layer it is important that the tip of the pipe is flexible in the vertical direction, otherwise it might break if settlements occur. The pipe usually has the dimension 50 mm (Bergdahl 1984, p.49).

The pipe is very flexible and will easily follow the movement of the soil. Inside the pipe a lod is installed. When the pipe moves the lod inside will follow the movements. From the reference value the inclination of the lod can then be determined. The movements are measured in two directions perpendicular to each other. One is assumed to be parallel with the expected direction of the movement and the other one perpendicular to it. The displacement is then usually presented as the resultant of the two directions. Measurements are usually performed on every meter and with a specific time interval (Bergdahl 1984, p.49).

2.3 Laboratory tests

Laboratory tests are performed on soil samples taken in field. It is important to make laboratory tests to be able to evaluate the soil properties and make a judgement of how the soil in the investigated area most probably will act when something is constructed in it. The tests used in this thesis are presented in this section.

2.3.1 Fall cone test

The fall cone test is a laboratory test used to evaluate undrained shear strength of clay. From a fall cone test you can also get the liquid limit and sensitivity. To test the undrained shear strength of clay a piston sample first has to be taken in field. The samples are then taken into the laboratory in tubes. The cone test is performed on the clay directly in the tubes right after the two first centimeters of the sample is removed, just to make sure the surface is absolutely smooth. Then the sample is placed under a cone shaped weight. The cone should just touch the surface of the clay, see *Figure 9*. Then it is released and the tip if the cone will penetrate the clay. This procedure is repeated three times. Approximately 1.5 times the penetration depth of clay is removed and put in a bowl after each test. The mean value of the three penetration

depths is then used for evaluation. This procedure will give the undisturbed shear strength of the clay (Sällfors 1993b, p.17).

The clay that was put away in a bowl is then remoulded before it is being tested again. The procedure is similar to the one mentioned above except that the sample is remoulded and put in a bowl. The cone test is performed in a device like the one in *Figure 9.* This gives the remoulded shear strength of the clay (Sällfors 1993b, p.17).

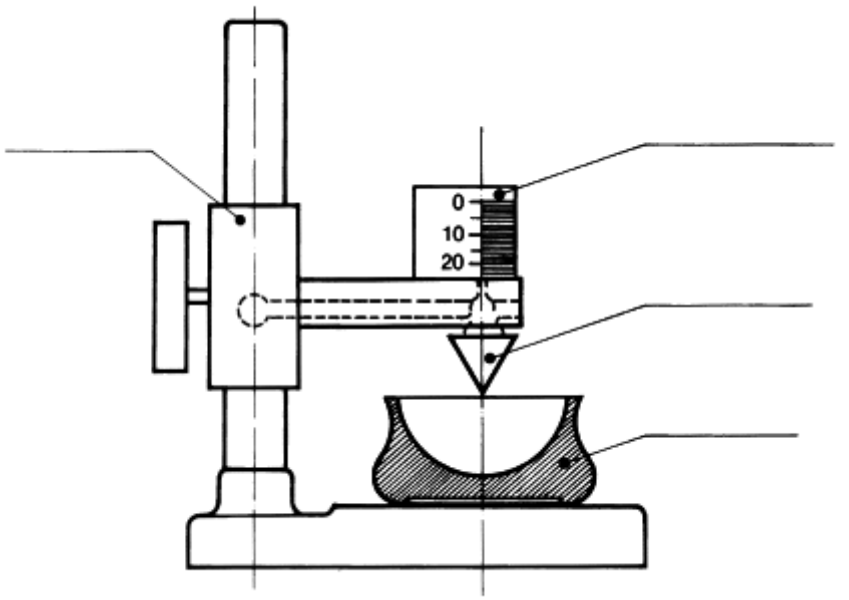

Figure 9 *Measuring equipment for fall cone test (Larsson 2008).*

As the shear strength evaluated from cone tests tend to be higher than the actual value for clay in field, it is necessary to reduce the shear strength with regard to the liquid limit, see Equation (5), in the same way as for vane shear test described in section 2.2.3.

$$\tau_{fu} = \mu \cdot \tau_k \qquad (5)$$

2.3.2 Oedometer test

Oedometer test are performed to determine the stresses in the soil and the deformation properties of the soil. Two types of tests can be performed; incremental strain or constant rate of strain, CRS. Only CRS-tests have been evaluated in this thesis and are presented here.

2.3.2.1 CRS-test

The CRS-method can give information about clays deformation properties in 1-2 days (Sällfors & Andréasson. 1986, p. 13). In this test the specimen is loaded in such a way

that it will be deformed at constant speed. The specimen is only drained at the top and the pore pressure is measured at the bottom where it is undrained conditions. The force and deformation in the vertical direction are also automatically recorded during the test. Unloading of the sample should normally not be performed at constant deformation speed (Sällfors & Andréasson. 1986, p. 33).

It is important that the sample is examined for possible organic variations since they can have a large impact on the pore pressure. Another part of the tube sample should be chosen if such a disturbance is anticipated (Sällfors & Andréasson 1986, p. 34).

The inside of the confining ring that the specimen is placed in is lubricated with silicon grease in order to reduce friction between the ring and the specimen (Claesson 2003, p. 45). An appropriate deformation speed is chosen on the press, a speed of 0,0025 mm/min is commonly used which gives a deformation of about 18 % during 24 hours. During the test the deformation, vertical force and pore pressure are measured about 200 times. After the gathered data has been processed the result are presented in different diagrams from where the preconsolidation pressure, compression modulus, permeability and consolidation coefficient can be evaluated (Sällfors & Andréasson.1986, p. 34).

2.3.3 Density

When talking about density in geotechnics there are mainly two kinds of densities, the bulk density and the compact density. These two densities differ when it comes to porous materials.

The bulk density describes as the mass divided by the volume, see Equation (6), when the soil is in its natural state (Sällfors 2001, p.2.6).

$$\rho = \frac{m}{V} \qquad (6)$$

Evaluation of the bulk density is performed on an undisturbed soil sample. The sample is brought to the laboratory in a tube. First the tube has to be weighted empty and then again with the soil sample within it. This makes it possible to calculate the weight of the soil sample. As the measures for the tube are known the volume can also be calculated. The ratio between them gives the bulk density (Sällfors 1993b, p.9).

The compact density on the other hand describes the density of the solid substance and is calculated as the ratio between the mass of the substance and the volume of the substance, see Equation (7) (Sällfors 2001, p. 2.6).

$$\rho_s = \frac{m_s}{V_s} \qquad (7)$$

To get the compact density of a material a method called the pyknometer method is used, where water is used to determine the volume of the solid material (Sällfors 1993b, p. 9).

2.3.4 Permeability

Permeability describes how water flows in a porous medium and the unit is [m/s]. For a porous material like soil the permeability will vary depending on what kind of fraction it is. Sand for instance has much higher permeability than clay. That is because the permeability is directly connected to the size and shape of the ingoing fractions. Since sand has larger grain size than clay, it is more porous and water can therefore flow more easily in the sand. Another aspect to consider regarding permeability is that it can vary in different directions (Sällfors 2001). Permeability in clay can be calculated with parameters given from a CRS-test (Sällfors 1993b, p.27).

2.3.5 Natural water ratio

The natural water ratio w_n, is usually determined from an undisturbed soil sample. The ratio between the weight of the water and the weight of the solid material will give the natural water ratio, see Equation (8) (Sällfors 2001, p. 2.7).

$$w_n = \frac{m_w}{m_s} \qquad (8)$$

It is a very easy test to determine this ratio. A 1 cm thick slice of the sample is removed and weighed. The sample is then put in an oven for 24 hours in 105°C. In the oven all the water in the sample will disappear as evaporation, then the sample is weighted again. The weight of the water can then be calculated as the total weight of the sample minus the weight of the sample after it has been dried in the oven (Sällfors 1993b, p. 11).

2.3.6 Liquid limit

The liquid limit, w_L, can as mentioned before be determined from a fall cone test. The water ratio where the sample goes from being plastic to being liquid is called the liquid limit. To decide this limit a 60 g 60° cone is used in the fall test. The liquid limit is when the cone penetrates the remoulded sample 10 mm (Sällfors 2001, p. 2.10).

Clay has different ability to bind water because the amount of organic material and the clay content varies, depending on where the clay is located. A high value on the liquid limit indicates high content of organic material in the clay (Sällfors 1993b, p. 11).

2.3.7 Sensitivity

The sensitivity, S_t, can be calculated as the undisturbed shear strength divided by the remoulded shear strength, see Equation (9) (Sällfors 2001, p. 2.13). These both shear strengths comes from a fall cone test which can be read more about in section 2.3.1.

$$S_t = \frac{\tau_{fu}}{\tau_{omr}} \qquad (9)$$

2.4 Empirics

Empiric relations are used to see how well values measured in field or in laboratory comply with the values calculated from empiric equations. If a measured value differs too much from an empiric value it might be a good idea to make some further investigations in the area. Empiric relations should be used carefully and only on soils with the same geological history as the empiric relations are based on. It is important to remember that empiric relations should not be seen as a substitute for other tests, but rather be a complement to the investigations.

2.4.1 Hansbo's relation

To control that values of the shear strength measured with vane shear test and fall cone test give normal values they can be compared to Hansbo's relation, see Equation (10);

$$\tau_{V,k} = \sigma'_c \cdot 0{,}45 w_L \qquad (10)$$

This relation is valid for normal consolidated and slightly overconsolidated Scandinavian soils. To be considered as reasonable values the reduced values of the shear strength should as good as possible comply with this relation.

By comparing the values with this relation one can make a simple judgment if they seem reasonable. If ones values are much higher than the one for Hansbo it can indicate that the correction factor should be higher while with lower values it can be possible that further investigations can give higher values of the shear strength (Larsson, et al. 2007, p. 18).

2.4.2 Undrained shear strength

The undrained shear strength can be expressed by Equation (11):

$$c_u = a \cdot \sigma'_c \cdot OCR^{-(1-b)} \quad \text{or as} \quad c_u = a \cdot \sigma'_{V0} \cdot OCR^b \qquad (11)$$

and is dependent on soil type, loading, preconsolidation pressure and the over consolidation ratio. The variables a and b are material parameters where a varies depending on the soil and the loading and b is normally assumed to be 0.8. The undrained shear strength is divided into three cases; active shear, direct shear and passive shear due to that the undrained shear strength varies with the direction of the loading, see *Figure 10* (Larsson, et al. 2007, p, 13).

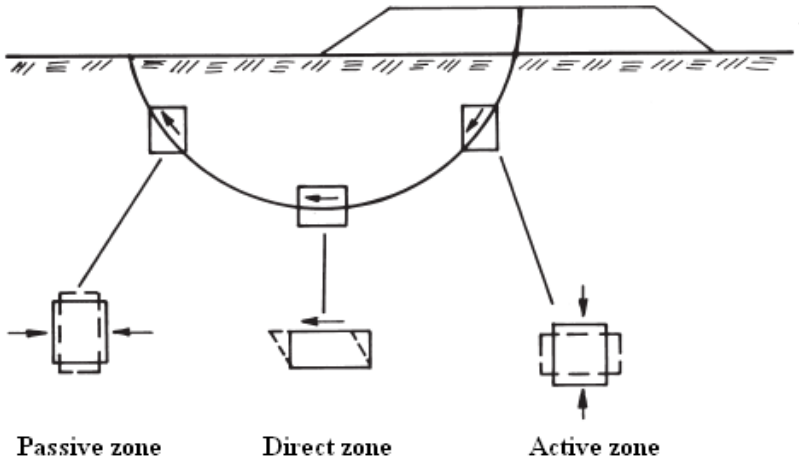

Figure 10 Zones where different kinds of shearing occur (Larsson, et al. 2007).

Below follows the empiric relations for the parameter a for clay, see Equation (12-14).

Active shear $$a \approx 0.33 \tag{12}$$

Direct shear $$a \approx 0.125 + 0.205 \cdot \frac{w_L}{1.17} \tag{13}$$

Passive shear $$a \approx 0.055 + 0.275 \cdot \frac{w_L}{1.17} \tag{14}$$

Especially for low plastic clays with high sensitivity these empiric relations can overestimate the undrained shear strength (Larsson, et al. 2007, p. 13).

2.4.3 Modulus

The oedometer modulus is, as mentioned before, evaluated from the CRS-test. To control that the modulus evaluated from the CRS-test is reliable it can be compared to an empiric relation for the oedometer-modulus, see Equation (15) below (Larsson 1994, p. 24);

$$M = m \cdot \sigma' \qquad (15)$$

Where m is the compression modulus number and σ' is the effective vertical pressure.

Field tests have shown that the modulus in the overconsolidated area evaluated from CRS-test is lower than the real values of the compression modulus, due to disturbance and stress relaxation of the soil sample. The best way to estimate the real compression modulus is to perform an unloading and reloading test. In cases where this test is not performed the empiric relation, see Equation (16), can be used to correct the oedometer modulus (Sällfors 2001, p. 6.16).

$$M_0 = 3 - 5 \cdot M_{0,CRS} \qquad (16)$$

2.4.4 Soil sample quality test

A completely undisturbed soil sample from field is almost impossible to get. When the testing device is driven into the ground it will disturb the soil which also will affect the soil sample. To get as accurate test results as possible it is important that the soil sample is of good quality. To simulate the stress state in the ground the soil sample is reconsolidated in laboratory before performing e.g. a triaxial test and a direct shear test. Since the soil sample already has been disturbed it is impossible to create the exact in situ stress state, but from the test results an evaluation can be made to see how reliable the results are, based on the soil sample quality. From an oedometer test the strain at the preconsolidation pressure can be evaluated see *Figure 11*. With the evaluated strain and the natural water ratio the soil sample quality can be determined see *Figure 12*, which indicates the reliability of the results (Larsson, et al. 2007, p. 15).

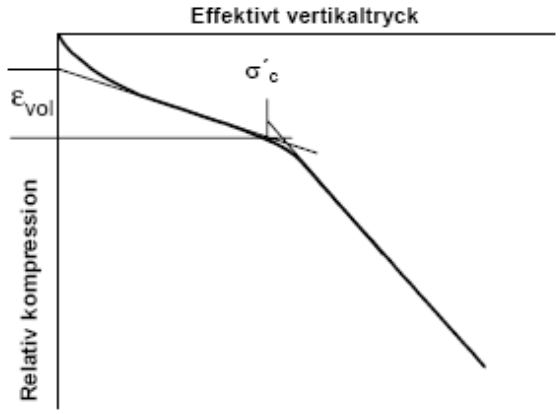

Figure 11 Strain at the preconsolidation pressure (Larsson, et al. 2007).

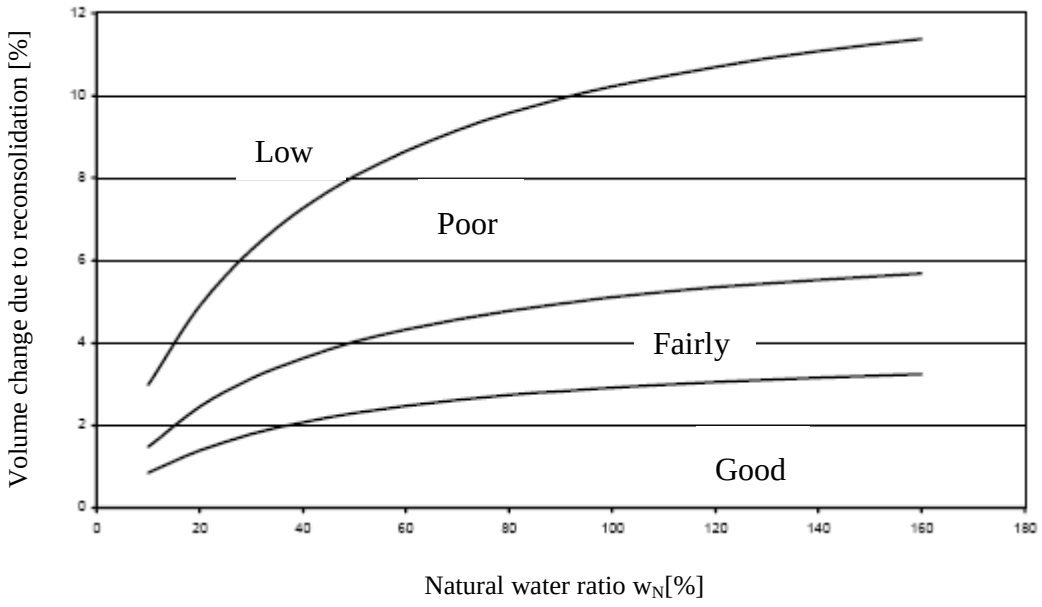

Figure 12 Diagram for evaluation of test sample quality (Larsson, et al. 2007).

2.5 Calculation program

To simulate pore water pressure changes and soil displacement due to installation of lime-cement columns the calculation program Plaxis has been used. The version that has been used is Plaxis 2D-version 9. All information in this section is taken from the handbook of Plaxis version 9 (Brinkgreve & Broere 2008).

2.5.1 Plaxis

Plaxis is a finite element program used to analyze geotechnical problems regarding stability and deformations. Several different calculation models are available in Plaxis. In this report the Mohr–Coulomb model is used. Because of the soil conditions the calculations in Plaxis are performed in an undrained analysis.

The modeling is divided into three main steps that are presented below:

Input
In this step the geometrical model is created. A model is built up with points, lines and clusters. Everything that will be included in the calculation steps has to be specified. It might be loads, prescribed displacements anchors, sheet pile walls and so forth. All the features will be given specific material properties. The model also has to have boundary conditions for how it is allowed to move. Then a mesh with triangular elements has to be created for the given geometry. It might be a 6-node element mesh or a 15-node element mesh. The 15–node element mesh is more detailed than the 6-node element mesh, so for more complex problems it is advisable to use the 15–node element mesh. If the geometry is changed, the mesh has to be regenerated. Finally the initial stresses have to be created, either by the K_0-procedure or by gravity loading. For more information about how to create initial stresses see the handbook of Plaxis.

Calculation

In this step all the calculation phases should be defined. Plaxis allows to use several different calculation types but in this report only the plastic analysis (deformations) and the consolidation analysis (time dependent) are used. In each calculation phase a define mode is available where soil layers and other features like an anchor can be selected or deselected depending on whether it should be included in the calculation or not. Stress points and displacement nodes can also be selected in the calculation step and can then later be used to create detailed curves in the curve program.

Output

In the output program the results are presented. It allows to view results after each calculation step. Horizontal- and vertical displacements, effective- and total stresses and excess pore pressure are examples of what can be viewed in the output program. Cross sections can also be created to study a particular area in more detail.

2.5.2 Mohr - Coulomb

Failure in soils can be described by the Mohr-Coulomb theory. Failure occurs when the shear stress becomes the same as the shear strength of the soil. The soils shear strength can be described by Coulomb's equation, see Equation (17). Since it is only the particles in the soil that can take shear stresses, the shear strength equation is based on effective stresses (Craig 2004, p. 91).

$$\tau_f = c' + \sigma_f \tan\phi' \qquad (17)$$

This equation, which describes the failure envelope, combined with Mohr's circle creates the Mohr-Coulomb diagram, see *Figure 13.*

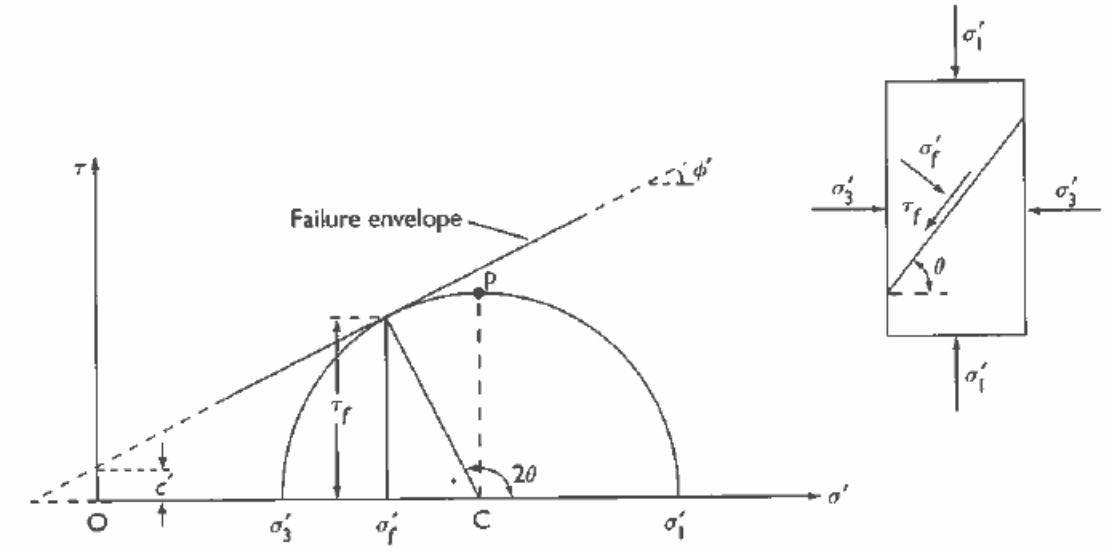

Figure 13 Mohr-Coulomb diagram and principal stress directions (Craig 2004).

As can be seen in *Figure 13,* σ'_1 is the principal stress in the vertical direction and σ'_3 is the principal stress in the horizontal direction. Mohr's circle is obtained by plotting a circle that connects the principal stresses σ'_1 and σ'_3. Mohr's circle shows the stress situation for all possible planes. The angle θ is the inclination of a plane compared to the horizontal plane. For a plane with an angle θ the shear stress and normal stress can be obtained by drawing a radius with an angle 2θ from the x-axis. The coordinates for the point where Mohr's circle and the drawn radius intersect is the shear stress and normal stress for the specific plane (Sällfors 2003, p. 3.8).

When the circle, in one specific point, is equal to the failure envelope the soil will collapse along the plane represented by the point. The plane where failure occurs will have an inclination of $45 + \phi'/2$ (Sällfors 2003, p. 5.4). From the failure envelope the cohesion, c' and the angle of internal friction, ϕ' can be determined.

As can be seen in the picture the shear strength is lower for smaller stresses. Because the stresses are effective stresses the shear strength in the soil will decrease when the

pore pressure increases, under the condition that the total stresses are unchanged. For undrained conditions the failure envelope in Mohr-Coulomb becomes horizontal, see *Figure 14*. This is due to that an increase in total stresses would result in an equal increase of the pore pressure because of the undrained conditions, and therefore the effective stresses will remain unchanged.

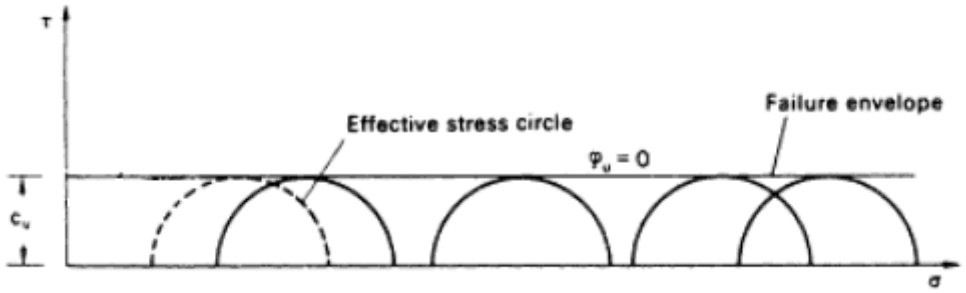

Figure 14 Failure envelope for undrained conditions (Craig 2004, modified).

In the figure are circles for different stress states shown, and the dotted circle represents the effective stresses, which are the same for all the different stress states.

Mohr-Coulomb is a simple model that is easy to use. However there are some limitations in the model. One of them is that there is no yield surface that sets the boundaries for failure when performing an undrained analysis.

To be able to obtain the total stresses, effective stresses and the excess pore pressure the undrained analysis has to be performed with effective parameters. These effective parameters have to be corrected so that they meet the values of the undrained shear strength, see *Figure 15*.

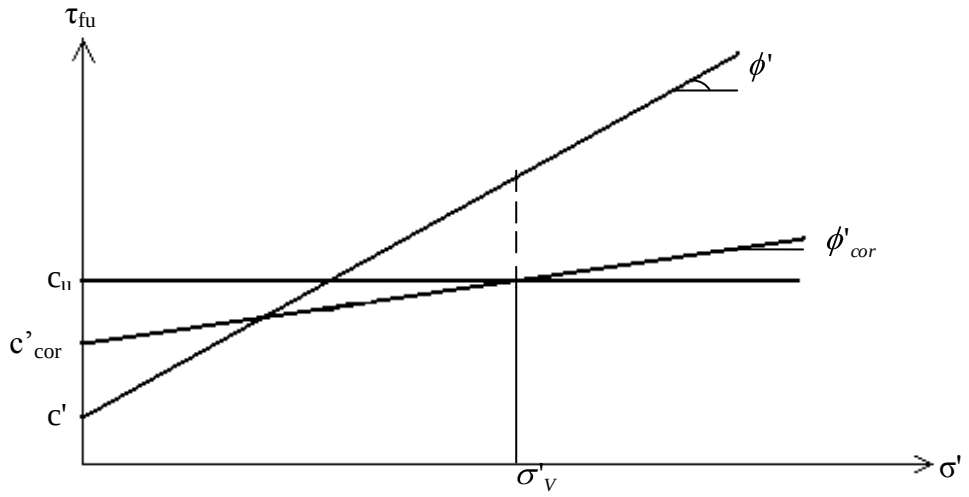

Figure 15 Correction of effective parameters.

The figure shows that if the effective parameters is not corrected they will give a shear strength that is too high for the given stress state. Another alternative is to use effective parameters but to set $c' = c_u$ and $\phi' = 0$ and to have an increment of c_u per m.

3 Area description

The area around section E32 is described below and is located about 20 km north of Göteborg. The parts about hydrogeology and topography is more site specific and involves information that is relevant for an area going from Bohus to Nödinge. The part about geology gives a more wide description of the geology around Göteborg and also short information about the latest deglaciation and how the clay around Göteborg was created.

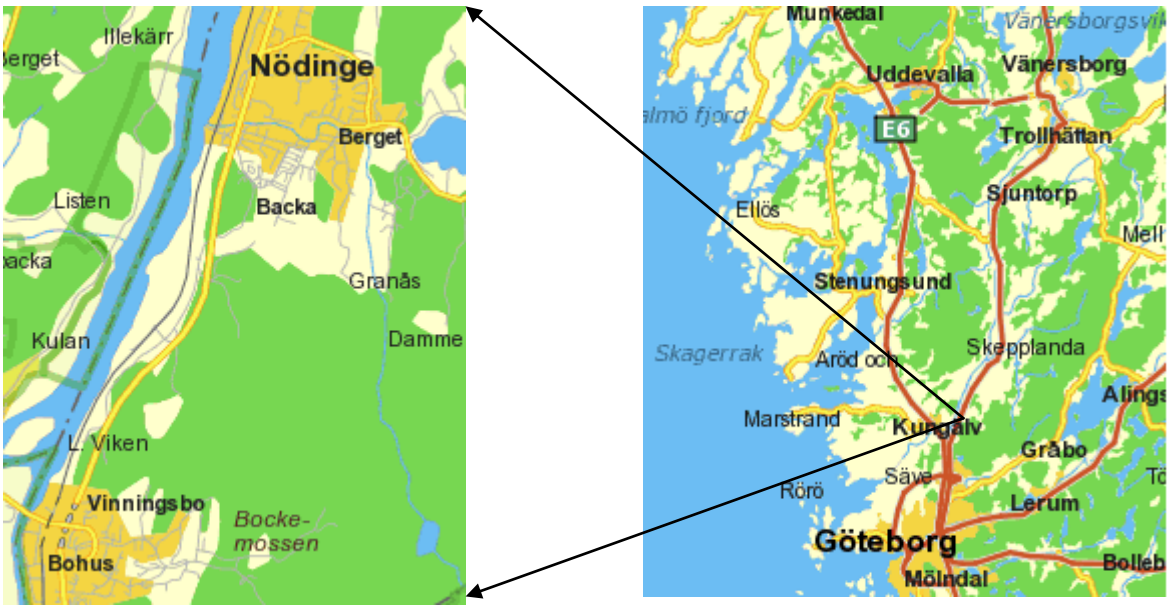

Figure 16 View of where Section E32 is located (Eniro).

3.1 Topography

The area between Bohus and Nödinge is a low-lying landscape between a rock in the east and the Göta älv river in the west. The rock have a level of +112 meters above sea level at its highest point and decline downwards Göta älv river that lies on a level of about +0,4 meters above sea level. The level of the low-lying landscape varies between about 1-10 meters above sea level (SGU 1976 & SGU 1979).

3.2 Geology

The soil layers in Sweden have come in to existence during the quaternary period and the post glacial period. During the latest ice age almost entire northern Europe was covered by a thick ice sheet. The thick ice layer pressed down the ground with its enormous weight. When the ice then started to melt the ground started to rise because of the unloading. The areas, where the ice sheet once had pressed down the ground,

became covered with water after the deglaciation, which is the case for the Göteborg area (Fredén 1986).

As the ice sheet started to melt, water began to flow and transported a lot of eroded material. When the water flow started to decrease, the eroded material could settle. The finest particles could only settle in calm water where the depth was great. That is why thick clay layers usually can be found in valleys. The sedimentation of fine particles has created the thick clay layers, up to 60-80 meter in some places, in the area (Fredén 1986). The structure of the clay is relatively even and is very little varved. That is because the clay particles have settled in a marine environment (SGU 1979). Since heavy particles settles first, the clay layers rests on layers of friction material with varying thicknesses, the friction material is then resting on the bedrock. Göta älv valley was once an inlet, but due to land uplift it has transformed into a river (Fredén 1986).

Typically for the west coast is the lack of till as top soil layer, which is probably because of the very small erosion in the end of the last deglaciation. The soil map (SGU 1979) shows that outcrops can be found in many places and that the bedrock in some places has a steep inclination towards Göta älv (Fredén 1986).

3.3 Hydrogeology

The groundwater surface in the area are basically following the ground and can be found approximately 0.5 m below the ground surface. The ground surface has a slightly inclination towards Göta älv. There are also some minor fracture zones in the area and the majority of them are in east west direction and in north-east to south-west direction (Aqualog 2007). Orientation of fracture zones and information about the inclination of the ground surface gives an indication of how the water flows. In this area it is most probably that the water flows towards Göta älv river from north-east to south-west direction.

4 Site specific data for section E32

Here is site specific data for Section A located at km 459+600, see Drawing 1 and 2, presented. The distance from the most westerly column row to Göta älv river is approximately 40 m, see Appendix 1. First the layer sequence for the area is presented. Then different ground properties and pore pressure are evaluated for the area. Specific information about when the different columns are installed is then presented. Last section contains information about pore pressure changes and soil displacements that occurred due to installation of lime-cement columns.

4.1 Layer sequence

The soil layers in section E32 have been determined from some commonly used test methods like; test pit and pressure probing. These tests are taken from several different places within the section and they give a similar view about the layer sequence. The first meter is considered as a dry crust followed by a homogeneous clay layer, approximately 28 m thick. Underneath the clay layer a friction material is found, see *Figure 17*. In Section A, no tests have been taken further down than to level -32 which is a few meters down in the friction material, but the friction material is most probably resting on the bedrock.

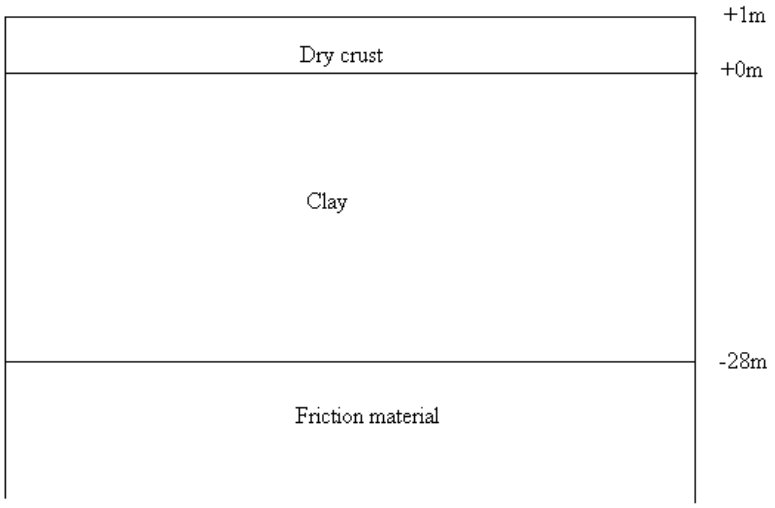

Figure 17 Soil profile in Section A.

4.2 Ground conditions

Results from the laboratory investigations are presented in diagrams in Appendix 2. The parameters have been evaluated in Appendix 3.

The water ratio, w_N, varies between approximately 70-110 % down to a depth of 30 m, while the liquid limit, w_L, varies between 80-100 % the first ten meters and then has a value of about 60-80 % down to a depth of 30 m, see *Figure 18*.

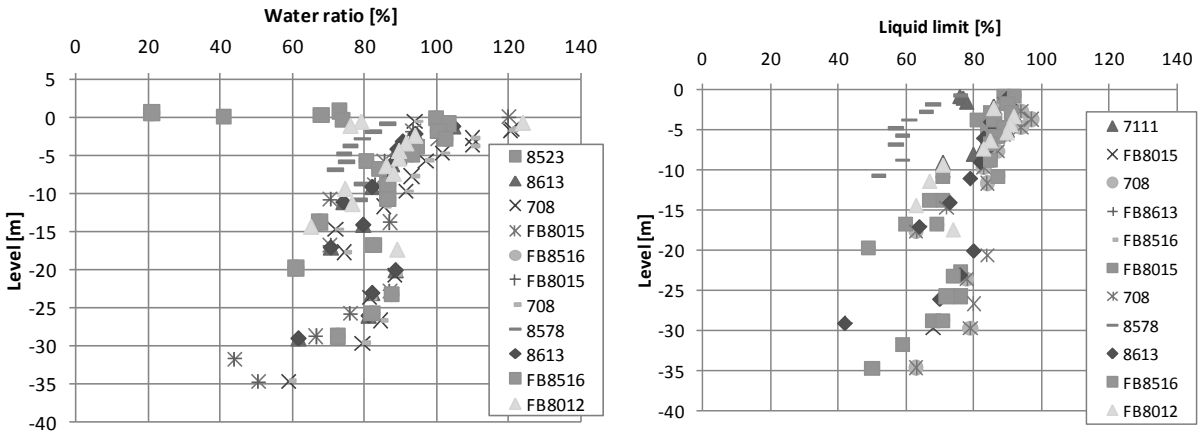

Figure 18 Water ratio and liquid limit from Section E32.

The permeability is quite even through the clay layer with values between 2-20$\cdot 10^{-10}$ m/s, see Appendix 2a and 2b.

The bulk density have been evaluated from laboratory investigations made on samples from three different boreholes, see Appendix 2c. The density of the clay range from 1.5 t/m^3 at the top to 1.8 t/m^3 at level -35 m.

The preconsolidation pressure evaluated from CRS-test are plotted in a diagram, see Appendix 2d. The preconsolidation pressure has been used to calculate an empiric value of the shear strength by using Hansbo's relation, see Section 2.4.1 It has also been used to calculate the empiric value of the active, passive and direct shear strength, see Section 2.4.2 The overconsolidation ratio is also required to calculate these empiric values. The OCR has been evaluated from the borehole closest to Section A, see Appendix 2e. It shows that the clay is normally consolidated with an OCR ranging from 1.5 at the surface to around 1 at level -30 m. In *Figure 19* the in situ and preconsolidation stresses are plotted.

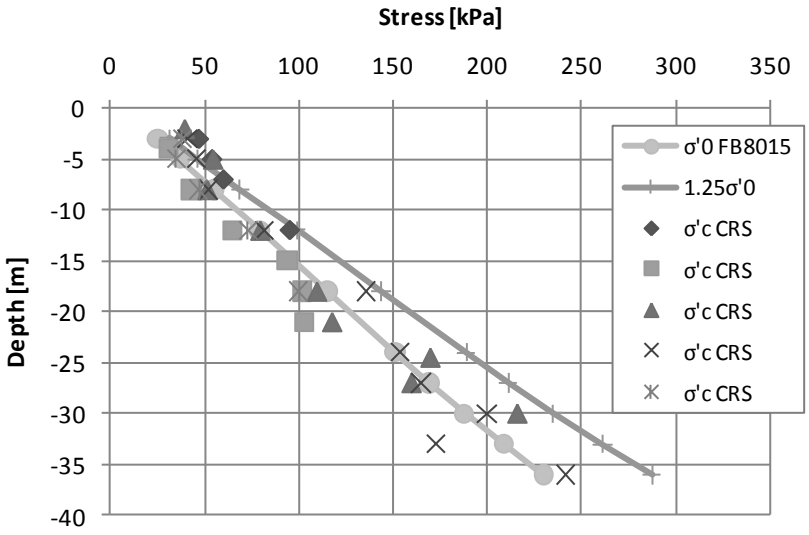

Figure 19 *In situ stress and preconsolidation pressure evaluated from CRS-tests.*

The quality of the soil samples have been evaluated according to the soil sample quality test described in Section 2.4.4. This test showed that the quality of the soil samples were fairly and close to good.

The shear strength measured from fall cone test and vane shear test have been reduced due to the liquid limit and plotted in a diagram, see Appendix 2g. In *Figure 20* the evaluated (assumed) shear strength is plotted together with measured values.

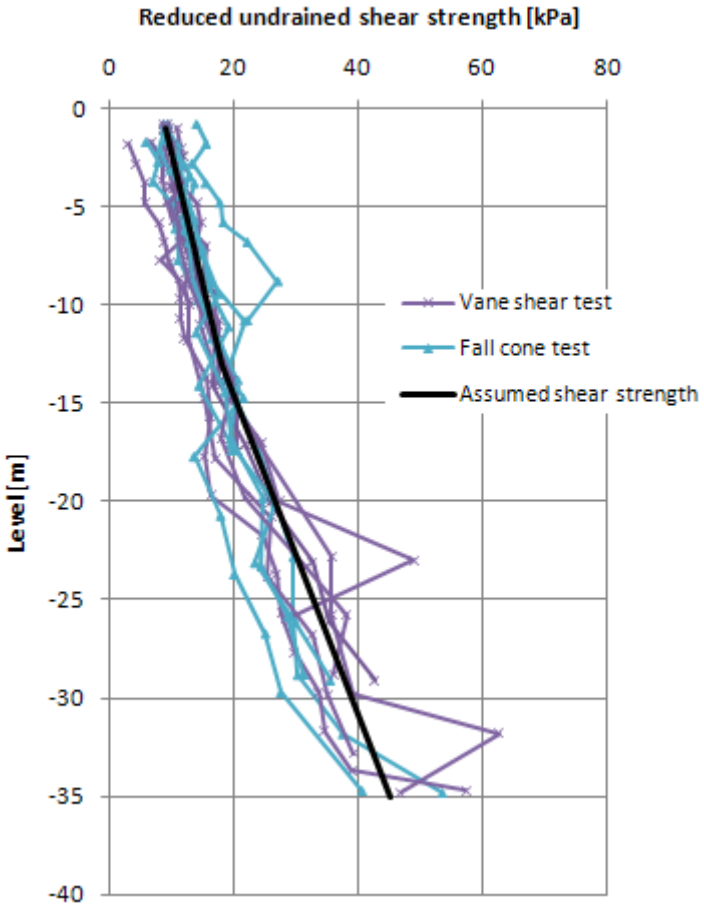

Figure 20 *Evaluated shear strength.*

The measured shear strength has also been compared to empiric relations by Hansbo and about undrained shear strength, see Section 2.4.1 and 2.4.2. The measured shear strength have been plotted in a diagram with the values of the shear strength from the above mentioned empiric relations, see Appendix 4a. When the different graphs are compared it can be seen that the empiric relations give higher values of the shear strength than measured from fall cone and vane shear test. This can indicate that the liquid limit used for reduction of the measured shear strength from fall cone and vane shear test is too high. This, because a high liquid limit gives high values of the empiric shear strength, see Equation (10). Additional investigations could result in higher shear strength.

The compression modulus has been evaluated from CRS-tests, see *Figure 21* for M_0 and Appendix 1h for M_L. In Appendix 4b the evaluated values are compared with the empirical relations in Section 2.4.3.

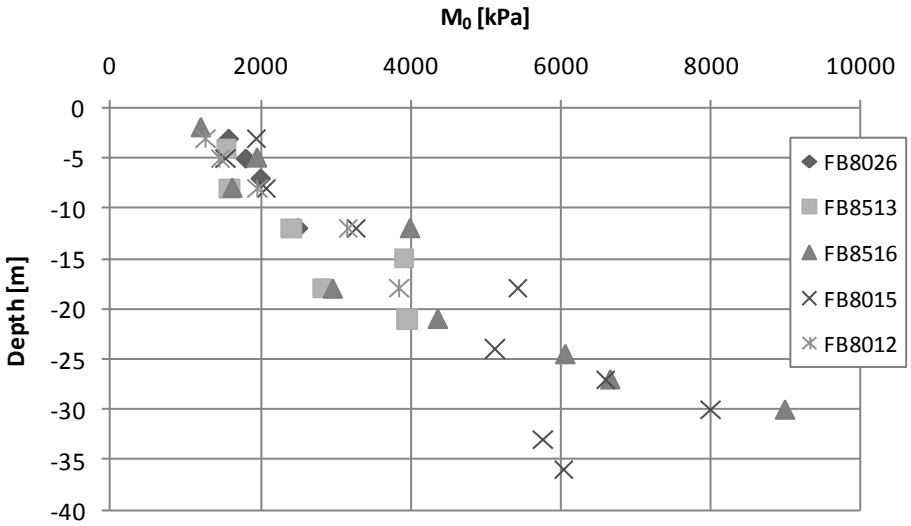

Figure 21 *Oedometer modulus evaluated from CRS-tests.*

4.3 Pore water pressure

The results from pore pressure measurements at nine different locations are shown in the diagram below, see *Figure 22.* The different piezometers are located within an area of about 500 m around section A and the pore pressure measurements have been performed at different times of the year.

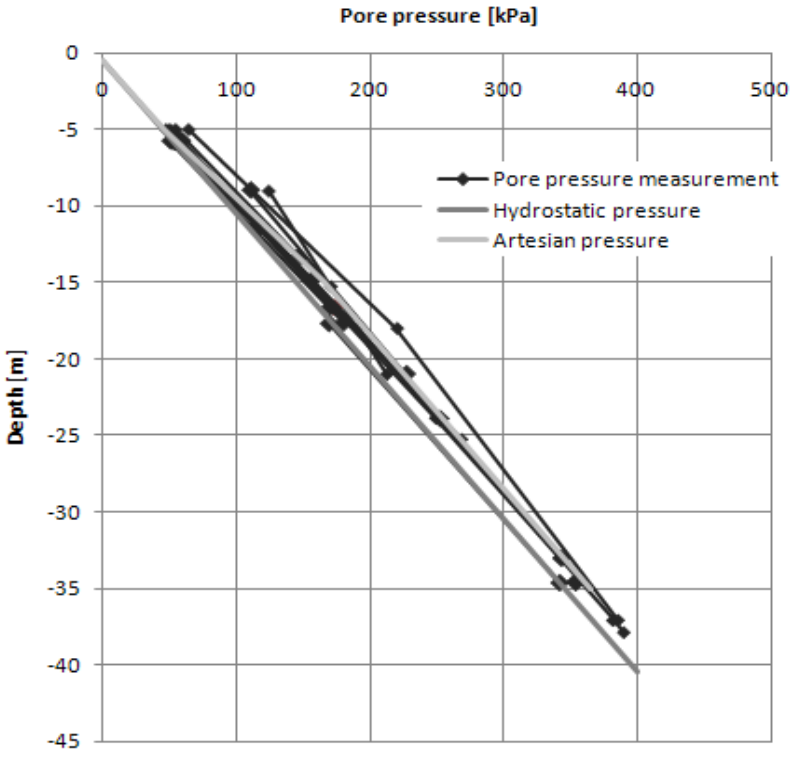

Figure 22 *Pore pressure measurements in section E32.*

As can be seen in the figure, most of the measurements show an artesian pore pressure of about 20 kPa around depth -15 m. The measure that stands out the most is taken in January 2008 and is located about 80 m away from Section A. Other measurements performed at the same date follows the hydrostatic line better, see Appendix 6. So because it is the only measurement that stands out this much it can be assumed that the excess pore pressure has arisen locally and not will affect the groundwater conditions in Section A. From the two test pits that have been made in the area the level of the groundwater table has been determined to lie about 0,5 m below the ground surface (Aqualog 2007). The evaluation of the pore pressure measurements give that the groundwater table is 0,5 m below the surface and the pore pressure can be assumed to be hydrostatic down to level -5 m and that there is an artesian pressure below this level. Because of the nearness to Göta älv river the groundwater table can vary depending on the water level in the river.

4.4 Installation of lime-cement columns

In section E32 there are three types of lime-cement columns installed; short columns installed as plates, long singular columns and dynamic columns also installed as plates, see *Figure 23*, and all columns are installed from level +0.5 m. Information about installation order are available for the short and the long columns but not for the dynamic columns. Therefore the installation order is assumed to be the same as for the long and the short columns. The data for the installation order combined with the coordinate system makes it possible to determine in which direction the columns are installed. For section E32 they are installed from north to south and each column from east to west. The columns are installed in Plaxis in the order that they are presented below.

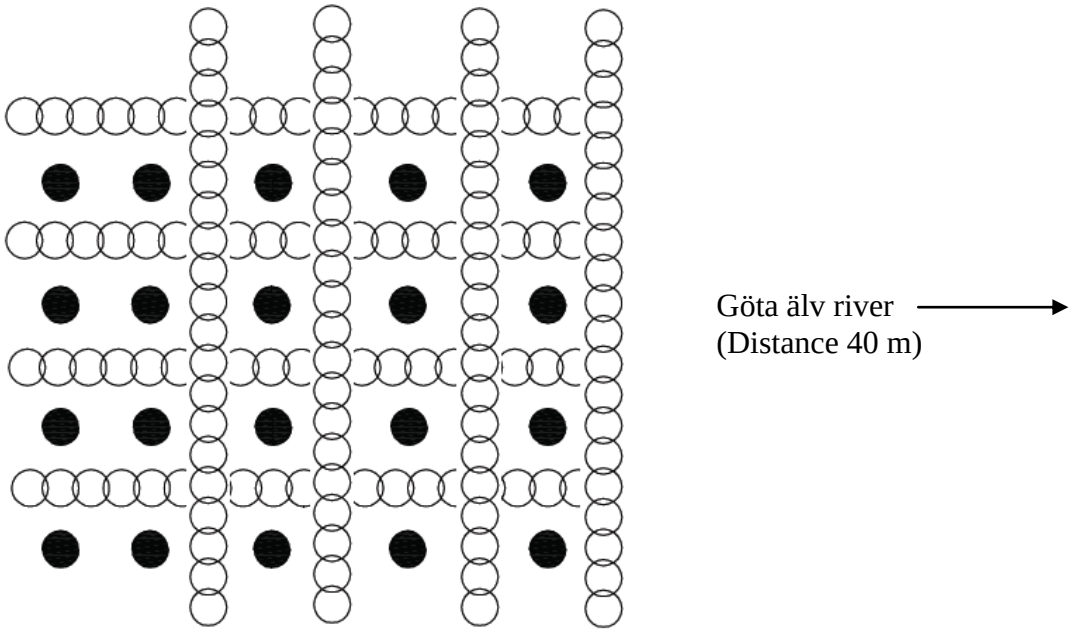

Figure 23 *Installation scheme where the horizontal rows are the short columns, the vertical rows are the dynamic columns and the black dots are the long columns. The railway goes in the vertical direction.*

Short columns

The short columns are installed with an overlap of 0.1 m which will form plates. The plates are perpendicular to the railway and have a center distance of 2 m, see Appendix 7 and Drawing 3. They are approximately 4.2 m long in whole section 459+600 and reaches down to level -3.7 m. One plate consists of 20 columns in a row. Installation of the short columns in the area was made the 3rd of March 2009.

Long columns

The long columns were installed the 6th of March, three days after the installation of the short columns, as singular columns. Five columns are installed in a row with a center distance of 2 m, see Appendix 7 and Drawing 3. They are 22.6 m long and goes down to level -22.1 m.

Dynamic columns

The dynamic columns are installed to prevent vibrations from the railway. They are 7 m long and goes down to level -6.5. These columns are, as the short ones, installed with 0.1 m overlap which will create a plate. The columns are parallel with the railway and will create a stabilized zone right under the rail, see Appendix 7 and Drawing 3. As mentioned before, there is no available data about the installation order for the dynamic columns so they are assumed to be installed 9th of March, three days after the long columns.

4.5 Horizontal displacements and pore pressures

Within section E32, a more detailed study regarding horizontal displacements and pore pressures has been made in Section A. In this section an inclinometer and a piezometer are installed 4 m west of the lime-cement column row closest to the river, see Appendix 8.

Data from the inclinometer measurement showing the horizontal displacements in Section A have been sorted out to be able to study specific dates in more detail. The dates of interest are between March 3rd and March 9th 2009, because that is when the different types of columns were installed. The figure below shows inclinometer data one time per day from March 1th to March 10th. It can be seen that there are three different periods where the inclinometer indicate movements in the ground, see *Figure 24*. It shows that the largest measured horizontal displacement is somewhere around 60 mm and it occurs in the upper part of the soil layer.

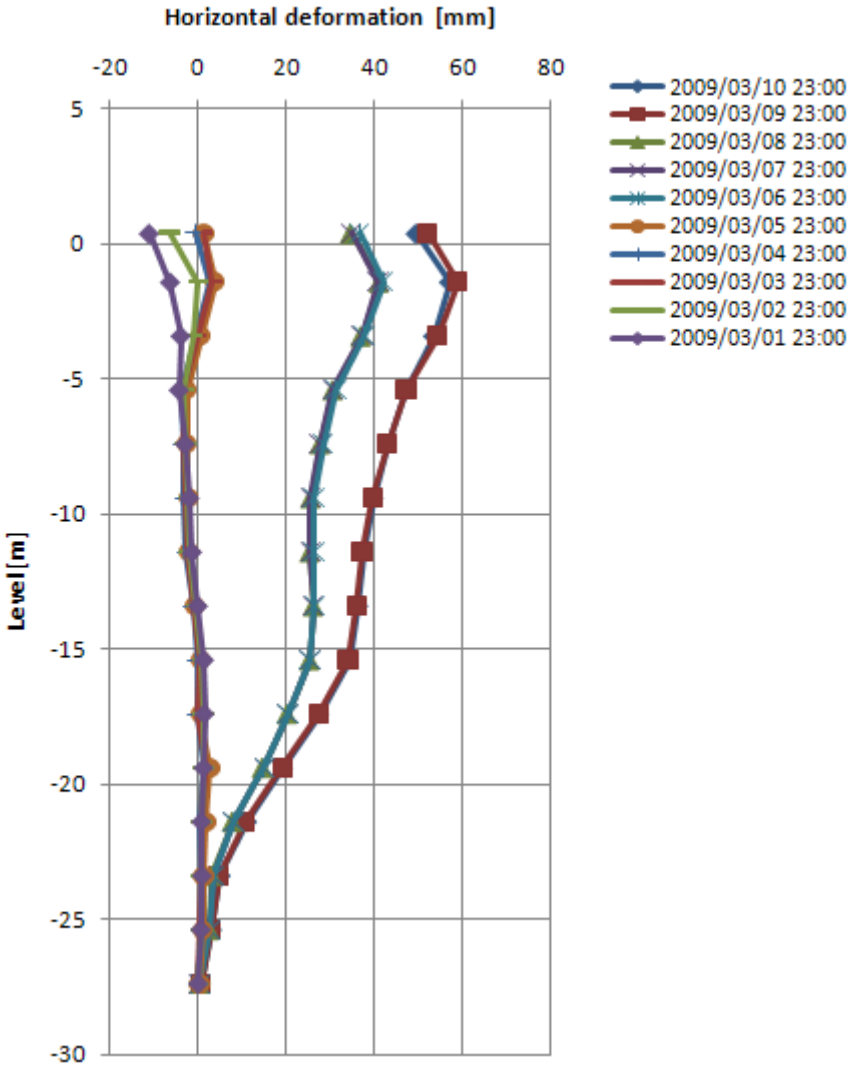

Figure 24 *Showing the measured horizontal displacements in Section A between March 1th and March 10th*

The piezometer is located at the same place as the inclinometer, see Appendix 8. The pore pressure is studied more in detail around the same dates as the different types of columns are installed, between March 3rd and March 9th, 2009. To be able to observe the pore pressure changes a few days before and after the installation dates are showed in the diagram. The piezometer register data from two different levels, -4 m and -9 m, see *Figure 25* and *Figure 26*.

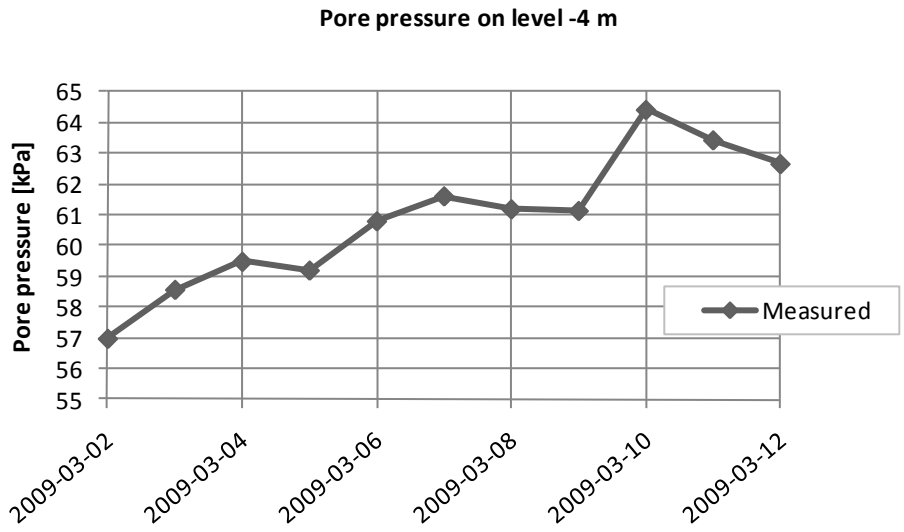

Figure 25 *Measured pore pressure on level -4 m.*

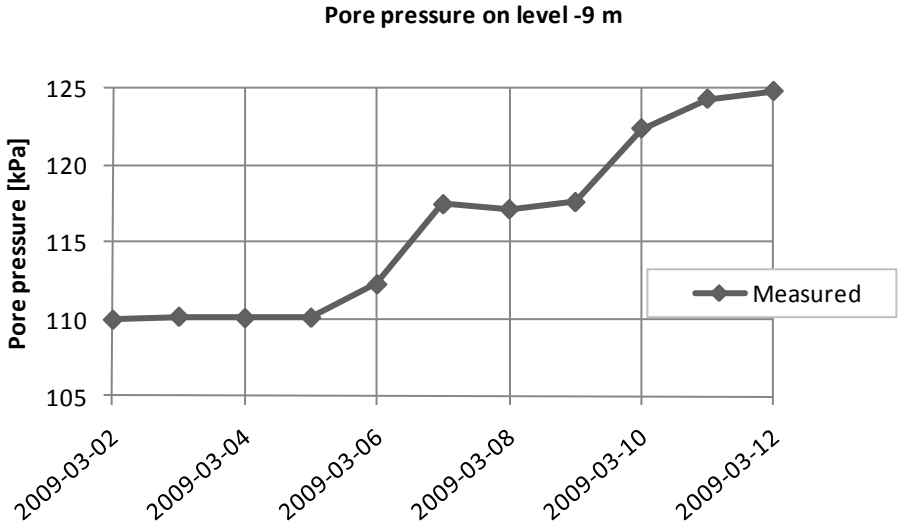

Figure 26 *Measured pore pressure on level -9 m.*

It can be seen in *Figure 25* that the pore pressure on level -4 m is increased at the three dates where the lime-cement columns are installed. At each installation phase the pore pressure raises with approximately 2.5 kPa during a two day period.

Figure 26 showing the pore pressure at level -9 m and it has a slightly different look than the one on level -4 m. The pore pressure is unchanged until 6th of March when the installation of the long columns starts. Since this piezometer is located around 6 m below the short columns the pore pressure will be unaffected when the short columns are installed. The increase of the pore pressure is highest when the long columns are installed which is expected since the long columns reaches approximately 12 m below the piezometer. In this phase the pore pressure increases with 8 kPa over a two day period. As a final step, the dynamic columns are installed around March 9th. In the

piezometer diagram for level -9 m it can be seen that the pore pressure increases even further with around 6 kPa over a two day period. One possible reason to why the increase is smaller is that the dynamic columns only go down 7 m below ground surface and will therefore affect the piezometer less than the long columns.

5 Calculations

This chapter presents the different calculation methods that have been used.

5.1 Plaxis

The program Plaxis has been used to simulate horizontal displacements and excess pore pressure that arises due to installation of lime-cement columns in Section A.

Information about the Plaxis program in this section is taken from the handbook of Plaxis version 9 (Brinkgreve & Broere 2008).

The simulations have been performed with an undrained analysis with effective and undrained parameters in order to obtain values of the excess pore pressure. For the derivation of the effective parameters see Appendix 5.

A plane strain model with 15-node elements was used for the simulations. The plane strain model is two-dimensional and has no strains or displacements in the z-direction, thus the model can be used for cross sections that are uniform and have the same loads and stress states perpendicular to the cross section. The boundary conditions is that there is full fixity at the base and horizontal fixity at the vertical sides. The model has to be long enough so that the boundary conditions do not affect the result, therefore the length of the model is set to 100 m. The mesh is coarse and has been refined around the columns, see *Figure 27*.

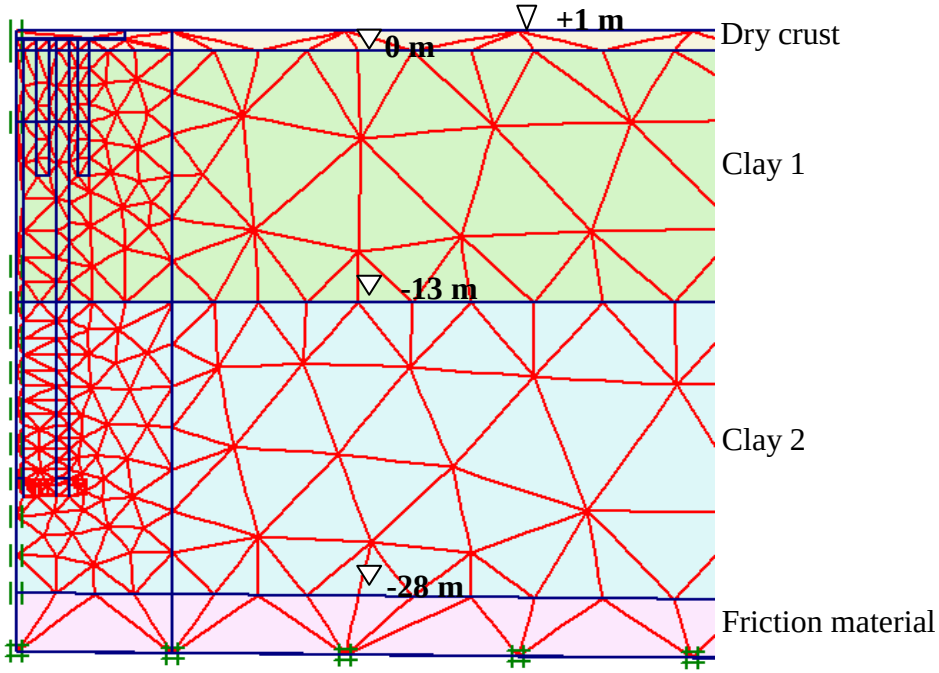

Figure 27 *Refined mesh around the lime-cement columns.*

Two different types of calculation have been performed; plastic calculation and consolidation analysis. Plastic calculation is an elastic-plastic deformation analysis

used for the installation of the columns and do not consider any time effects or any reduction of excess pore pressure. To simulate this reduction of pore pressure between the different installations a consolidation analyses are used. A consolidation analysis considers dissipation of excess pore pressure over time.

Volume strain and prescribed displacement have been applied in the model to simulate the installation of the lime-cement columns. Volume strain is used to simulate the volume expansion of the clay caused by the columns, while the prescribed displacement is set to zero over the columns to prevent soil heave right above the installation. The volume strains for the different columns are presented in *Table 1*. The volume strains are calculated based on a mixture density of 1 800 kg/m^3 and with an amount of mixture of 25 kg/m. For calculations of the applied volume strain in Section A, see Appendix 9.

Table 1 *Assumed volume strains for the different columns.*

	Volume strain [%]
Short columns	1.6
Long columns	1.2
Dynamic columns	4.6

5.1.1 Input parameters

The unit weight of the dry crust are chosen to 18 kN/m^3, for the clay 16 kN/m^3 and for the friction material the unit weight is set to 17 kN/m^3, see Appendix 2a. The pore pressure is assumed to be hydrostatic because the artesian pressure is considered not to affect the results.

The shear strength is assumed to be 9 kPa at level -1 m and increases with 0.75 kPa/m down to level -13 m and from that level increases with 1.22 kPa/m.

The values of the cohesion, *c'*, and angle of internal friction, ϕ', are chosen so that they will correspond to the assumed shear strength, see Appendix 4. To make sure that these input values result in a shear strength in Plaxis that corresponds to the assumed shear strength as evaluated from field measurements the values have been controlled with the soil test in Plaxis. These input values are controlled to make sure that they result in a shear strength in Plaxis that corresponds to the shear strength assumed from the field measurements, see Appendix 4a. This control is made through the performance of a soil test in Plaxis where the behavior of the different soil layers can be tested.

The assumed modulus is chosen to be approximately 3 times the mean value. From this assumed modulus, Young´s modulus is calculated and since the simulation in Plaxis requires effective parameters, Young´s effective modulus is also calculated, see Appendix 5.

In *Table 2* are the input parameters used for the simulations in Plaxis gathered.

Table 2 *Input parameters for simulations in Plaxis.*

	Dry crust	*Clay 1*	*Clay 2*	*Friction material*
Material type	Drained	Undrained	Undrained	Drained
γ *[kN/m^3]*	18	16	16	17
$k_x=k_y$ *[m/day]*	0,001	0,00005	0,00005	1
E' [kPa]	5 000	1 730	5 060	8 900
E'_{incr} *[kPa]*	0	256	256	256
v' [-]	0,35	0,35	0,35	0,35
c' [kPa]	5	6	2	0,2
ϕ' *[°]*	30	10	11,5	32
ψ *[°]*	0	0	0	0

5.1.2 Calculation phases

To be able to simulate the installation process and the effects of the lime-cement columns as accurate as possible, the simulation has been divided into several calculation phases, which are presented below in the order they are run in Plaxis.

Since the model contains non horizontal layers the ordinary K_0 *procedure* to create the initial stresses cannot be used. Instead the feature *Gravity loading* is used, which means that the multiplier for the soil weight is increased from 0 to 1. Since this procedure results in unrealistic displacements, it is important to select the option, *Reset displacement to zero*.

In the next phase the working bed is installed, which is simulated by just activating the cluster that represent the working bed. A *prescribed displacement*, put to zero, is placed right under the working bed to avoid vertical displacements above the columns.

In calculation phase three, the short columns are installed. Since it only takes a few minutes to create a lime-cement column, the short ones are modeled as a block where all columns are installed at the same time. This is a simplification made to avoid all small clusters that otherwise have to be drawn. Here the *prescribed displacement is* removed due to the unrealistic horizontal displacements that occur on an unexpected depth.

After the short columns have been installed, there is a pause in the installation process for three days. A consolidation analysis is performed for those three days.

The long singular columns are then installed one by one. Since it takes longer time to install these than the short ones it is more realistic to simulate the installation with one long column at time. In this step the *prescribed displacement* is activated.

It is assumed that there is a pause in the installation process for three days after the singular columns are installed and a second consolidation analysis is performed for those three days.

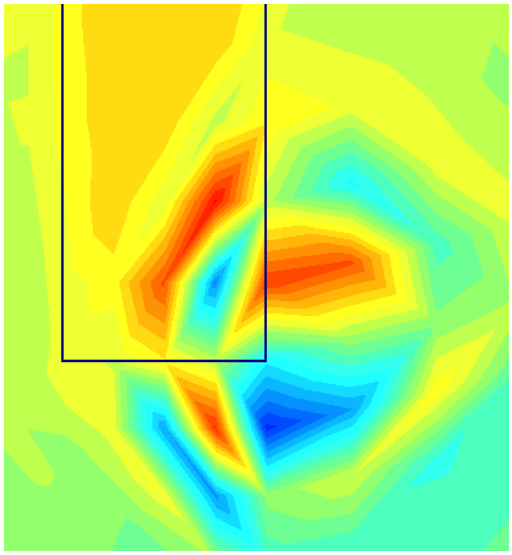

The dynamic columns are installed as plates one by one in Plaxis. Since there is no available information about installation date or pattern, the dynamic columns are assumed to be installed three days after the long columns and also in the same direction as the short and long columns.

The last phase is a consolidation analysis for two days which is made to reduce the unrealistic high excess pore pressure that appears around the toe of some columns, see *Figure 28*. Since this high excess pore pressure only appears in a very small area it can be neglected.

Figure 28 *Locally high excess pore pressure around column toe.*

5.2 Rehnman

Rehnmans piling theory is, as mentioned before, a simple analytical method to calculate vertical and horizontal displacements due to pile driving. Here this theory is applied on installation of lime-cement columns.

The heave can be calculated with Equation (18) where all input parameters and results can be found in Appendix 10.1 – 10.4.

$$x = \frac{\eta(V_{piles} - V_{pre-coring})}{d\left[(\alpha+\beta)\left(\frac{l}{2}+\frac{d}{3}\right)+(\gamma+\delta)\left(\frac{b}{2}+\frac{d}{3}\right)+\frac{b\cdot l}{d}\right]} \qquad (18)$$

Where;

α	[-]	Heave factor of building
β	[-]	Heave factor of building
δ	[-]	Heave factor of building
γ	[-]	Heave factor of building

η	[-]	Heave factor
b	[m]	Width of the area
d	[m]	Pile depth below ground surface
l	[m]	Length of area
V_{piles}	[m^3]	Volume of piles
$V_{pre-coring}$	[m^3]	Volume of piles

The heave factor η is related to how compressible the soil is. The factor can vary between 0.5 and 1.0. The factor is chosen to 0.75 for section E32, which is the most commonly used value. (Olsson & Holm 1993, p. 260) The factors α, β, δ and γ are used to include the effects of surrounding constructions like buildings, roads or existing piles to the heave calculation. The factors vary between 0 and 1, where 0 is for heavy building and 1 is for light building. The result from Equation (18) combined with *Figure 29* makes it possible to calculate the soil displacement in the horizontal direction.

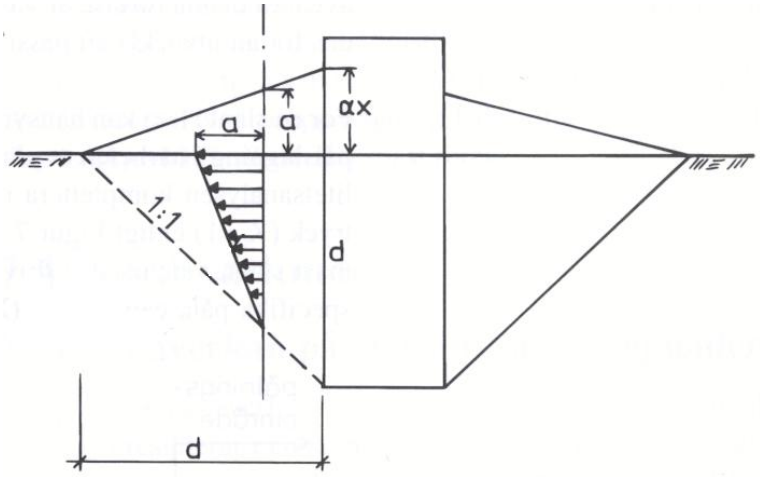

Figure 29 *Principle sketch from where the horizontal displacement can be calculated from the vertical displacement (Olsson & Holm 1993)*

At the ground surface the horizontal displacement is assumed to be the same as the heave. With the assumption that the affected area is within one pile length with an inclination of 45° from the pile toe, see *Figure 29*, the horizontal displacement through the soil profile can be calculated (Olsson & Holm 1993, p.261).

Equation (18) assumes a specific area where piling is performed and since the area where the columns are installed in Section E32 is very long, four calculations with different lengths are made. In the first calculation the length is assumed to be 1 m, see

Appendix 10.1. In the second calculation the length is assumed to be 10 m, see Appendix 10.2. In the third calculation the length is assumed to be 50 m, see Appendix 10.3. For these three calculations α, β, δ and γ are put to 1, i.e. the heave will be able to spread equally in all directions without any forces that reduces the heave. In the fourth calculation the length is assumed to be 50 m, see Appendix 10.4, and in this calculation δ and γ are put to 0. This is because the heave in the longitudinal direction is assumed to be reduced by the columns already installed.

5.3 The Sagaseta method

The calculations have been performed with help from Anders Kullingsjö.

To verify this method a lime-cement column is modelled as an expansion of a soil volume with a diameter of 600 mm. The radial distance, r, in Equation (1) see Section 2.1.3.2 is calculated from the edge of the column. With the assumption that the only expansion is due to the added mixture of lime and cement, about 25 kg/m column with a density of 2 500 kg/m^3, this expansion is put to 3.54 %. This assumption is only valid for saturated soil and neglects all affects from water and air used in the installation process. However, since the method is linearly related to the volume increase, the results can be scaled against any other expansion.

Since the monitoring took place 4 metres west of the centre of the most westerly lime-cement column this column was used as an origin of coordinates. The pattern of lime-cement columns is complex due to the dynamic effect and the aspects on stability and settlements. This gives that the columns have different length, which is the reason that every single column was modelled separately.

15 perpendicular plates (rows) are included in the model and the lime-cement columns installed in parallel plates includes 1 column each. Note that the intersection columns are modelled as short columns. 320 single columns are included in the model. The closest column not included in the model has a normalized distance, i.e. distance divided by column length, of 2.8.

5.4 Analytic model for excess pore pressure

As mentioned in section 2.1.4 the clay around a column installation is affected by a shearing force T_Q and an injection pressure P_j where the maximum value of the shearing force is equal to the undrained shear strength of the clay (Shen et al. 2003). This analytical model considers the excess pore pressure that are created around a lime-cement column during installation caused by the shearing force and the injection pressure.

The model is based on a shearing-expanding process of a cylindrical cavity. Henkel´s pore pressure parameter is also considered in this method and it can be calculated from Skempton´s pressure parameter A_f, see Equation (19-21). For information about the values of the parameters that are used in the calculations, see Appendix 11.

$$p'_0 = \frac{\sigma'_1 + \sigma'_2 + \sigma'_3}{3} \quad (19)$$

$$A_f = \frac{c_u}{p'_0} + \frac{1 - \sin\phi'}{2 \cdot \sin\phi'} \quad (20)$$

$$\alpha_f = 0.707(3 \cdot A_f - 1) \quad (21)$$

Where α_f is Henkel´s pore pressure parameter at failure.

The injection pressure of the slurry is usually somewhere around 2 to 4 times the in situ shear strength. The excess pore pressure can for saturated soils ($\beta = 1$) in the plastic zone be calculated with Equation (22).

$$\Delta u = \frac{\Delta p'_c \cdot c_u}{c_u} - 2\ln\left(\frac{r}{R_c}\right) - \ln\left(\frac{1 + B_{rl}}{1 + B_{rt}}\right) - B_{rt} + 0.816 \cdot \alpha_f \quad (22)$$

Where;

$$B_{rl} = \sqrt{\left(1 - \left(\frac{T_Q}{c_u}\right)^2 \cdot \left(\frac{R_c}{r}\right)^4\right)} \quad (23)$$

$$B_{rt} = \sqrt{\left(1 - \left(\frac{T_Q}{c_u}\right)^2\right)} \quad (24)$$

The calculations can be made for both a plastic and elastic zone, but since the highest excess pore pressures will occur in the plastic zone near the column this report only consider the plastic zone. The excess pore pressure is very much affected by the injection pressure that is used where a higher injection pressure gives higher excess pore pressure. The variation of the shearing force T_Q will also affect the excess pore pressure, but in this report $T_Q = c_u$ is only considered.

6 Results

In this chapter the results from the different calculation methods are presented.

6.1 Plaxis

Results from Plaxis compared with measured results regarding horizontal displacements and pore pressure changes in Section A are presented below.

6.1.1 Horizontal displacements and pore pressure changes

The three installation phases are modeled one by one in Plaxis to be able to see how the different types of columns affect the horizontal displacements and the pore pressure. In the diagrams regarding horizontal displacements the measured displacements at the inclinometer is compared with the displacements calculated in Plaxis. In the diagrams regarding pore pressure the measured pore pressure on level -4 m respectively -9 m are compared with results from Plaxis.

The horizontal displacements caused by the short columns can be seen in *Figure 30*

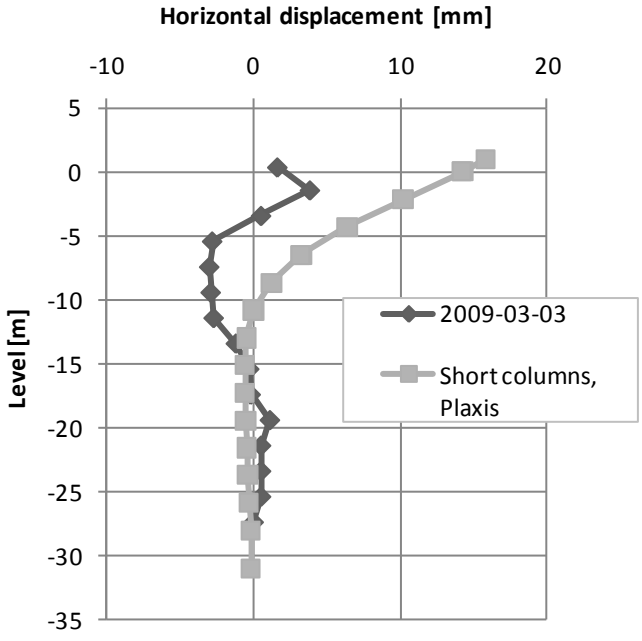

Figure 30 Horizontal displacements after installation of short columns.

It can be seen that the measured displacements are smaller than the displacements in Plaxis down to level -15 m. Below that level there are almost no measured displacements and no displacements at all in Plaxis.

The horizontal displacements caused by the short and the long columns can be seen in *Figure 31*.

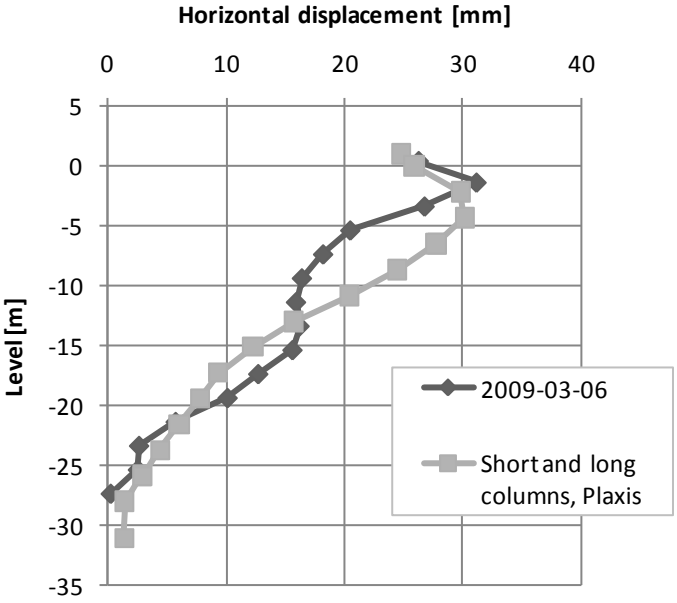

Figure 31 *Horizontal displacements after installation of short and long columns.*

The result complies better with each other in this phase than after the installation of the short columns. Between level -4 m and -12 m the results differ with a maximum value of 10 mm.

The horizontal displacements caused by all columns can be seen in *Figure 32*.

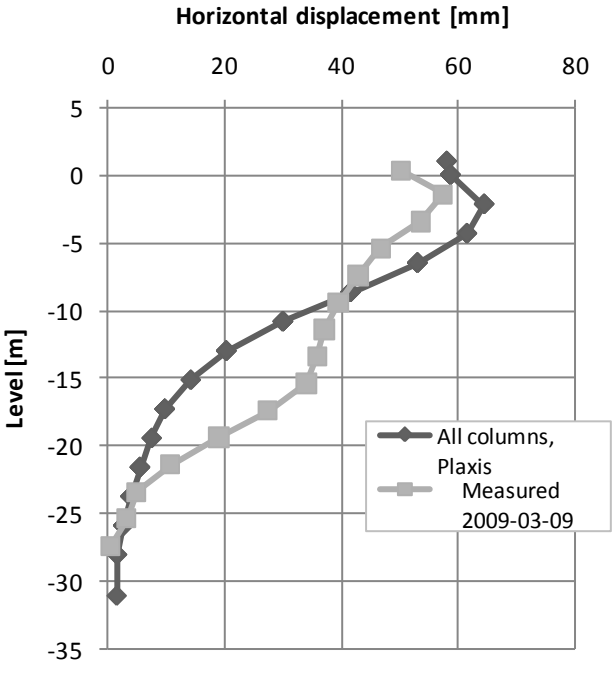

Figure 32 *Horizontal displacements after installation of all columns.*

It can be seen in the diagram that down to approximately level -10 m the measured horizontal displacements are smaller than the calculated. Below this level the measured displacements are larger than the calculated ones and the difference is as a maximum 20 mm.

The measured and the calculated pore pressures at level -4 m can be seen in *Figure 33*.

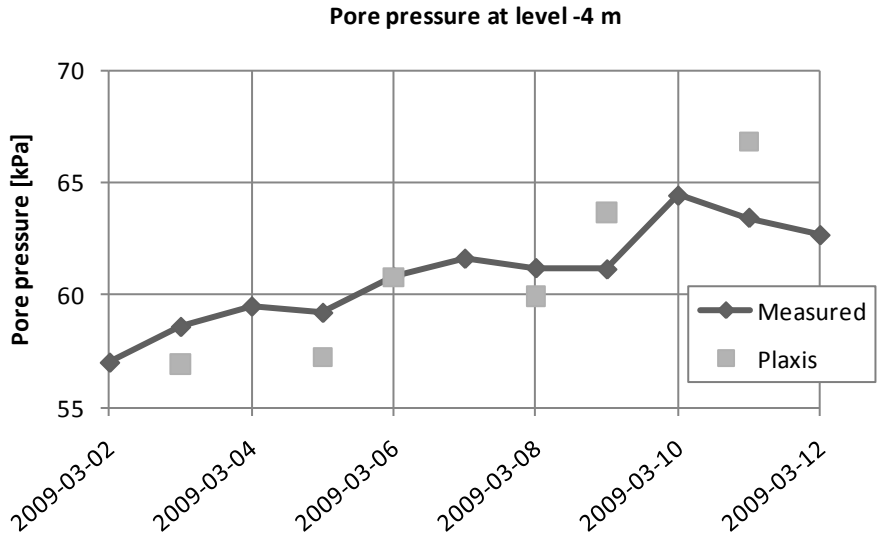

Figure 33 Pore pressure at level -4 m. Installation dates are 3rd, 6th and 9th of March.

It can be seen that the measured pore pressure and the pore pressure calculated in Plaxis complies well with each other. The difference in pore pressure varies depending on at which date the values are compared, but in general the pore pressure differ with 1-3 kPa.

The measured and the calculated pore pressures on level -9 m can be seen in *Figure 34.*

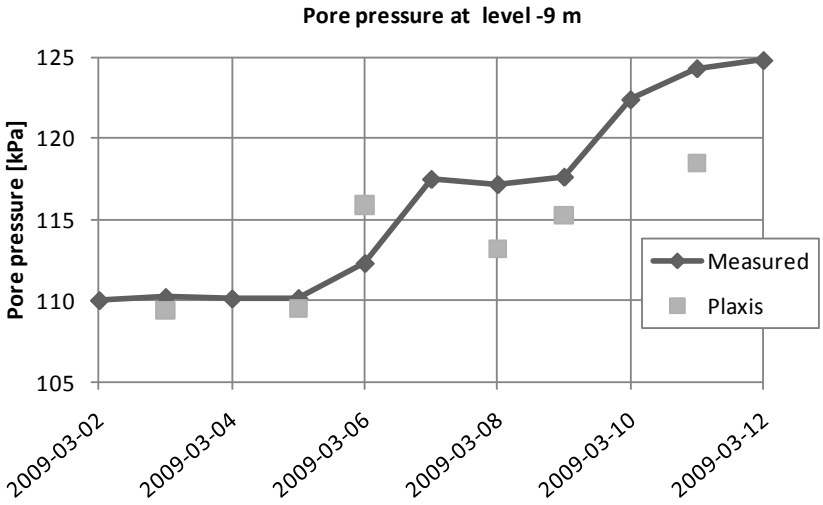

Figure 34 *Pore pressure at level -9 m. Installation dates are 3rd, 6th and 9th of March.*

It can be seen that the calculated values from Plaxis follows the measured values well. It is only after the last column installation the values differ a bit more, approximately 6 kPa. The excess pore pressure in the whole soil profile can be seen in *Figure 35*.

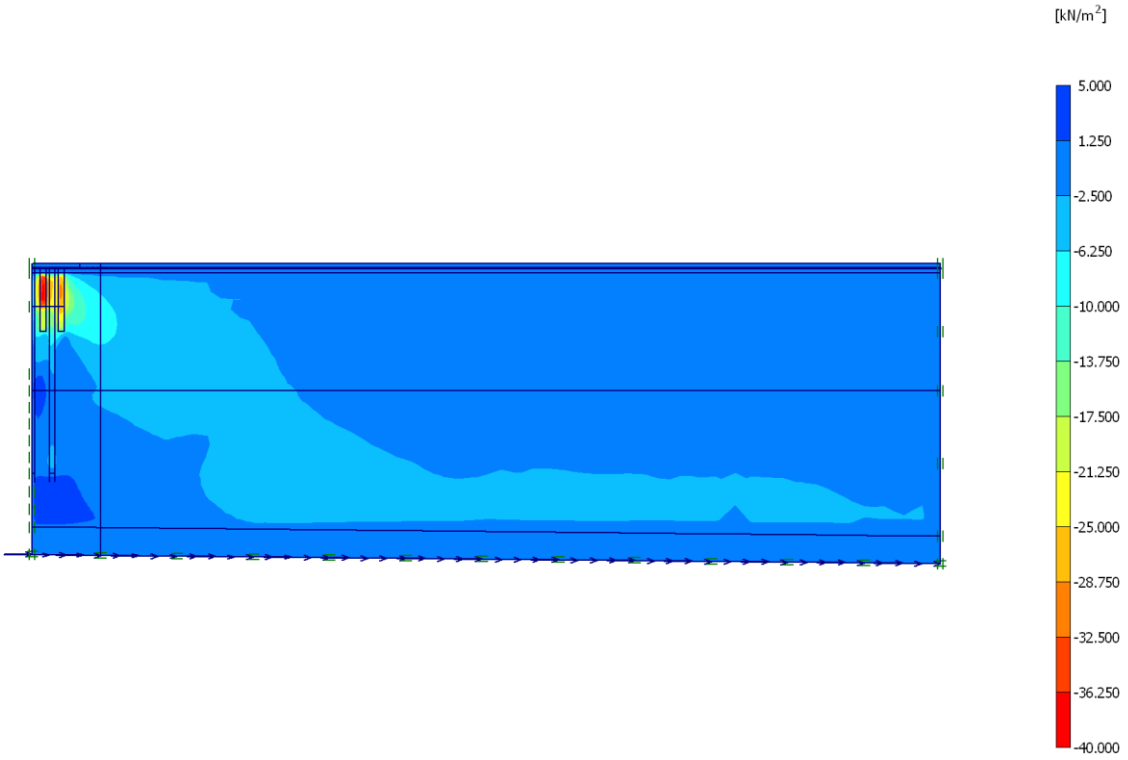

Figure 35 *Soil profile with excess pore pressure after all columns are installed and after two days of consolidation. Negative values represent pressure.*

New information about the columns in the intersection of the perpendicular and parallel plates came up in a late stage in the project, see *Figure 36*. According to this

new information these columns are installed to level -15 m. Therefore a new simulation in Plaxis has been performed and the results for the horizontal displacements are presented in *Figure 37*.

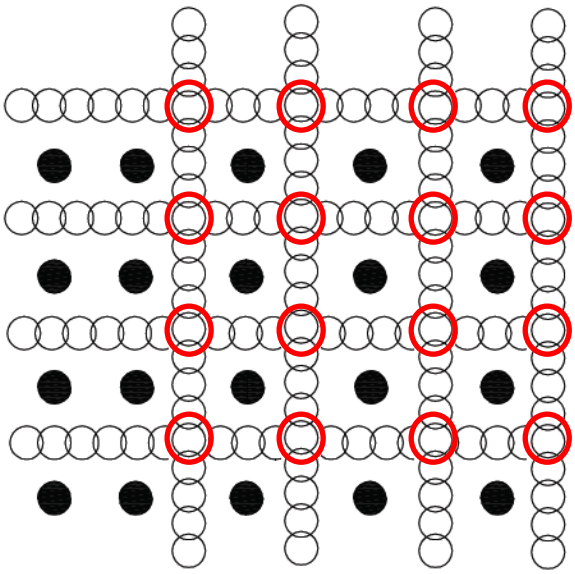

Figure 36 *Location of corner columns.*

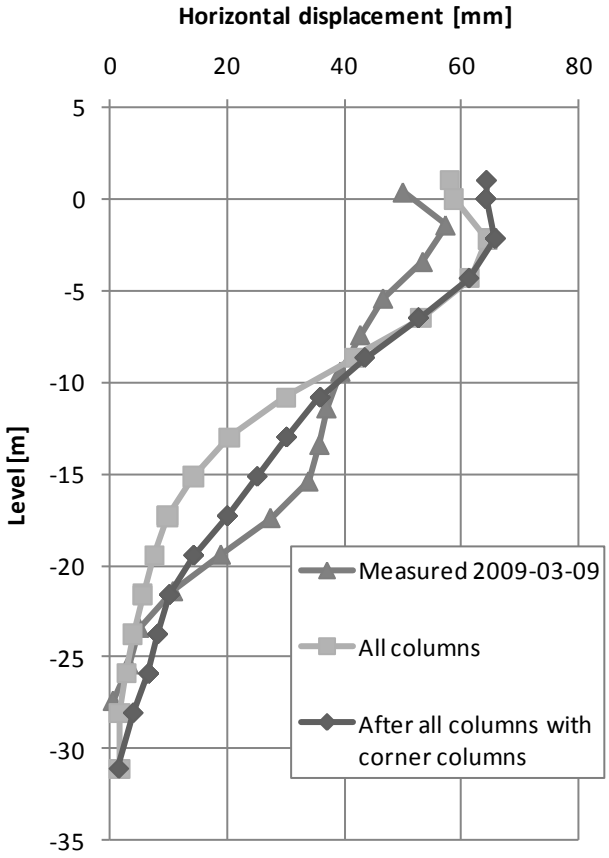

Figure 37 *Horizontal displacements with corner columns.*

As can be seen in the figure this new simulation give larger displacements from level -10 m than the previous simulation, while above this level the displacements are almost the same for the two simulations. The new simulation has better accordance with the measured displacements, but has still smaller displacements around level -15 m.

The change of the corner columns length gives almost no change in the pore pressure compared to the previous simulation, less than 1 kPa, and is therefore not presented.

6.1.2 Parameter analysis

A sensitivity analysis has been made in Plaxis where different parameters have been changed in order to see what influence they have on the horizontal displacement and the pore pressure changes. The analysis that are made are decrease and increase of; effective Young's modulus, volume strain, Poisson ratio, shear strength in the clay layers and one analysis where the cohesion is set to the undrained shear strength and the friction angle is equal to zero. The input values of the changed parameter for the different analyses are presented in Appendix 12. The results from the analysis with Young's modulus and the volume strain are presented here because they have the biggest influence on the results. The results from the other analyses made can be seen in Appendix 13.

In the case where undrained parameters for the shear strength are used, i.e. $c' = c_u$ and $\phi' = 0$, there is no significant difference between using undrained or effective parameters. This is expected since it is only two different ways of describing the shear strength.

The value of the increase of Young's modulus is calculated from the initial shear modulus, see Appendix 12 and the value of the decrease of Young's modulus is 200 kPa lower than the assumed Young's modulus for the clay layers and the friction material, a larger decrease gave unrealistic results in Plaxis. The horizontal displacement for the analyses compared to the measured displacement can be seen in *Figure 38*.

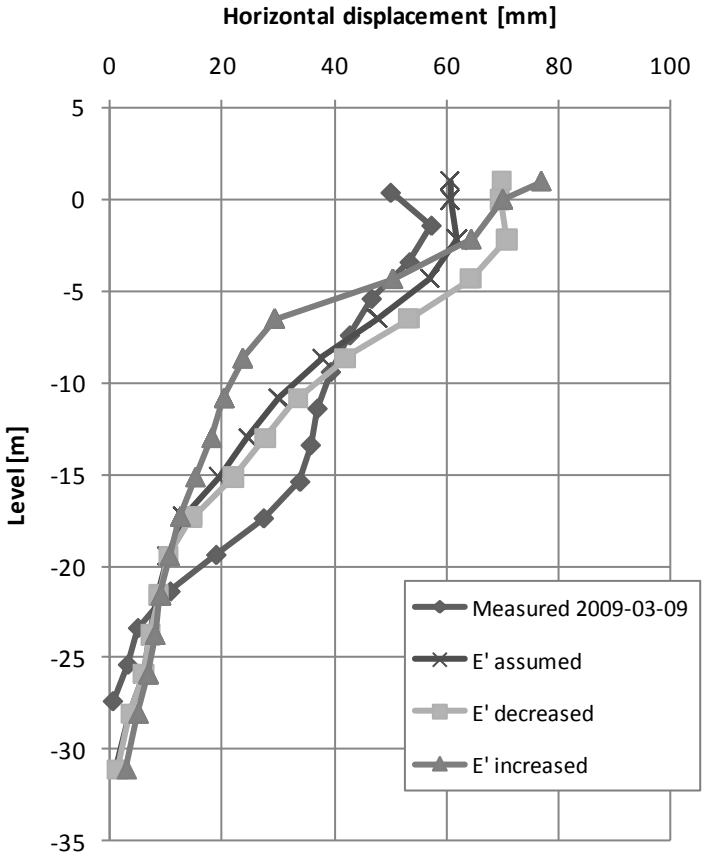

Figure 38 Horizontal displacements after installation of all columns.

As can be seen in the figure the three simulations made in Plaxis show approximately the same horizontal displacement from the level -22 m, which is where the long columns ends. The decrease of Young's modulus give higher displacement than the assumed but the difference is not so big due to that the decrease is small. An increase of Young's modulus give smaller displacements which can be expected, but the increase of Young's modulus also gives higher displacement in the top which probably is due to that Young's modulus of the dry crust is the same in the three Plaxis simulations. The behavior of the decreased and increased Young's modulus differ from each other because the decrease is constant, 200 kPa, while the increase varies with depth, see Appendix 12.

The pore pressure at level -4 m and -9 m for the analyses are presented in *Figure 39* and *Figure 40* respectively. The pore pressures for the assumed and decreased Young's modulus are quite even due to that the difference between Young's moduli are small. In *Figure 41* are the excess pore pressure for the whole soil profile shown.

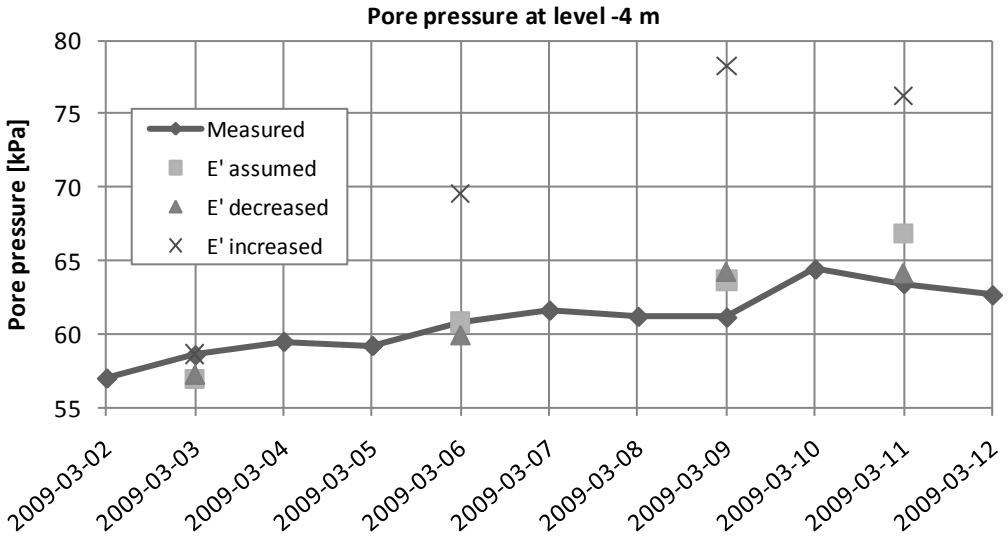

Figure 39 *Pore pressure at level -4 m. Installation dates are 3rd, 6th and 9th of March.*

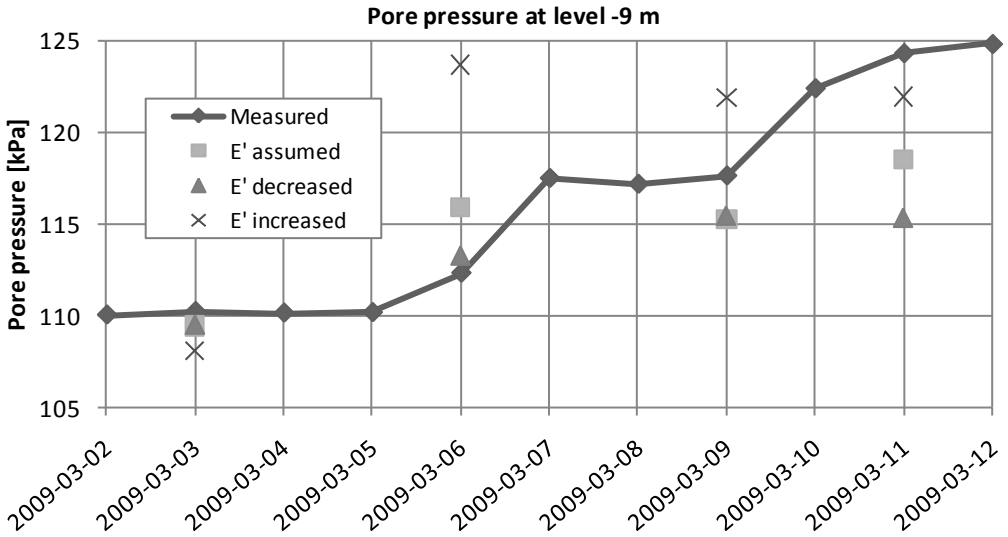

Figure 40 *Pore pressure at level -9 m. Installation dates are 3rd, 6th and 9th of March.*

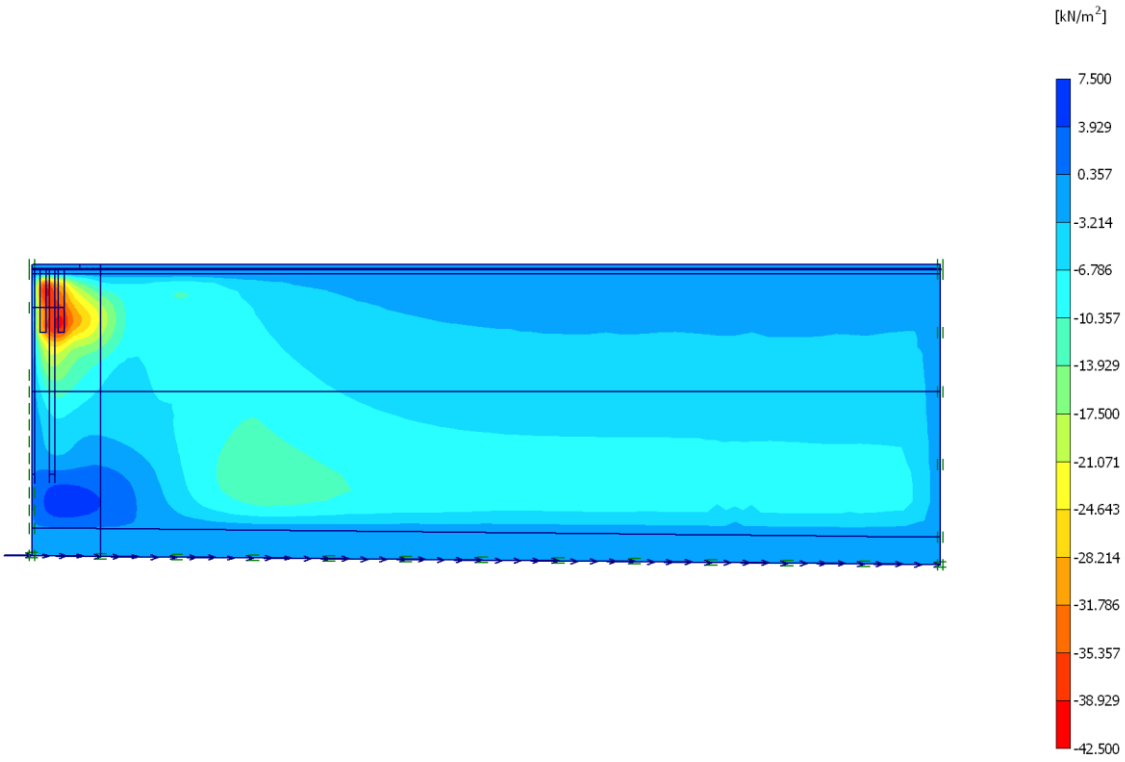

Figure 41 *Soil profile with excess pore pressure for increased Young's modulus after all columns are installed and after two days of consolidation. Negative values represent pressure.*

The increase of Young's modulus gives the highest values of the pore pressure, which was not expected because higher Young's modulus should give lower pore pressures due to that the soil is stiffer.

The decreased and increased volume strains have been calculated from different densities of the lime-cement mixture, see Appendix 12. A decreased or increased volume strain has, as can be seen in *Figure 42*, a big impact on the horizontal displacements.

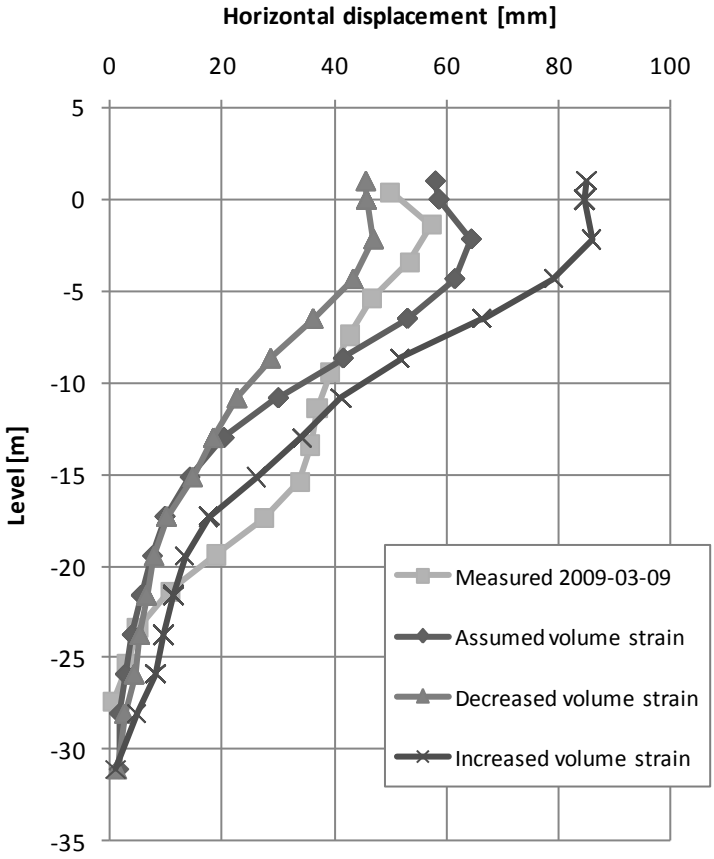

Figure 42 *Horizontal displacement after installation of all columns.*

Figure 43 and *Figure 44* show the pore pressures at level -4 m and -9 m respectively. The decreased volume strain give as expected somewhat lower pore pressure than the assumed volume strain and the increased volume strain give also lower pore pressures than for the assumed volume strain but the variation in pore pressures are small, the difference are about 3 kPa at largest.

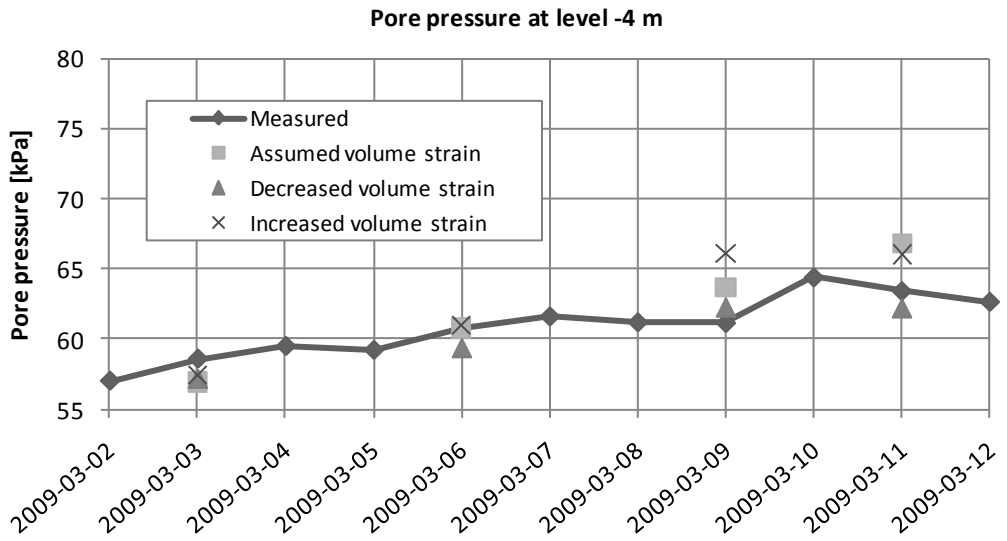

Figure 43 *Pore pressure at level -4 m. Installation dates are 3rd, 6th and 9th of March.*

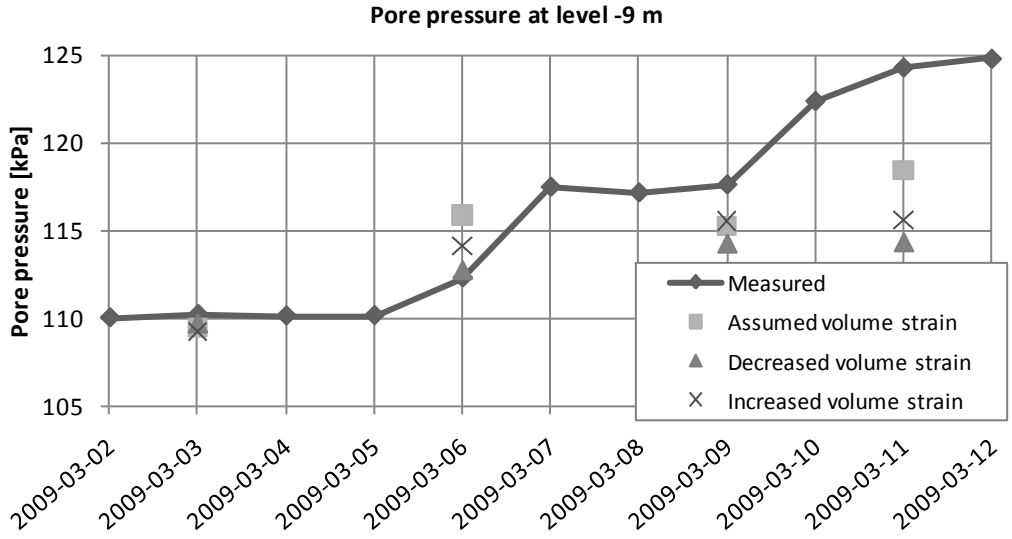

Figure 44 *Pore pressure at level -9 m. Installation dates are 3rd, 6th and 9th of March.*

6.1.3 Discussion

It can be noticed that the measured horizontal displacements in Section A differ from the horizontal displacements calculated in Plaxis. The simulations in Plaxis capture the behavior of the soil displacement quite well. The simulations that involved corner columns give even better accordance with the measured displacements, although the displacements are smaller than the measured values below level -10 m. The reason for this could be that the inclinometer is located 4 m right in front of the perpendicular plate, where the corner columns are located. Therefore it could be more realistic to use a higher volume strain in the corner columns.

Plaxis simulates the installation of the columns as a volume strain, which means that the soil volume will expand, but in reality there are more things that affect the displacements. Some of the things that are hard to predict is the injection pressure, shearing force and compaction of the soil, where the injection pressure is the factor that has the biggest impact on the installation effects. It is hard to determine a volume strain which account for all these things. The pore pressure calculated in Plaxis do not change the way it is expected to do when the volume strain is increased, see *Figure 43* and *Figure 44*. The pore pressure was expected to be higher when the volume strain was increased but that did not happen.

After the first installation phase the measured displacements are negative in some places and it can be seen that there has also been negative movements during a period before the first installation phase. This might be because the inclinometer is located between the installation area and a service road. The service road is used by heavy vehicles which can cause ground movements in the east direction, towards the inclinometer. The displacements from the installation of the lime-cement columns are measured as positive in the west direction, which is why the possible displacements from the service road will give negative results at the inclinometer. The measured displacements should in reality be larger if there were no negative soil movements. In *Figure 45* the negative displacements have been accounted for.

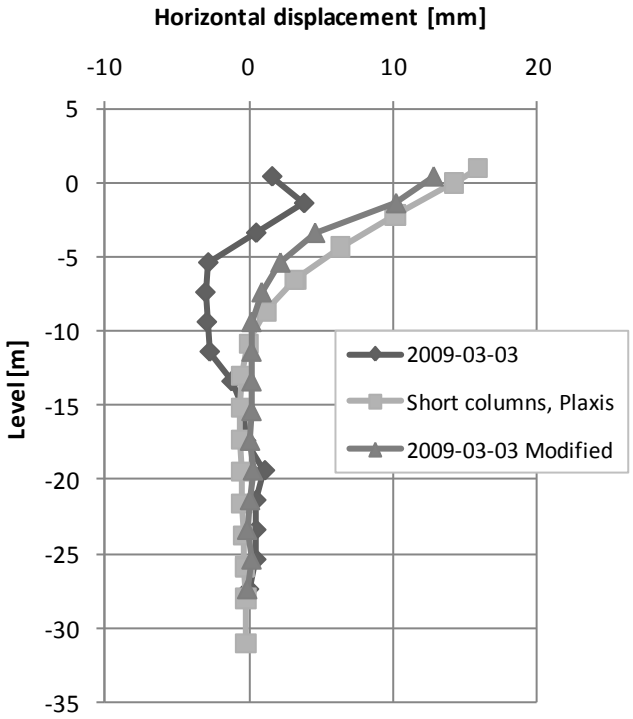

Figure 45 Modified soil displacement after short columns.

It can be seen in the figure that the modified displacements complies well with the simulations from Plaxis.

In Plaxis the dynamic columns are installed in the final phase, three days after the installation of the long columns. Since there is no available data of the dates when the dynamic columns are installed it is an assumption, based on pore pressure changes and inclinometer data, that they are installed three days after the long ones. In some of the graphs, both regarding pore pressure and horizontal displacements, the values from Plaxis and the measured values differ more after or around 9th of March than in the rest of the graph. The pore pressure changes that are observed around 9th of March might have another explanation and not necessarily caused by the assumed installation of the dynamic columns.

The horizontal displacements in Plaxis are presented as vectors, while the measured displacements are resultants of the displacements in the horizontal plane. Since the resultant will be larger than the vector, the measured displacements should be slightly higher than the displacements calculated in Plaxis. The different ways of presenting the horizontal displacements have almost no effect on the results, but it is worth to be noticed.

The pore pressure in Section A has a small artesian pressure in the lower aquifer. This artesian pressure has very little impact on the pore pressure results and is therefore assumed to be hydrostatic in Plaxis.

6.2 Rehnman

In *Figure 46* below the results from Rehnmans method are plotted against the measured horizontal displacements after installation of all columns. It can be seen that the results not comply very well. Rehnmans method gives less displacements and do not give any displacements below level -18 m.

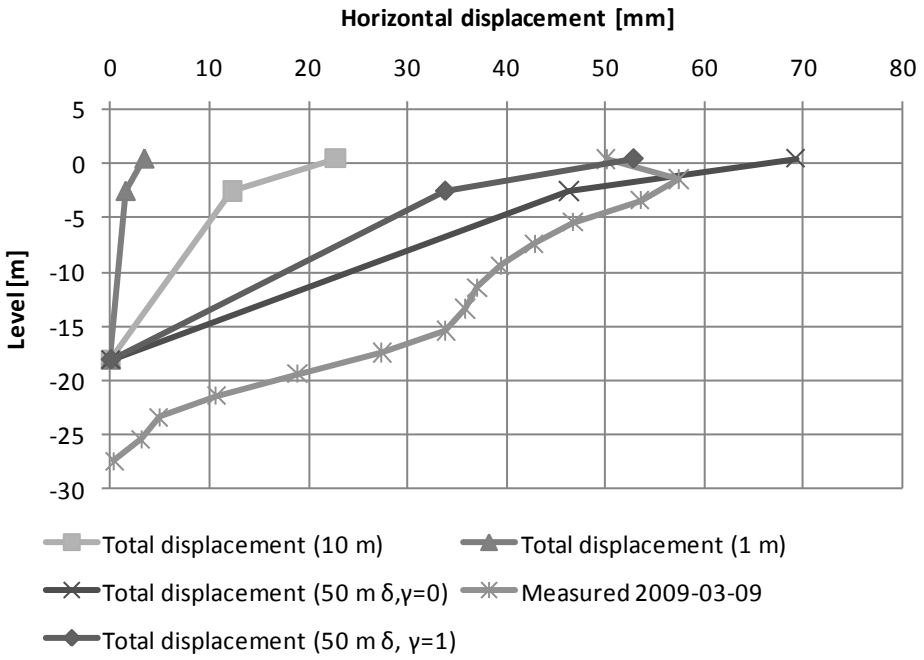

Figure 46 Comparison between Rehnmans method and measured displacements.

6.2.1 Discussion

In *Figure 46* it can be seen that the graph representing the calculation for 50 m length and δ, γ are equal to 0 comply best with the measured displacements. Here the displacements are not allowed in the longitudinal direction which seems reasonable since other columns may have been installed that will prevent horizontal displacements in this direction.

The assumption made in Rehnman that the displacements start from the pile toe does not comply with the measured results. The other assumption made in Rehnman about the influence area being one pile length does not reflect the real behavior either. The real displacements are of larger magnitude and starts at a greater depth. In Appendix 10.1 – 10.4 it can be seen that the short columns does not contribute to any displacements at the inclinometer. This is because the distance to the inclinometer is equal to the length of the short columns. It can be seen in *Figure 45* that the short columns give displacements, which show that the assumption about the influence area in Rehnmans is not true in this case with lime-cement columns.

As can be seen in *Figure 46* the measured displacements start much deeper than the toe of the column. One possibility is to increase the influence area to more than one

pile length. This will make the displacements calculated in Rehnman´s method to start deeper down and will therefore probably give better accordance with the measured values.

6.3 The Sagaseta method

Only the horizontal displacements at the ground surface are calculated in this method. The inclinometer is located at (4,0), where the x-axis is perpendicular to the dynamic columns and the y-axis is parallel to the dynamic columns. It is apparent in all the diagrams below that the columns closest to the inclinometer are the ones that have biggest impact on the horizontal displacements. In *Figure 47* the horizontal displacements, at the inclinometer, induced by the short columns are presented. The short columns are as previously mentioned installed as perpendicular plates so in the diagram the displacements caused by each plate is shown. The maximum horizontal displacement at the inclinometer is caused by row 1 and is around 0.7 mm.

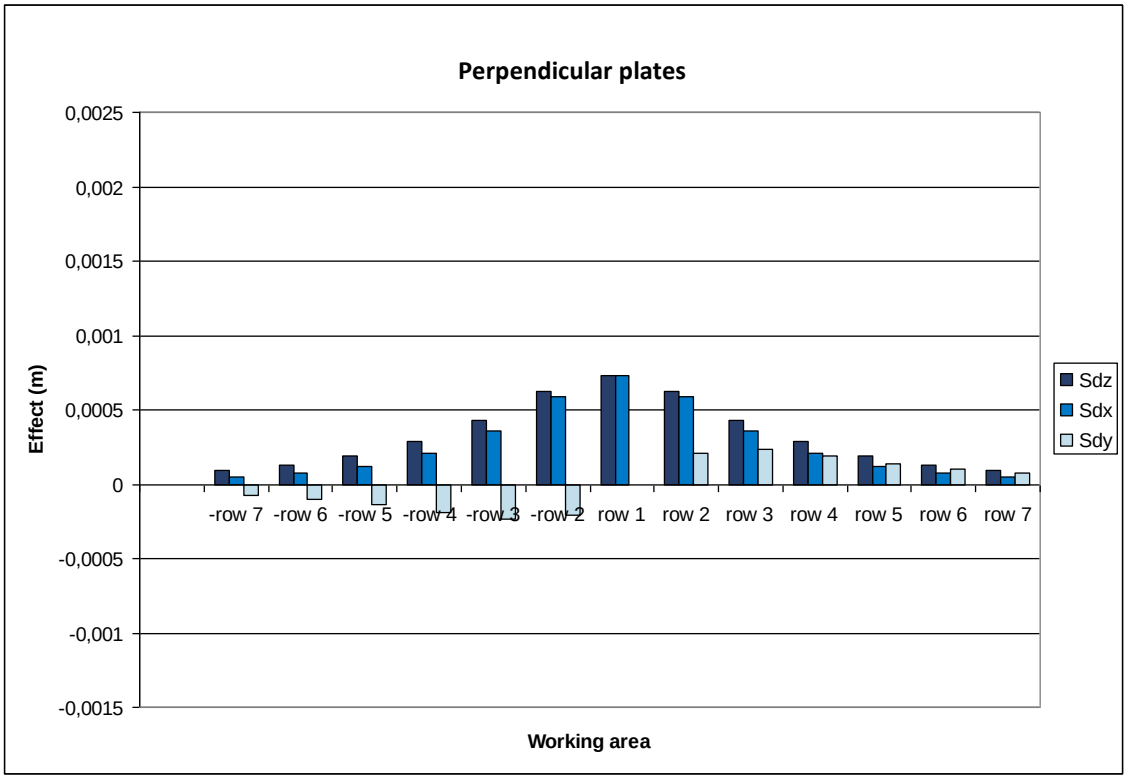

Figure 47 *Horizontal displacements (x-direction) at the inclinometer caused by each perpendicular plate (short columns).*

The singular columns in *Figure 48* are modelled as four rows with five columns in each row, i.e. 20 columns are installed at the same time. It can be seen in the figure that the maximum horizontal displacement caused by the singular columns are about 2.3 mm.

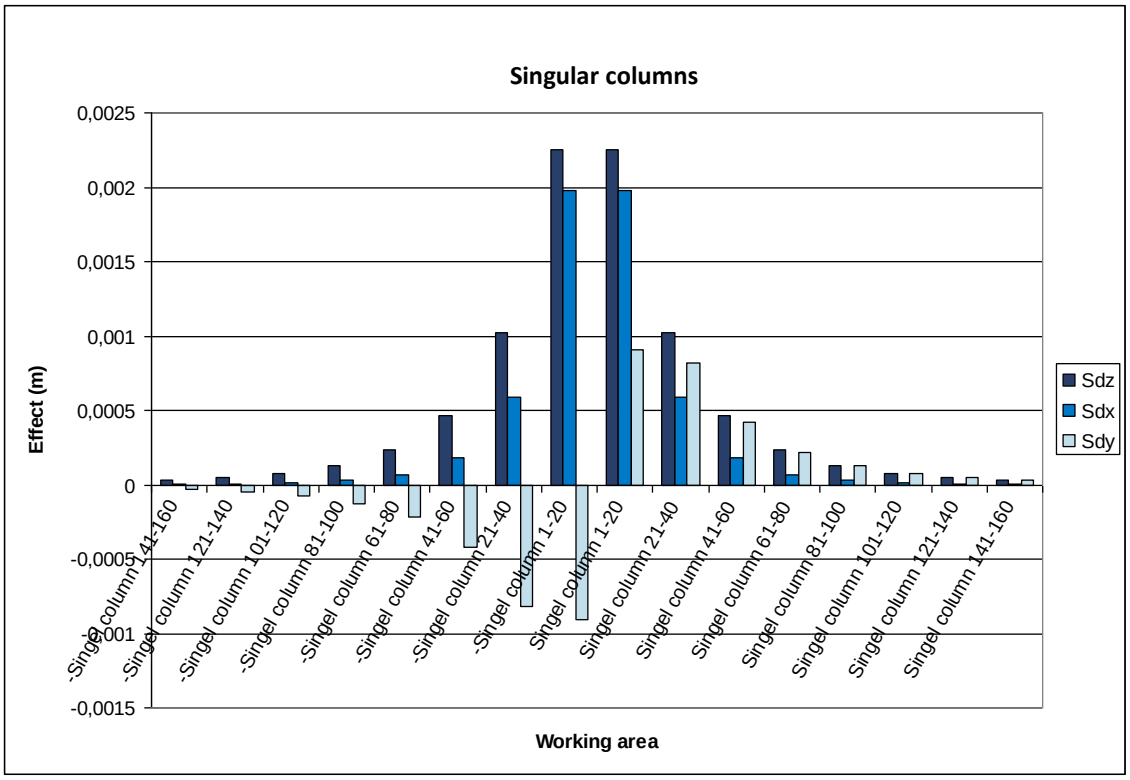

Figure 48 *Horizontal displacements (x-direction) at the inclinometer caused by the singular columns.*

In *Figure 49* column 1 represent the parallel plate closest to the inclinometer and column 4 is the parallel plate farthest from the inclinometer. As can be seen in the figure the maximum displacement is around 1.7 mm.

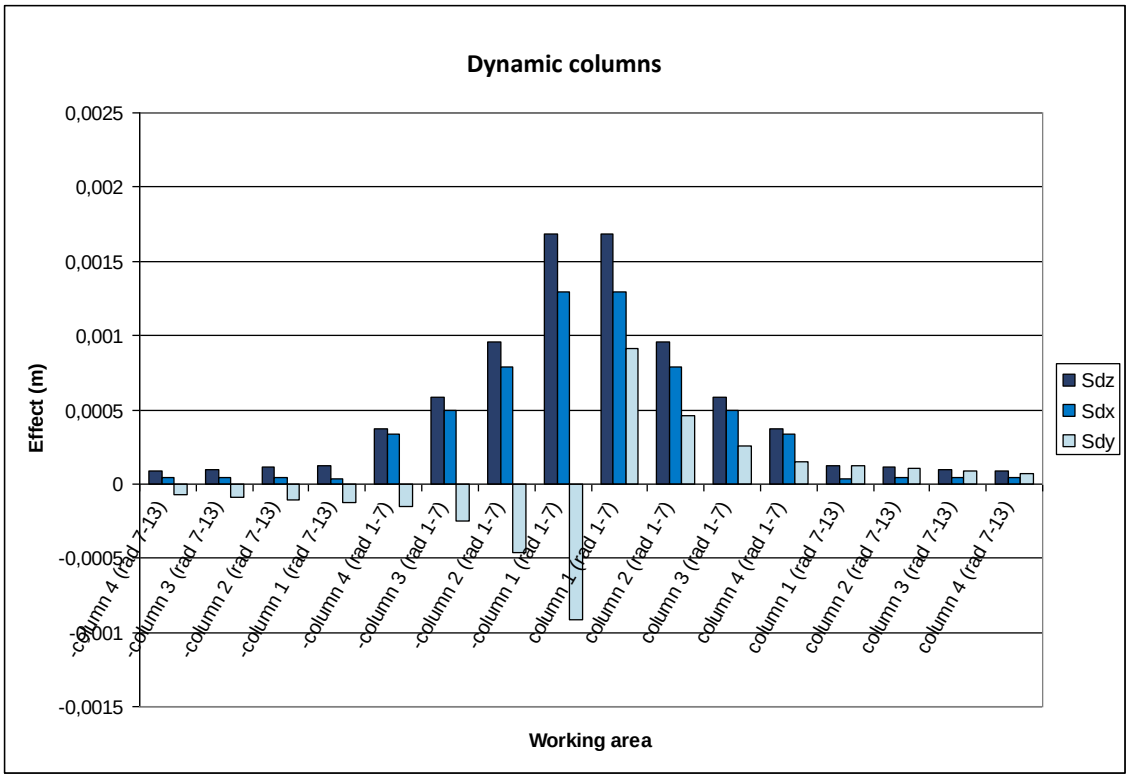

Figure 49 *Horizontal displacements (x-direction) at the inclinometer caused by the dynamic columns.*

The accumulated horizontal displacement for all column installations are presented in *Figure 50*, where the horizontal displacement towards the inclinometer is on the x-axis. The displacements on the y-axis in *Figure 50* are the displacements parallel to the railway, which not are of interest in this thesis. In the figure the letters A, C and E shows when the installation of the different columns pass by the inclinometer and the letters B and D shows when there is no installation. A is for the short colums, C is for the singular columns and E is for the dynamic columns. As can be seen in the figure the largest displacements occur when the installations passes the inclinometer. The total displacement at the ground surface is approximately 15 mm after all columns are installed.

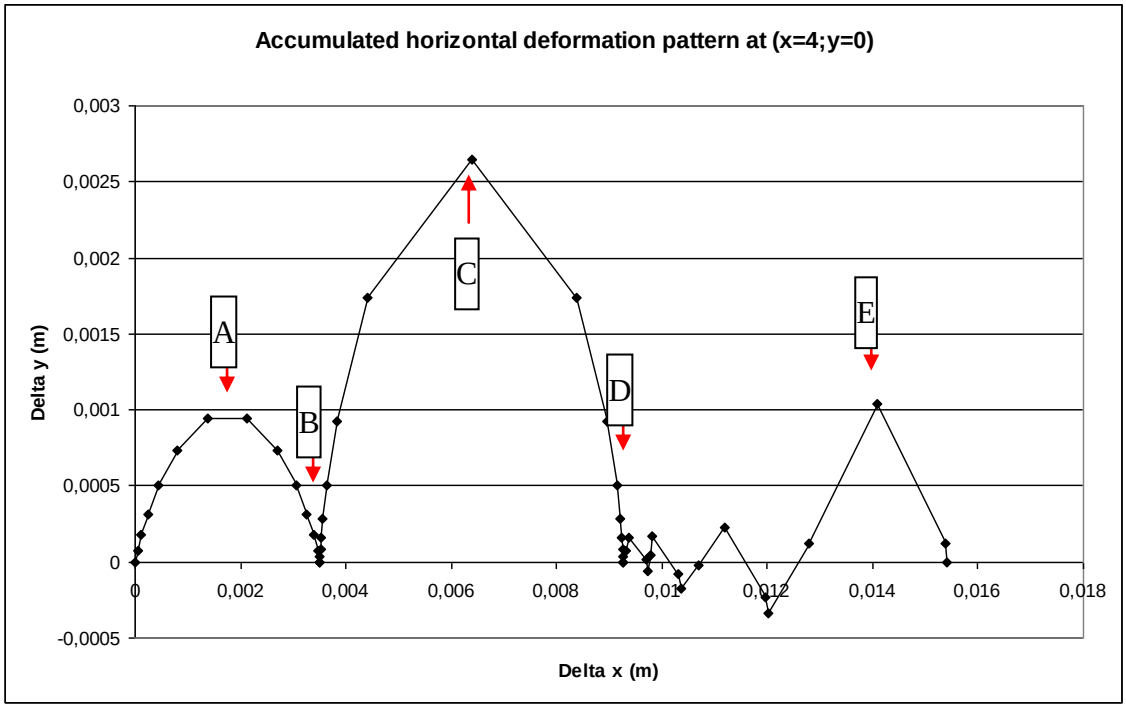

Figure 50 *Accumulated horizontal displacements (x-direction) at inclinometer.*

As mentioned in Section 5.3 the calculations are based on a volume expansion of 3.54 %, but the results are possible to scale up. So for a volume expansion of 4.9 %, for calculations see Appendix 9, calculated for a mixture density of 1 800 kg/m^3 the results will be 1.4 times larger. In *Table 3* are the horizontal displacements at the ground surface for the measured, calculated and the up-scaled displacements presented.

Table 3 *Comparison of horizontal displacements at ground surface.*

	Measured	*3.54 %*	*4.9 %*
Short columns	1 mm	3 mm	4.2 mm
Long columns	36.5 mm	9 mm	12.6 mm
Dynamic columns	52 mm	15 mm	21 mm

It can be seen in the table that the calculated and up-scaled displacement after the installation of the short columns are small and in the same range as the measured displacement. For the long and dynamic columns the measured displacement is much larger than both the calculated and up-scaled displacement. For more detailed results, see Appendix 14.

6.3.1 Discussion

Because the pattern of the lime-cement columns is symmetric the calculations are made in one direction and then reversed in the other direction the displacements become exactly the same at both sides of the inclinometer. This is not how it will work in reality because the soil will always move in the direction where the resistance is smallest.

Since this method only give the displacement at the ground surface the result can only be compared in one point with the measured displacement. The measured displacement at the ground surface can have been disturbed, for example by heavy vehicles. Therefore the comparison can be very misleading and as can be seen in *Table 3* the results differ much from the measured displacement.

6.4 Analytic model for excess pore pressure

Below is the excess pore pressure on 5 m and 10 m depth presented in a graph, see *Figure 51*.

The excess pore pressure is calculated for different injection pressure, 2-4 times the undrained shear strength, but with the same pore pressure parameter. Results from the analytical model are compared with results from Plaxis.

The graph is divided in two parts by a horizontal line where the line defines the border between the plastic and elastic zone. As can be seen in *Figure 51* the excess pore pressure in Plaxis on 10 m depth is in the elastic zone. That is probably because only the long columns affect the pore pressure on this level. On 5 m depth, all columns will have influence on the pore pressure and therefore will a higher excess pore pressure be created here.

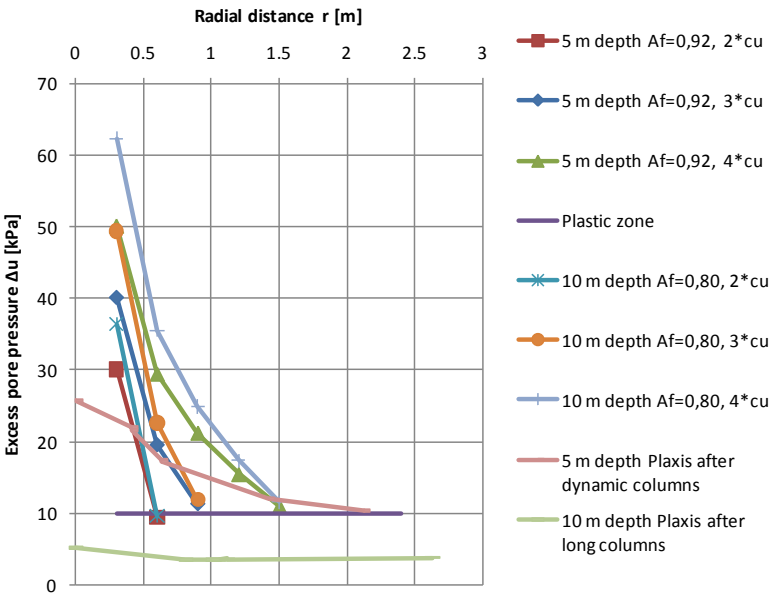

Figure 51 *Declining of pore pressure in radial direction from the column on 5 m and 10 m depth.*

6.4.1 Discussion

The results from the analytical model are based on the assumptions that the shearing force is equal to the undrained shear strength and that the injection pressure is 2-4 times larger than the in situ shear strength. The results in Plaxis are instead based on a volume expansion that will occur when a lime-cement column is installed. The volume expansion does not account for any injection pressure or any shearing force created from the mixing tool. It only takes the volume change into account.

The fact that these two ways of calculating the excess pore pressure is based on different assumptions makes it understandable to see why the results from the different calculation methods do not comply very well.

7 Conclusions

Of all calculation methods that have been used, Plaxis was the one that gave the best accordance with the measured values. The Rehnman method is a simple method that underestimates the area of influence which make the results comply bad with the measured displacements. The displacements from the Sagaseta method are hard to compare with the measured values because it only gives the displacement at the ground surface and it is a big risk that the measured values are disturbed. A possible source to disturbance can be heavy vehicles due to construction in the area. The analytical method to calculate excess pore pressure is also hard to compare in this case. This is because it calculates the excess pore pressure very close to the installation where no pore pressure measurements are made. It is likely that the excess pore pressure close to the column calculated with this method is more realistic than the ones calculated by Plaxis since the analytical method considers the injection pressure and the shearing force.

The parameters that have biggest impact on the results in Plaxis are the volume strain and Young´s modulus. Since the volume strain is strongly connected to the horizontal displacements it is important to choose volume strain with care. When Young´s modulus is increased the soil will be stiffer, which will reduce the horizontal displacements.

The overall conclusion is that the simulations made in Plaxis captures the behavior of the measured horizontal displacements relatively well.

8 Propose to further investigations

A service road is located west of the installation area, between the river and the inclinometer. This road embankment may have had a reducing effect on the horizontal displacements. In further investigations it could be interesting to include this service road in the simulations to see how it will affect the results.

In other sections where the bedrock surface has a steeper inclination towards the river the horizontal displacements in this direction could be affected. If the bedrock is blocking the soil movement in one direction it will force the soil to move in the opposite direction and thereby increase the horizontal displacements. Since the level of the bedrock varies within Section E32 it could be interesting to investigate another section with a steeper inclination of the bedrock.

Since it is a complex problem where several parameters affect the result it could be interesting to simulate the problem in 3-dimensions. Especially since the choice of volume strain has a big impact on the results.

In some places the railway is located very close to the river. If there is a slope near the river, it could be interesting to investigate which impact the horizontal displacements and pore pressure changes would have on the stability.

9 References

Aqualog. (2007): *PM - Provgropar vid Stora Viken utförda 071022*, Göteborg.

ASCE, American Society of Civil Engineers. Available at: http://www.asce.org/ conferences /deepfound2002/pdf/cptdata.pdf. [Accessed 11 March 2009]

Bergdahl, U. (1984): *Geotekniska undersökningar i fält.* Statens geotekniska institut, Information 2, Linköping, 72 pp.

Brinkgreve, R.B.J., & Broere, W. ed. (2008): *Plaxis 2D – version 9*.

Brookfield Viscosity Specialists. Avaliable at: http://www.viscometers.org/images/ accessories/Vane-spindles.jpg [Accessed 12 March 2010]

Carlsten, P. (1989): Lime and Lime/Cement Columns. In J. Harlén, W. Wolski eds. 1996. *Embankments on soft soils.* Amsterdam: Elsevier. Ch. 10.

Claesson, P. (2003): *Long term settlements in soft clays*. Ph.D. Thesis. Department of Geotechnical Engineering, Chalmers University of Technology, Göteborg 188 pp.

Craig, R.F. (1974): *Craig's soil mechanics.* 7th ed. E & FN Spon, London, 2004.

Edstam, T. et al. (2010): Partihallsbron – Ingen koloss på lerfötter. SGF. *Grundläggningsdagen 2010: Geoteknik att grunn(d)a på.* Stockholm, 11 March 2010.

Eniro. Available at: http://kartor.eniro.se/ [Accessed 28 April 2010]

Fredén, C. (1986): *Beskrivning till jordartskartan Göteborg NO.*Serie Ae nr 40. SGU, Uppsala.

Geotechnics (2009): *BOM 045 – Course Literature 2009, Research group Geotechnical Engineering.* Chalmers University of Technology, Göteborg, 2009.

Hedman, P. & Kuokkanen, M. (2003): *Hållfasthetsfördelning i kalkcementpelare – Fältförstök i Strängnäs.* Arbetsrapport 29. Svensk Djupstabilisering, Linköping, 2003.

Honkanen, J. & Olofsson, J. (2001): *Kalkcementpelare i skivor – Modell försök.* Arbetsrapport 19. Svensk Djupstabilisering, Linköping, 2001.

Johansson, B. & Jendeby, L. (1998): *Portrycksökningar till följd av pålslagning och dess betydelse för stabiliteten*. Rapport B 1998:4. Institutionen för geoteknik, Chalmers tekniska högskola, Göteborg.

Larsson, R. (1994): *Deformationsegenskaper i jord.* Rapport B 1994:6. Institutionen för geoteknik, Chalmers tekniska högskola, Göteborg.

Larsson, R. et al. (2007): *Skjuvhålllfasthet – utvärdering i kohesionsjord*. Andra utgåvan. Statens geotekniska institut och Geo, Chalmers tekniska högskola, Information 3, Linköping.

Larsson, R. (2008): Jords egenskaper. Statens geotekniska institut, Information 1, Linköping, 62 pp. Available at: http://www.swedgeo.se/upload/publikationer /Info/pdf/SGI-I1.pdf [Accessed 12 March 2010]

Olsson, C. & Holm, G. (1993): *Pålgrundläggning*. Svensk byggtjänst och Statens geotekniska institut, Solna.

Sagaseta, C., Whittle, A.J., Santagata, M. (1997): Deformation analysis of shallow penetration in clay. *International Journal for numerical and analytical methods in geomechanics*, 21, pp. 687-719.

School of Civil & Environmental Engineering. Available at: http://geosystems.ce gatech.edu/Faculty/Mayne/Research/devices/cpt.htm [Accessed 12 March 2010]

SGF (1996): *Geoteknisk fälthandbok – allmänna råd och metodbeskrivningar*. Svenska geotekniska föreningen, SGF Rapport 1:96, Linköping, 173 pp.

SGF (1999): *Kalk- och kalkcementpelare – Vägledning för projektering, utförande och kontroll.* Svenska Geotekniska Föreningen, SGF Rapport 4:95, Stockholm, 11 pp.

SGF (2005): Kalkcementpelare, Metodblad 1 [Online] (Updated October 2005) http://www.sgf.net/web/page.aspx?pageid=81751 [Accessed 6 February 2010]

SGU (1976): Jordartskartan Göteborg SO. *Serie Ae*, nr 26, 1:50 000, Stockholm: SGU.

SGU (1979): Jordartskartan 7B Göteborg NO. *Serie Ae*, nr 40, 1:50 000, Stockholm: SGU.

SGU (2007): *Lera – sediment på havs- och sjöbottnar.* [Online] (Updated May 2007) Available at: http://www.sgu.se/sgu/sv/geologi/jordtacket/under-istiden/lera.html [Accessed 9 April 2010]

Shen, S.-L., Miura, N. & Koga, H. (2003): Interaction mechanism between deep mixing column and surrounding clay during installation. *Canadian Geotechnical Journal*, 40 (2), pp. 293-307.

Sällfors, G., & Andréasson, L. i samarbete med SGF:s laboratoriekommitté (1986): *Kompressionsegenskaper – Geotekniska* laboratorieanvisningar, del 10. Statens råd för byggnadsforskning, Byggforskningsrådets informationsblad T2:1985, Stockholm.

Sällfors, G. (1993a): *Handledning till laborationer i Geoteknik – Fältundersökningar*. Chalmers tekniska högskola, Göteborg, 29 pp.

Sällfors, G. (1993b): *Handledning till laborationer i Geoteknik – Laboratorie-undersökningar*. Chalmers tekniska högskola, Göteborg, 41 pp.

Sällfors, G. (2001): *Geoteknik, Jordmateriallära – Jordmekanik.* 3:e upplagan. Chalmers tekniska högskola, Göteborg, 2003.

Appendix

Appendix 1.

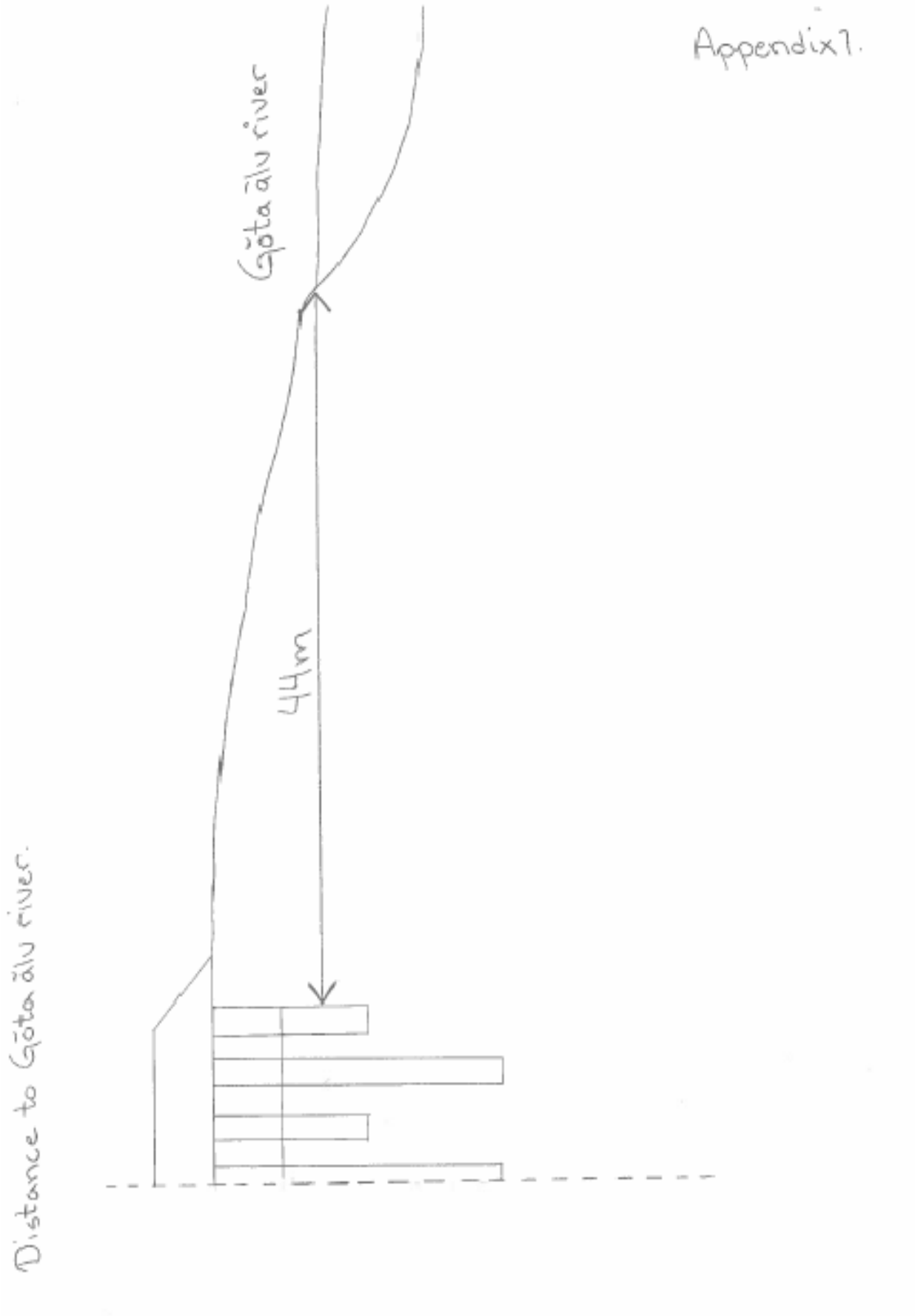

The boreholes are located within a radius of 100 m from Section A.

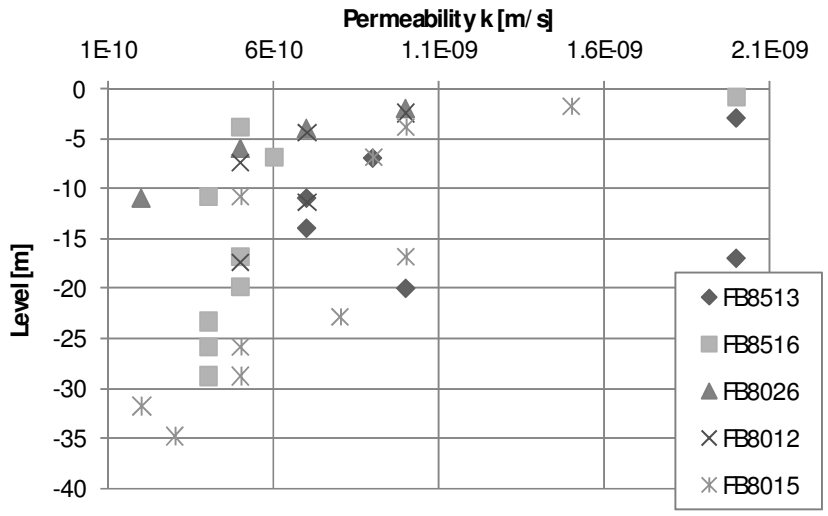

(a)

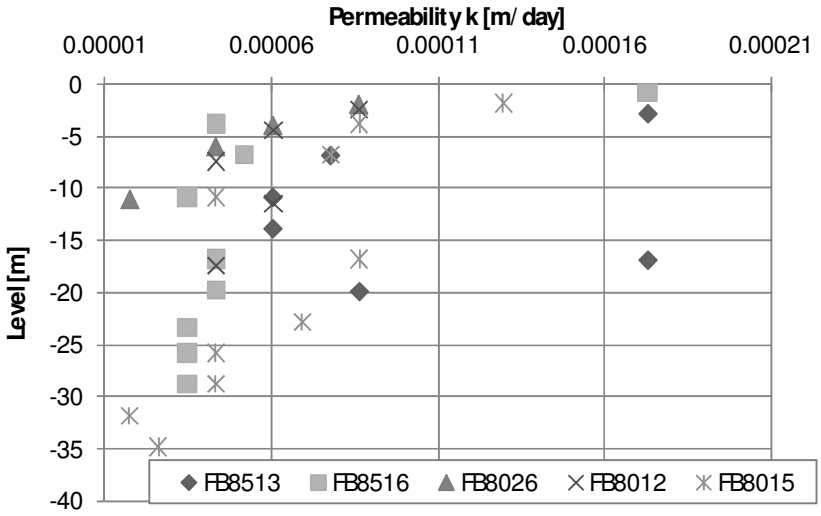

(b)

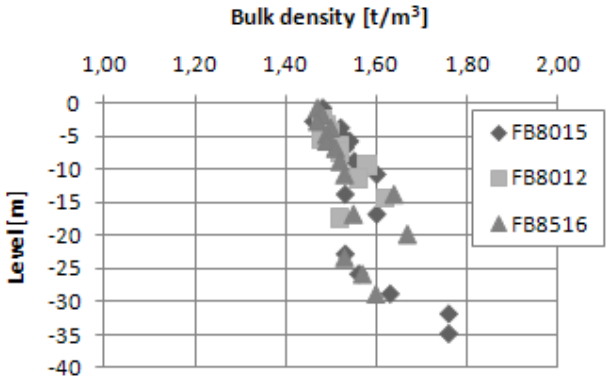
Bulk density [t/m³]
1,00
1,20
1,40
1,60
1,80
2,00
0
-5
-10
-15
-20
-25
-30
-35
-40
Level [m]
FB8015
FB8012
FB8516

(c)

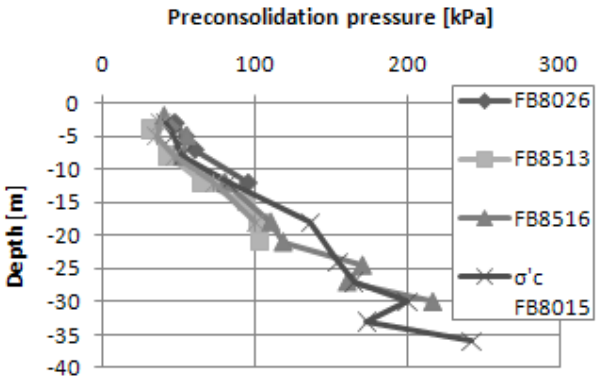
Preconsolidation pressure [kPa]
0
100
200
300
0
-5
-10
-15
-20
-25
-30
-35
-40
Depth [m]
FB8026
FB8513
FB8516
σ'c FB8015

(d)

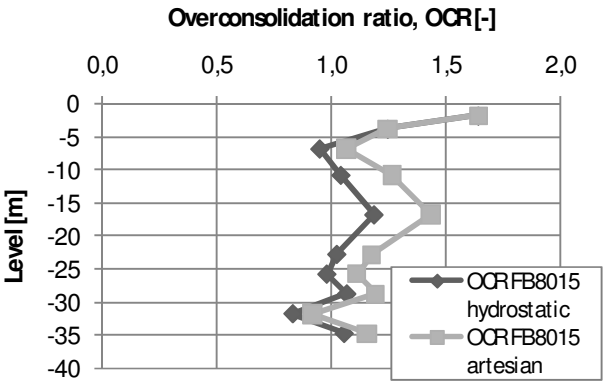
Overconsolidation ratio, OCR [-]
0,0
0,5
1,0
1,5
2,0
0
-5
-10
-15
-20
-25
-30
-35
-40
Level [m]
OCR FB8015 hydrostatic
OCR FB8015 artesian

(e)

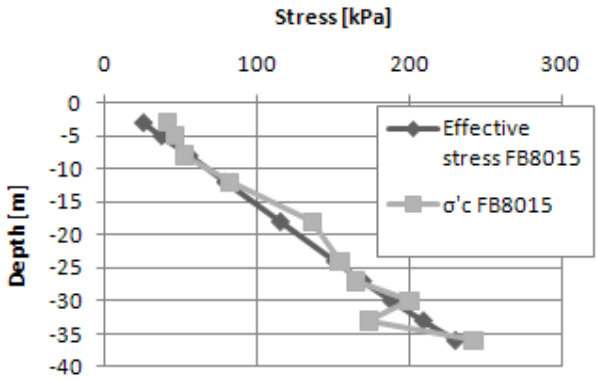
Stress [kPa]
0
100
200
300
0
-5
-10
-15
-20
-25
-30
-35
-40
Depth [m]
Effective stress FB8015
σ'c FB8015

(f)

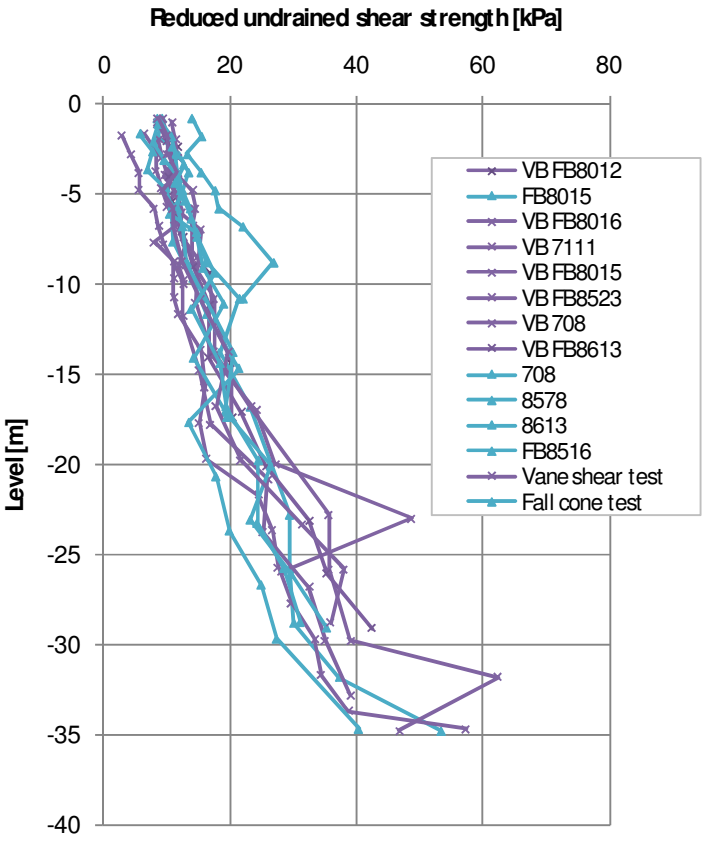
Reduced undrained shear strength [kPa]
0
20
40
60
80
0
-5
-10
-15
-20
-25
-30
-35
-40
Level [m]
VB FB8012
FB8015
VB FB8016
VB 7111
VB FB8015
VB FB8523
VB 708
VB FB8613
708
8578
8613
FB8516
Vane shear test
Fall cone test

(g)

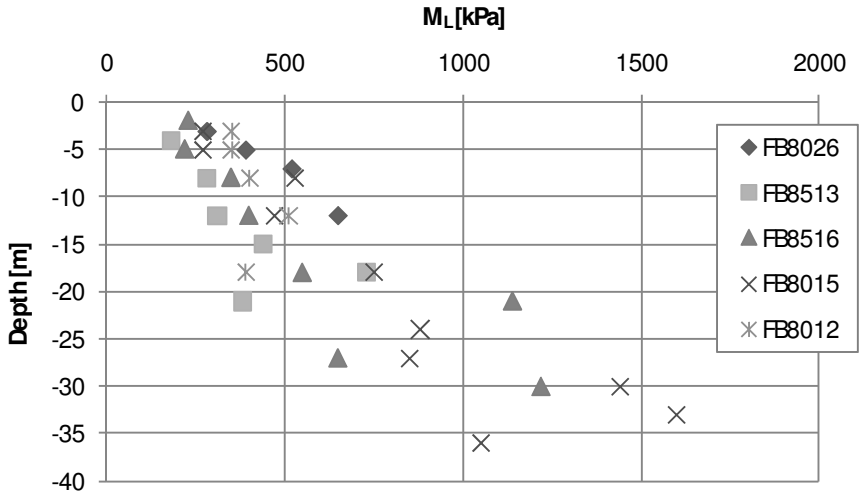
M_L [kPa]
0
500
1000
1500
2000
0
-5
-10
-15
-20
-25
-30
-35
-40
Depth [m]
FB8026
FB8513
FB8516
FB8015
FB8012

(h)

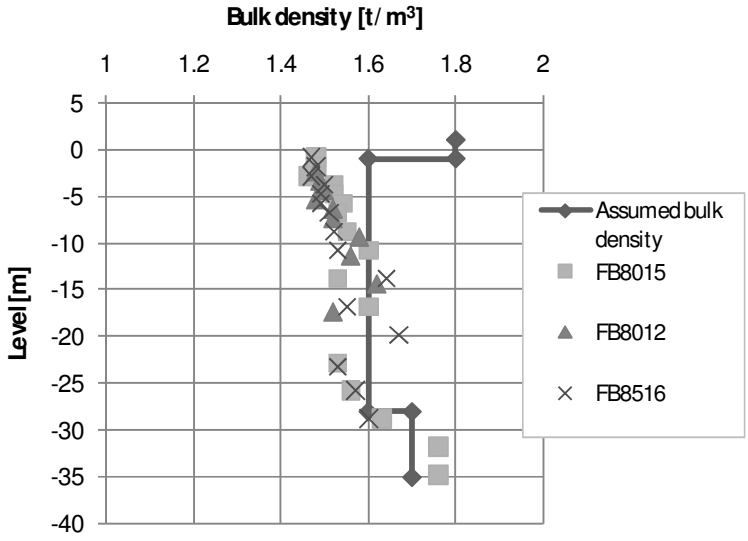
Bulk density [t/ m3]
1
1.2
1.4
1.6
1.8
2
5
0
-5
-10
-15
-20
-25
-30
-35
-40
Level [m]
Assumed bulk density
FB8015
FB8012
FB8516

(a)

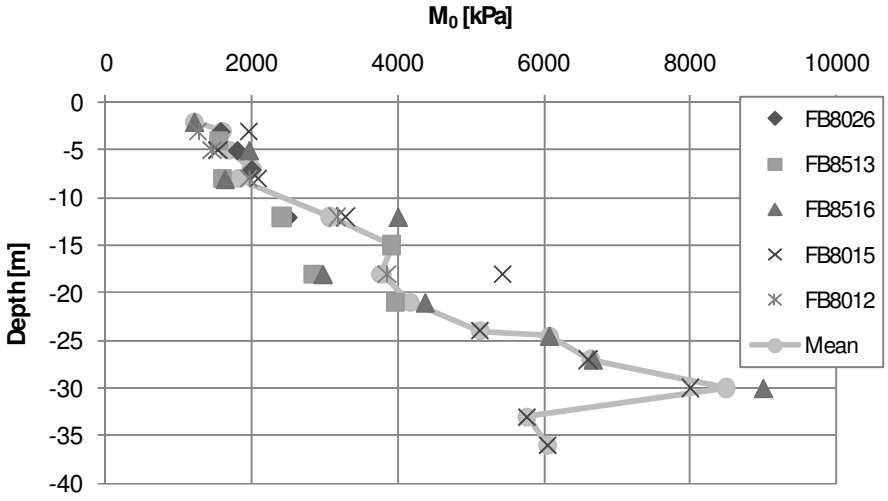
M0 [kPa]
0
2000
4000
6000
8000
10000
0
-5
-10
-15
-20
-25
-30
-35
-40
Depth [m]
FB8026
FB8513
FB8516
FB8015
FB8012
Mean

(b)

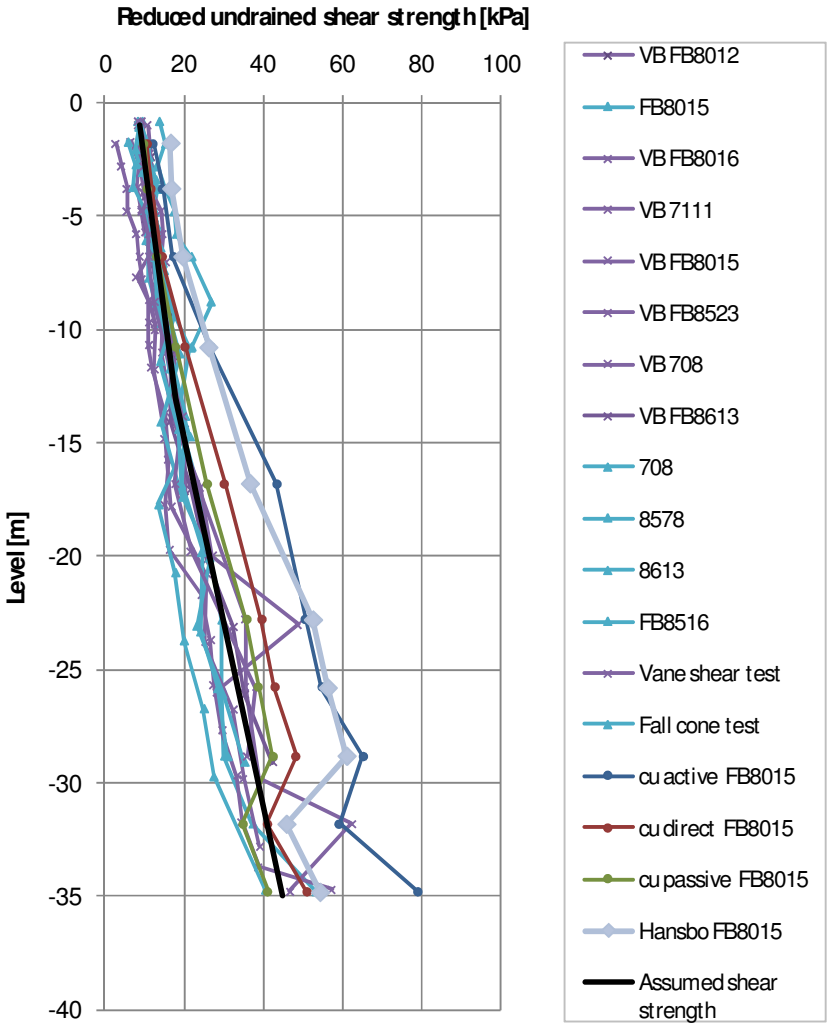
Reduced undrained shear strength [kPa]
0
20
40
60
80
100
0
-5
-10
-15
-20
-25
-30
-35
-40
Level [m]
VB FB8012
FB8015
VB FB8016
VB 7111
VB FB8015
VB FB8523
VB 708
VB FB8613
708
8578
8613
FB8516
Vane shear test
Fall cone test
cu active FB8015
cu direct FB8015
cu passive FB8015
Hansbo FB8015
Assumed shear strength

(a)

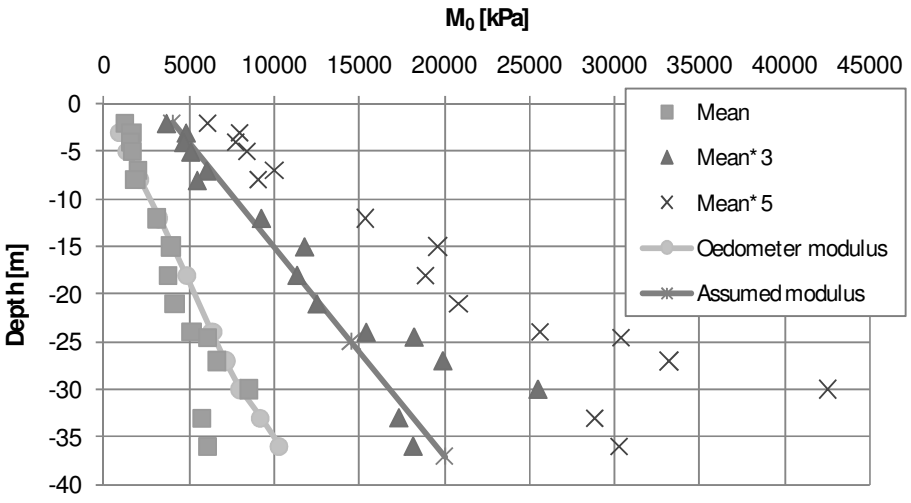
M0 [kPa]
0
5000
10000
15000
20000
25000
30000
35000
40000
45000
Depth [m]
0
-5
-10
-15
-20
-25
-30
-35
-40
Mean
Mean* 3
Mean* 5
Oedometer modulus
Assumed modulus

(b)

The vertical and horizontal effective stresses are calculated by the equations below; (Sällfors 2001)

$\sigma'_{0v} = \gamma \cdot z - u$ and $\sigma'_{0h} = K_0 \cdot \sigma'_{0v}$

The centre of the Mohr-Coulomb circle s'_0, and the undrained shear strength τ_{fu} are calculated by following equations[1]

$$s'_0 = \frac{\sigma'_{0v} + \sigma'_{0h}}{2}$$

$$\tau_{fu} = c' \cdot \cos\phi' + s'_0 \cdot \sin\phi'$$

The input data and the results are presented in the table below;

Linear elastic Mohr-Coulomb

Level [m]	*z [m]*	*γ [kN/m³]*	*u [kPa]*	*K_0 [-]*	*c' [kPa]*	*φ' [°]*	*σ'_{0h} [kPa]*	*σ'_{0v} [kPa]*	*s'_0 [kPa]*	*τ_{fu} [kPa]*
1	0	18	0	1	5	30	0	0	0,0	4,3
0	1	18	5	1	5	30	13	13	13,0	10,8
-1	2	16	15	0,7	6	10	13,3	19	16,2	8,7
-13	14	16	135	0,7	6	10	62,3	89	75,7	19,0
-13	14	16	135	0,7	2	13	62,3	89	75,7	19,0
-28	29	17	285	0,7	2	13	126,7	181	153,9	36,6

The values of c' and ϕ' from LEMC are used as a first approximation for the input data in Plaxis. The parameters are then changed in order to obtain the same mobilized shear strength in the Plaxis soil test as the shear strength assumed from the field investigations. The results from the Plaxis soil test are presented in the table below;

[1] Olsson, M., 2010. *Odränerad hållfasthet enligt "Effective-undrained analysis" och "Dränerad totalspänningsanalys".* (Personal communication, 24 March 2010)

Appendix 5.2

Plaxis soil test

Level [m]	*c' [kPa]*	*ϕ' [°]*	*τ_{fu} [kPa]*
0,5	5	30	9
0	5	30	11
0	6	10	8
-1	6	10	9
-13	6	10	21
-13	2	11,5	20
-28	2	11,5	37

The results from the LEMC and the Plaxis soil test are plotted in the diagram below along with the assumed shear strength.

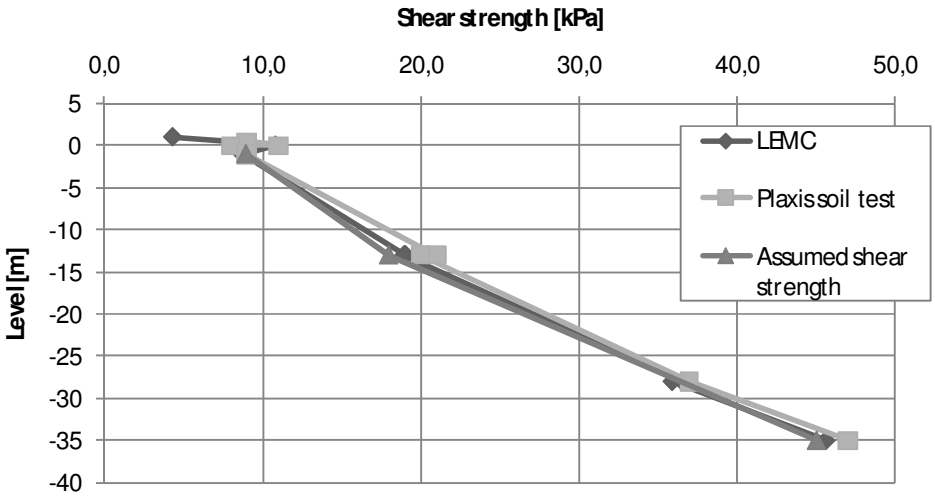

(a)

Young´s modulus is calculated by following equation, (Larsson 1994, p. 22)

$$E = M \cdot \frac{(1+\nu)\cdot(1-2\cdot\nu)}{(1-\nu)}$$

Young´s effective modulus is calculated by following equation, (Brinkgreve 2002)

$$E' = \frac{2\cdot(1+\nu)}{3}\cdot E_u \qquad \text{Where } E_u = E$$

Pore pressure measurements **Appendix 6.1**

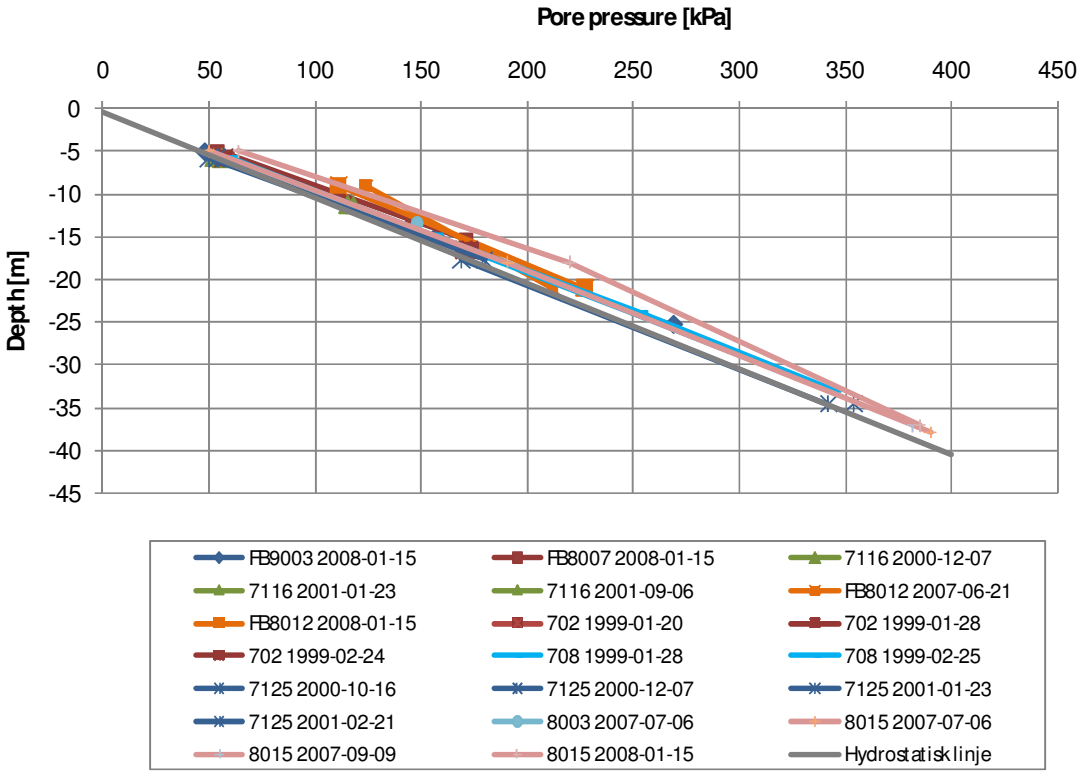

Installation scheme **Appendix 7.1**

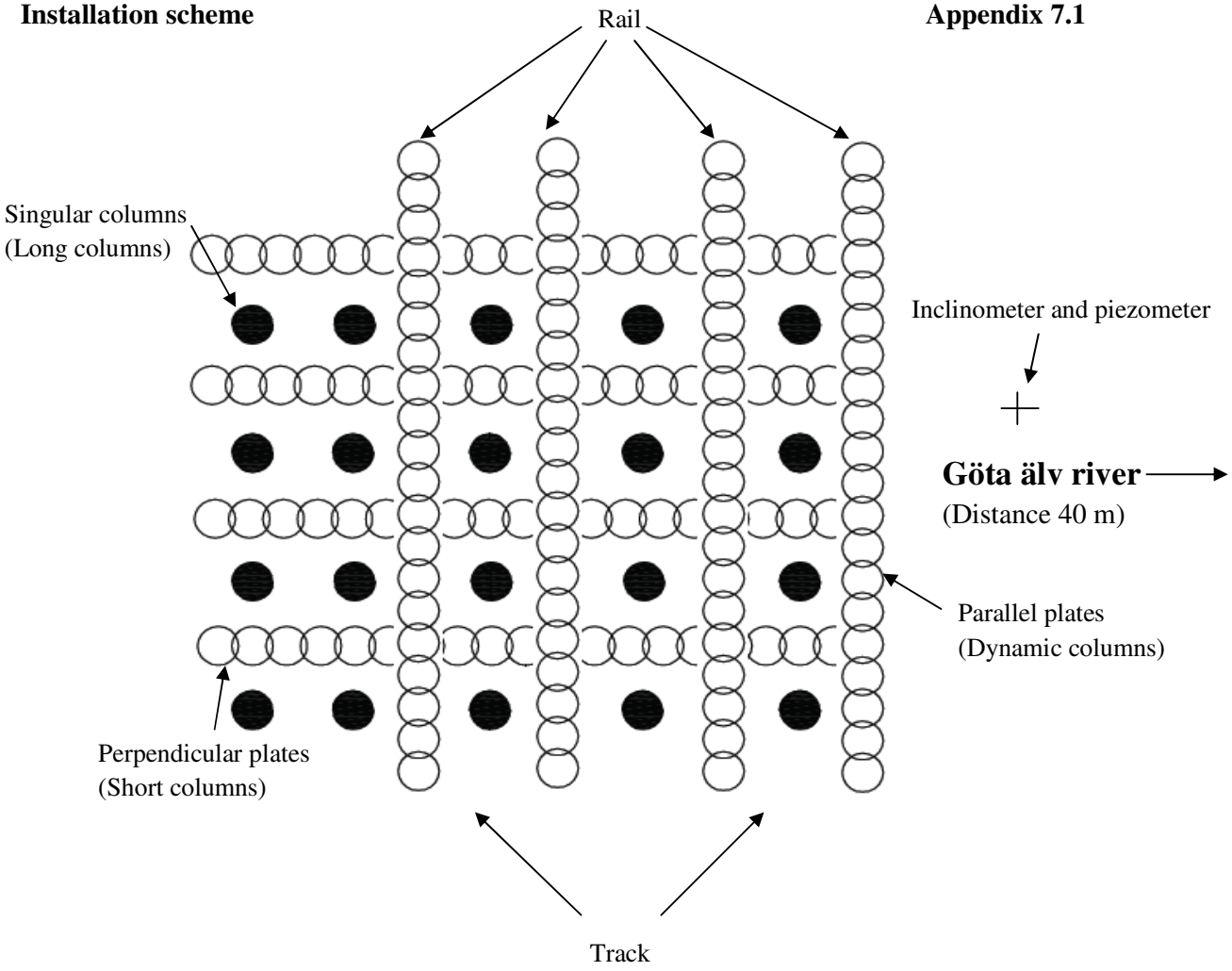

cc – distance between the perpendicular plates (short columns) is 2 m.

cc - distance between rails are 2 m.

cc – distance between the two tracks are 2.5 m.

cc – distance between the singular (long) columns in the vertical direction is 2 m.

cc – distance between the singular (long) columns in the horizontal direction is 2.25 m.

Location of piezometer and inclinometer, Section A **Appendix 8.1**

The drawing is not in scale. The symbols show the location of the piezometer and the inclinometer. They are located 4 m from the most westerly column row.

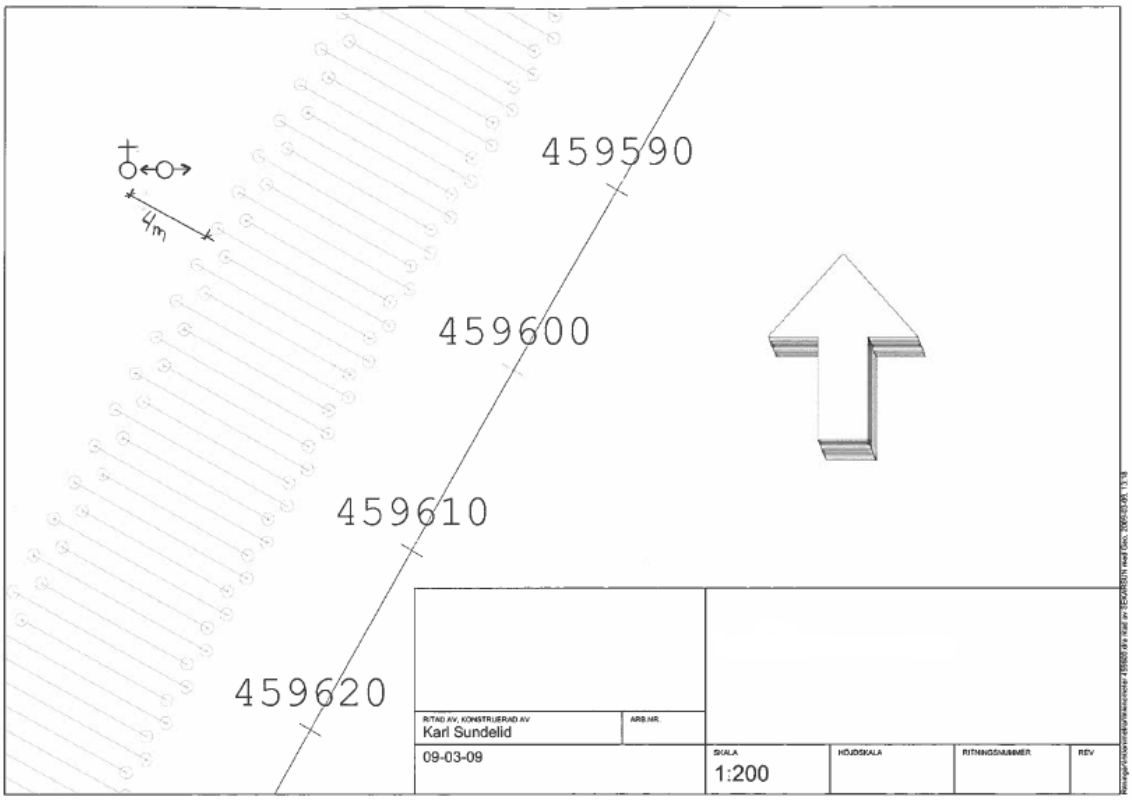

Volume strain **Appendix 9.1**

Density of mixture[1]	1800	[kg/m^3]
Amount of mixture	25	[kg/m]
Diameter of column	0,6	[m]
Volume column	0,283	[1/m]
Volume mixture	0,014	[m^3/m]

Short columns

Length of area	7	[m]
Width of area	10,1	[m]
Number of columns	80	
Length of columns	4,2	[m]
Total column length	336,0	[m]
Mixture volume	4,67	[m^3]
Soil volume	296,94	[m^3]
Volume strain, V_{strain}	0,016	[-]

Long columns

Length of area	2	[m]
Width of area	0,6	[m]
Number of columns	1	
Length of columns	22,6	[m]
Total column length	22,6	[m]
Mixture volume	0,31	[m^3]
Soil volume	27,12	[m^3]
Volume strain, V_{strain}	0,012	[-]

Dynamic columns

Length of area	1	[m]
Width of area	0,6	[m]
Number of columns	2	
Length of columns	7	[m]
Total column length	14,0	[m]
Mixture volume	0,19	[m^3]
Soil volume	4,2	[m^3]
Volume strain, V_{strain}	0,046	[-]

Appendix 9.2

Corner columns		
Length of area	2	[m]
Width of area	0,6	[m]
Number of columns	1	
Length of columns	15,5	[m]
Total column length	15,5	[m]
Mixture volume	0,22	[m^3]
Soil volume	18,6	[m^3]
Volume strain, V_{strain}	0,012	[-]

Sagaseta		
Volume column	0,283	[m^3/m]
Volume mixture	0,014	[m^3/m]
$V_{strain\ per\ column}$	0,049	[-]

[1](Bruk KC, p. 50) Byström, P.G. (2007): *Byggnadsmaterial - Uppbyggnad, tillverkning och egenskaper*. 2d ed. Studentlitteratur.

Rehnman – length 1 m **Appendix 10.1**

Diameter of column	0,6	[m]
Length of pile area, l	1	[m]
Width of pile area, b	10,1	[m]
Rows with dynamic columns	4	[-]
Heave factor, η	0,75	[-]
Volume of pre-coring, $V_{pre\text{-}coring}$	0	[m^3]
α	1	[-]
β	1	[-]
γ	1	[-]
δ	1	[-]

	Short columns	*Long columns*	*Dynamic columns*
Piledepth below ground surface, d [m]	4	22,6	7
Volume strain [-], V_{strain}	0,016	0,012	0,046
Total soil volume [m^3]	40,4	228,26	16,8
Pile volume [m^3], V_{pile}	0,6	2,7	0,7728
Heave, x [m]	0,0063	0,0022	0,0038

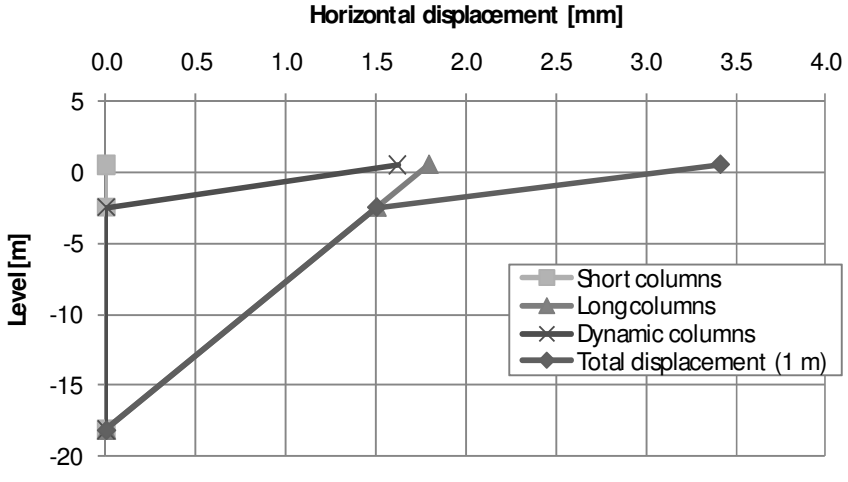

(a)

Rehnman – length 10 m. **Appendix 10.2**

Diameter of column	0,6	[m]
Length of pile area, l	10	[m]
Width of pile area, b	10,1	[m]
Rows with dynamic columns	4	[-]
Heave factor, η	0,75	[-]
Volume of pre-coring, $V_{pre\text{-}coring}$	0	[m^3]
α	1	[-]
β	1	[-]
γ	1	[-]
δ	1	[-]

	Short columns	*Long columns*	*Dynamic columns*
Piledepth below ground surface, d [m]	4	22,6	7
Volume strain [-], V_{strain}	0,016	0,012	0,046
Total soil volume [m^3]	404	2282,6	168
Pile volume [m^3], V_{pile}	6,5	27,4	7,728
Heave, x [m]	0,0398	0,0178	0,0189

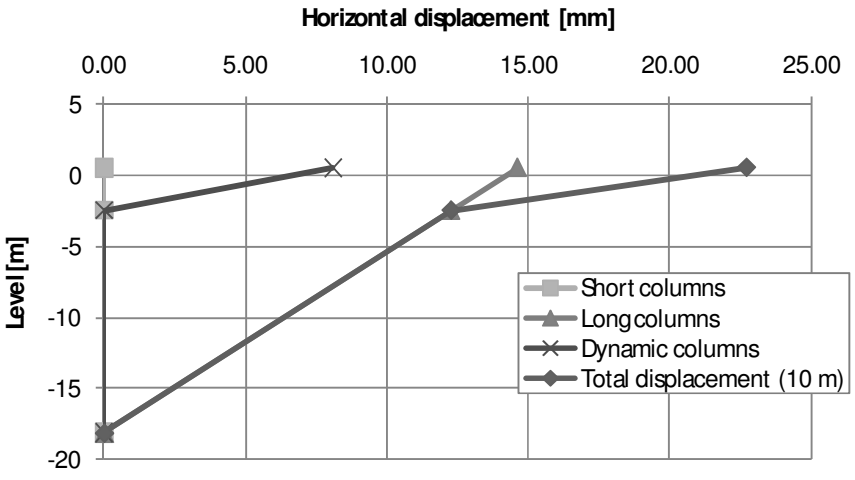

(a)

Rehnman – 50 m length (γ,δ=1) **Appendix 10.3**

Diameter of column	0,6	[m]
Length of pile area, l	50	[m]
Width of pile area, b	10,1	[m]
Rows dynamic columns	4	[-]
Heave factor, η	0,75	[-]
Volume of pre-coring, $V_{pre\text{-}coring}$	0	[m^3]
α	1	[-]
β	1	[-]
γ	1	[-]
δ	1	[-]

	Short columns	*Long columns*	*Dynamic columns*
Piledepth below ground surface, d [m]	4	22,6	7
Volume strain [-]	0,016	0,012	0,046
Total soil volume [m^3]	2020	11413	840
Pile volume [m^3]	32,3	137,0	38,64
Heave, x [m]	0,0753	0,0489	0,0292

Horizontal deformation at distance: 4 [m]

Total displacement [mm]

Level [m]	Short columns	Long columns	Dynamic columns	Total displacement
0,5	0,00	40,27	12,53	52,80
-2,5	0,00	33,77	0,00	33,77
-18,1	0,00	0,00	0,00	0,00

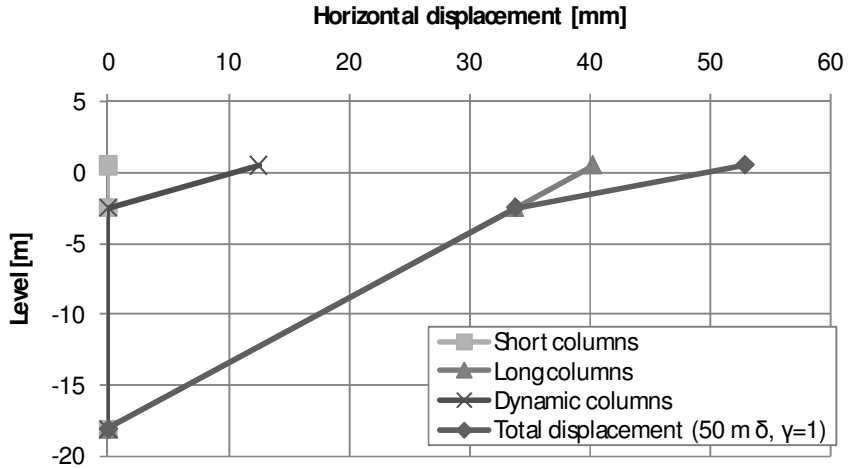

(a)

Diameter of column	0,6	[m]
Length of pile area, l	50	[m]
Width of pile area, b	10,1	[m]
Rows dynamic columns	4	[-]
Heave factor, η	0,75	[-]
Volume of pre-coring, $V_{pre\text{-}coring}$	0	[m^3]
α	1	[-]
β	1	[-]
γ	0	[-]
δ	0	[-]

	Short columns	*Long columns*	*Dynamic columns*
Piledepth below ground surface, d [m]	4	22,6	7
Volume strain [-]	0,016	0,012	0,046
Total soil volume [m^3]	2020	11413	840
Pile volume [m^3]	32,3	137,0	38,64
Heave, x [m]	0,0895	0,0671	0,0326

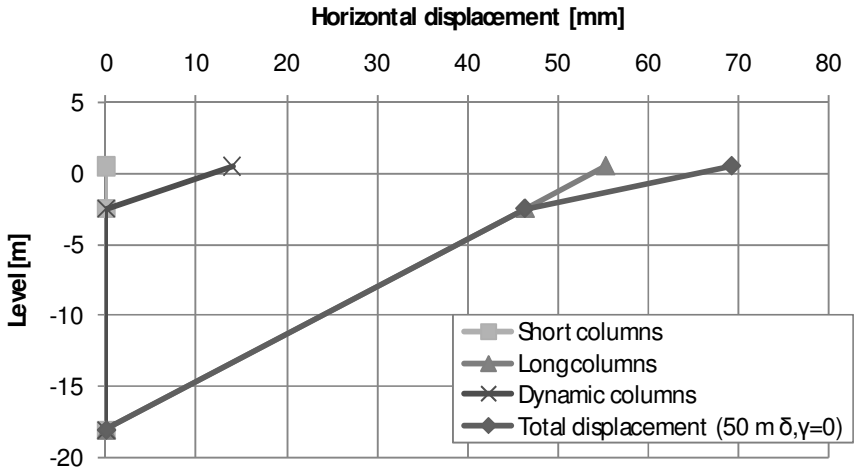

(a)

Input parameters for excess pore pressure calculation **Appendix 11.1**

Valid for both 5 m and 10 m

$\Delta p'_c = 2\text{-}4 \cdot c_u$

r = starts at 0.3 m and are then increased 0.3 m every step

$R_c = 0.3$

$T_Q = c_u$

$\phi = 30°$

---

5 m

$\sigma'_1 = 30$ kPa $\sigma'_2 = 21$ kPa $\sigma'_3 = 21$ kPa

$p'_0 = 24$ kPa

$c_u = 10$ kPa

$A_f = 0.92 \longrightarrow \alpha_f = 1.24$

---

10 m

$\sigma'_1 = 55$ kPa $\sigma'_1 = 38.5$ kPa $\sigma'_1 = 38.5$ kPa

$p'_0 = 44$ kPa

$c_u = 13$ kPa

$A_f = 0.80 \longrightarrow \alpha_f = 0.98$

Input data for parameter analysis **Appendix 12.1**

Young's modulus

	E' assumed [kPa]	*E' decreased [kPa]*	*E' increased [kPa]*
Dry crust (+1 to 0)	5 000	5 000	5 000
Clay layer 1 (0 to -13)	1 730 + 256 kPa/m	1530 + 256 kPa/m	11 138 + 1 547 kPa/m
Clay layer 2 (-13 to -28)	5 060 + 256 kPa/m	4 860 + 256 kPa/m	31 243 + 2 454 kPa/m
Friction layer (-28 to --)	8 900 + 256 kPa/m	8 700 + 256 kPa/m	68 059 + 4 375 kPa/m

The effective Young's modulus $E^{'}$ can be calculated with the equation below (Brinkgreve 2002)

$$E^{'} = \frac{2 \cdot (1+\nu)}{3} \cdot E_u$$

where the undrained Young's modulus E_u is set equal to the initial Young's modulus E_0. The initial Young's modulus E_0 can be calculated with equation; (Larsson 1994, p. 36)

$$E_0 = 2 \cdot G_0 \cdot (1+\nu)$$

and the initial shear modulus G_0 can be calculated with equation; (Larsson 1994, p. 35)

$$G_0 = \frac{500 \cdot \tau_{fu}}{w_L}$$

Values for τ_{fu} and w_L for different levels can be read from *Figure 20* and *Figure 18* respectively.

Appendix 12.2

Volume strain

	Assumed volume strain [%]	*Decreased volume strain [%]*	*Increased volume strain [%]*
Short columns	1.6	1.2	2.2
Long columns	1.2	0.9	1.6
Dynamic columns	4.6	3.6	6.4

The decreased and increased volume strain are calculated in the same way as the assumed volume strain, see Appendix 9, but with different densities of the lime-cement mixture. The decreased volume strain is calculated with a density of 2 300 kg/m^3 and the increased volume strain is calculated with a density of 1 300 kg/m^3 of the lime-cement mixture.

Poisson

	Assumed Poisson [-]	*Decreased Poisson [-]*	*Increased Poisson [-]*
Dry crust (+1 to 0)	0.35	0.25	0.45
Clay layer 1 (0 to -13)	0.35	0.25	0.45
Clay layer 2 (-13 to -28)	0.35	0.25	0.45
Friction layer (-28 to --)	0.35	0.25	0.45

Appendix 12.3

Shear strength

	Assumed shear strength		*Decreased shear strength*		*Increased shear strength*	
	c' *[kPa]*	ϕ' *[°]*	c' *[kPa]*	ϕ' *[°]*	c' *[kPa]*	ϕ' *[°]*
Dry crust (+1 to 0)	5	30	5	30	5	30
Clay layer 1 (0 to -13)	6	10	2	8	10	9
Clay layer 2 (-13 to -28)	2	11.5	2	9	5	11.5
Friction layer (-28 to --)	0,2	12	0.2	13.5	0,2	12

In this analysis the assumed shear strength is decreased with 5 kPa and increased with 5 kPa. The effective parameters c' and ϕ' are calculated in the same way as for the assumed shear strength, see Appendix 5.

Undrained parameters

	Undrained parameters	
	c' *[kPa]*	ϕ' *[°]*
Dry crust (+1 to 0)	5	30
Clay layer 1 (0 to -13)	8.25 + 0.75 kPa/m	0
Clay layer 2 (-13 to -28)	18 + 1.23 kPa/m	0
Friction layer (-28 to --)	0,2	12

In this analysis undrained parameters are used instead of effective parameters, that is $c' = c_u$ and $\phi = 0$, where c_u is set to the assumed shear strength, see *Figure 20.*

Here the horizontal displacements after the last installation phase and the pore pressure during the three installation phases for every parameter analysis are presented. The short columns are installed 3rd of March, the long columns 6th of March and the dynamic columns 9th of March.

Poisson

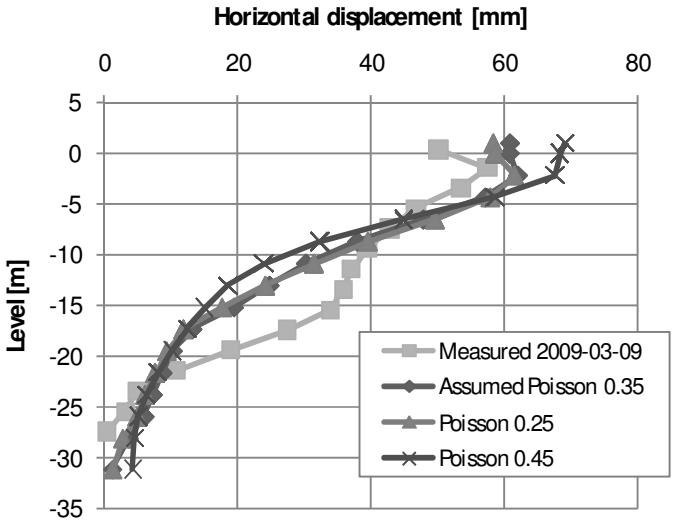

(a)

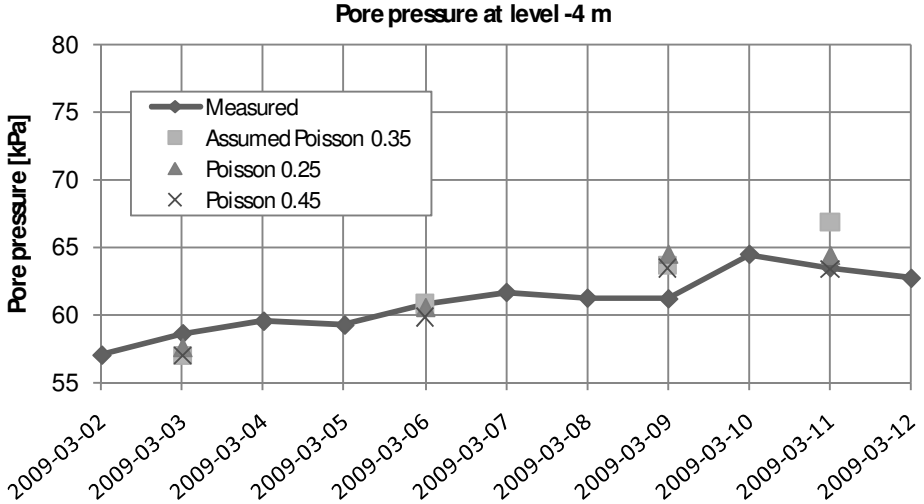

(b)

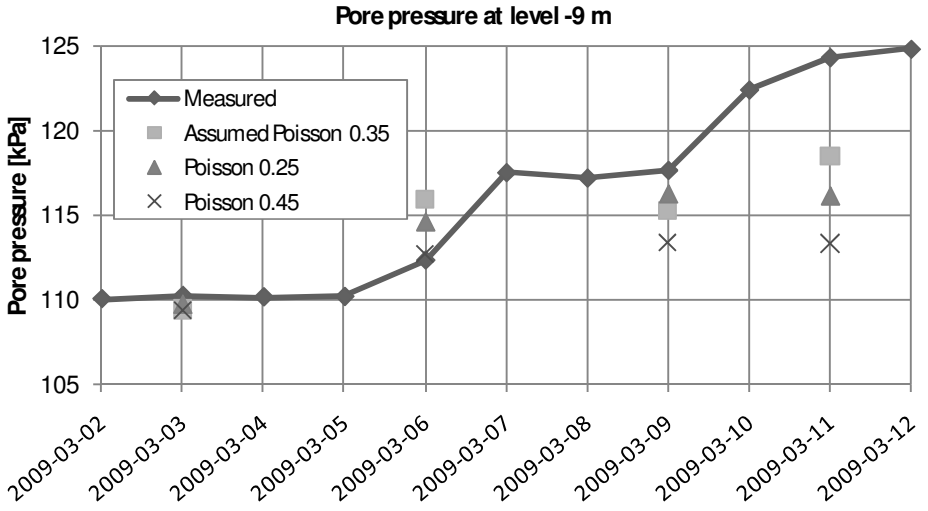
Pore pressure at level -9 m
Pore pressure [kPa]
125
120
115
110
105
Measured
Assumed Poisson 0.35
Poisson 0.25
Poisson 0.45
2009-03-02
2009-03-03
2009-03-04
2009-03-05
2009-03-06
2009-03-07
2009-03-08
2009-03-09
2009-03-10
2009-03-11
2009-03-12

(c)

Shear strength

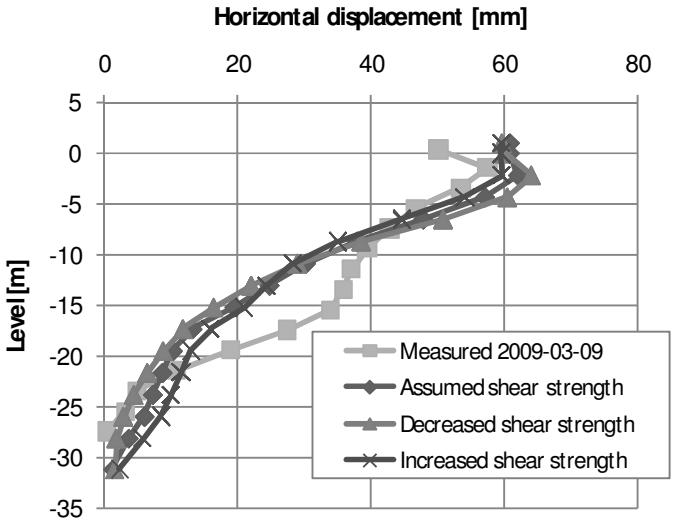

(d)

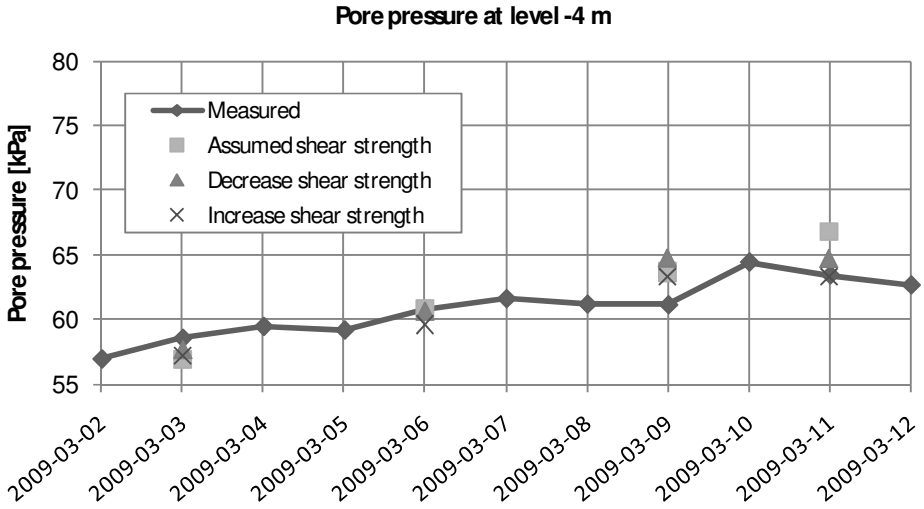

(e)

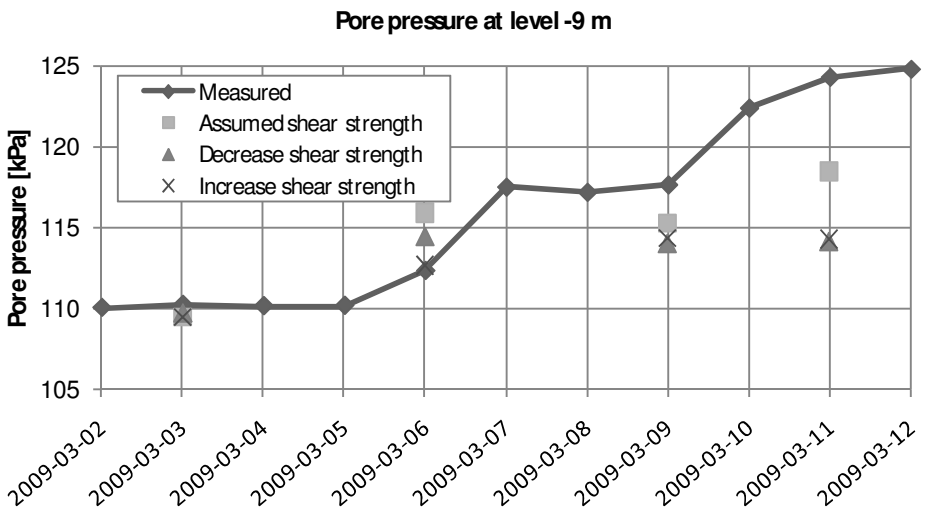
Pore pressure at level -9 m
Pore pressure [kPa]
125
120
115
110
105
Measured
Assumed shear strength
Decrease shear strength
Increase shear strength
2009-03-02
2009-03-03
2009-03-04
2009-03-05
2009-03-06
2009-03-07
2009-03-08
2009-03-09
2009-03-10
2009-03-11
2009-03-12

(f)

Undrained parameters

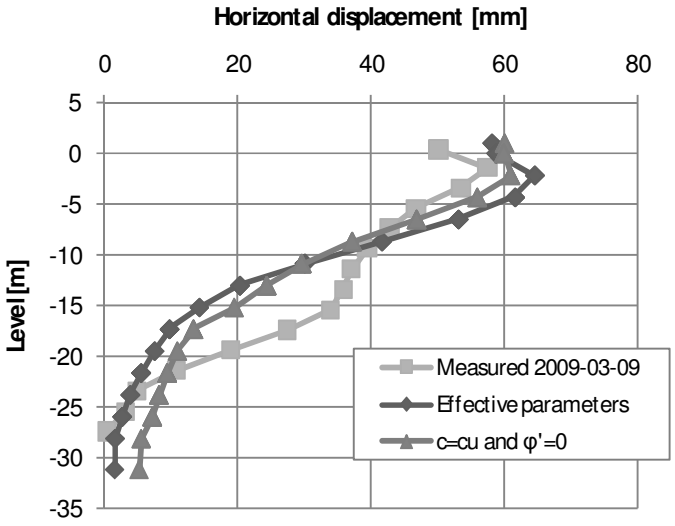

(g)

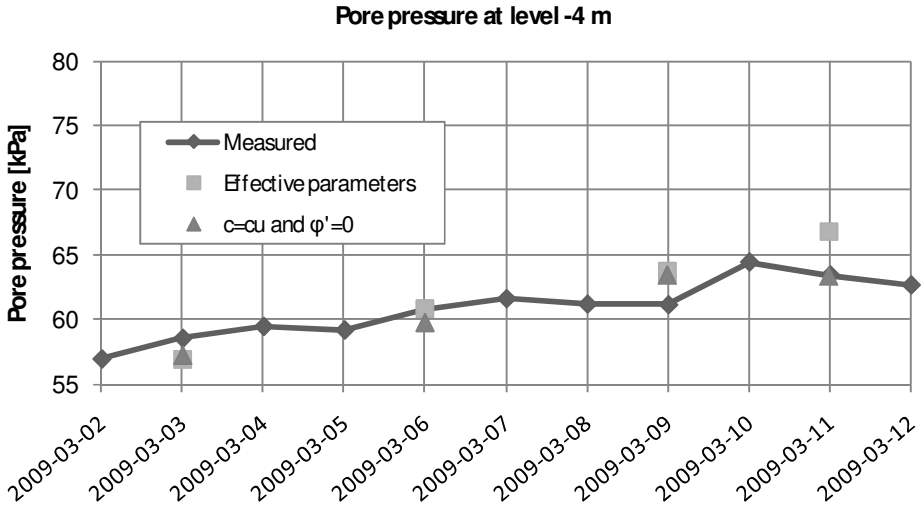

(h)

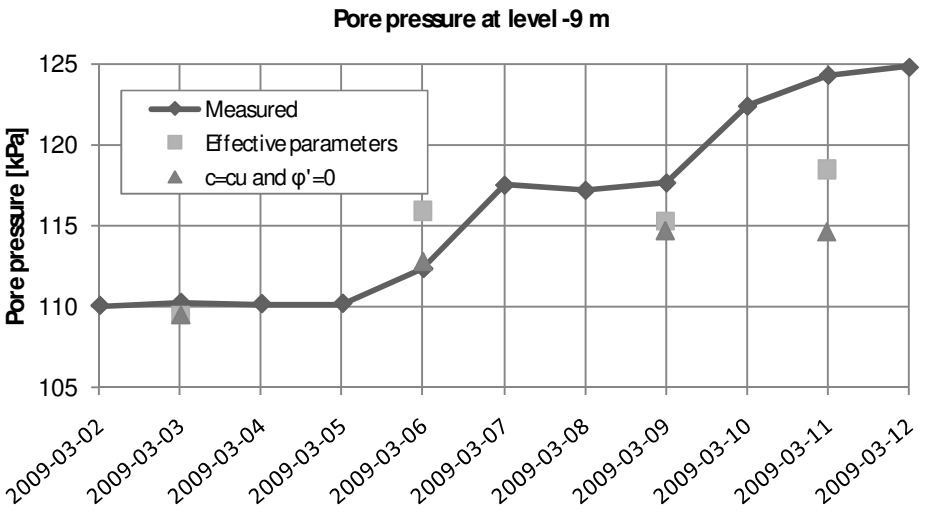
Pore pressure at level -9 m
Pore pressure [kPa]
125
120
115
110
105
Measured
Effective parameters
c=cu and φ'=0
2009-03-02
2009-03-03
2009-03-04
2009-03-05
2009-03-06
2009-03-07
2009-03-08
2009-03-09
2009-03-10
2009-03-11
2009-03-12

(i)

Results from Sagaseta calculations **Appendix 14.1**

The results are based on calculations with a volume expansion of 3.54 %. The inclinometer is located at (4,0), where the x-axis is perpendicular to the dynamic columns and the y-axis is parallel to the dynamic columns.

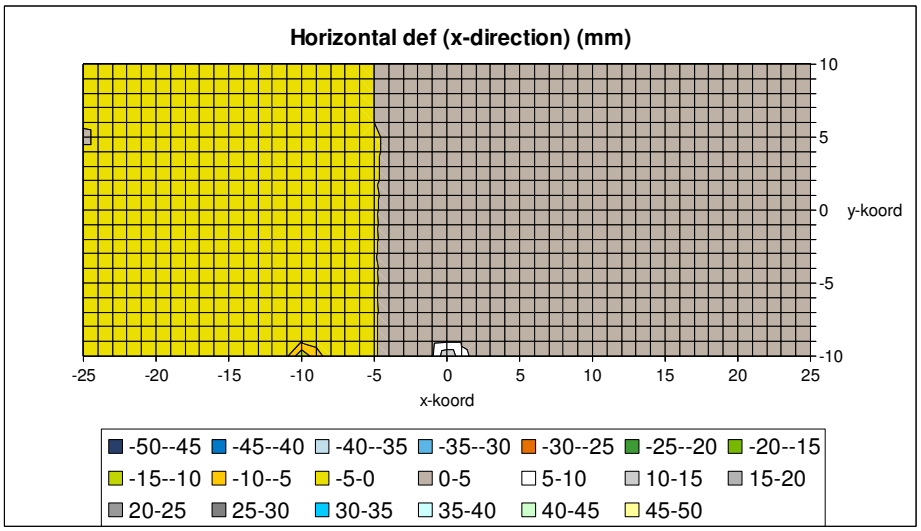

(a)

Horizontal displacement after installation of perpendicular plates (short columns), at a distance ≥10 m in y-direction from the inclinometer.

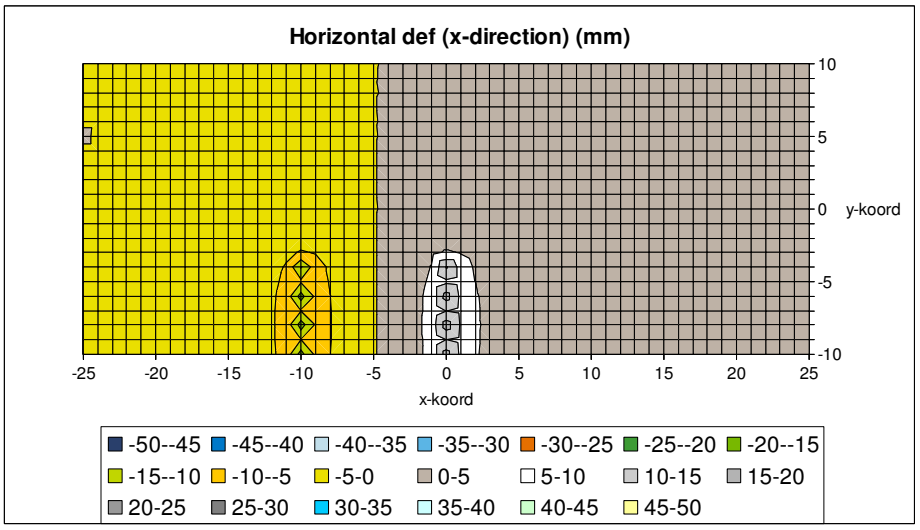

(b)

Horizontal displacement after installation of perpendicular plates (short columns), at a distance ≥4 m in y-direction from the inclinometer.

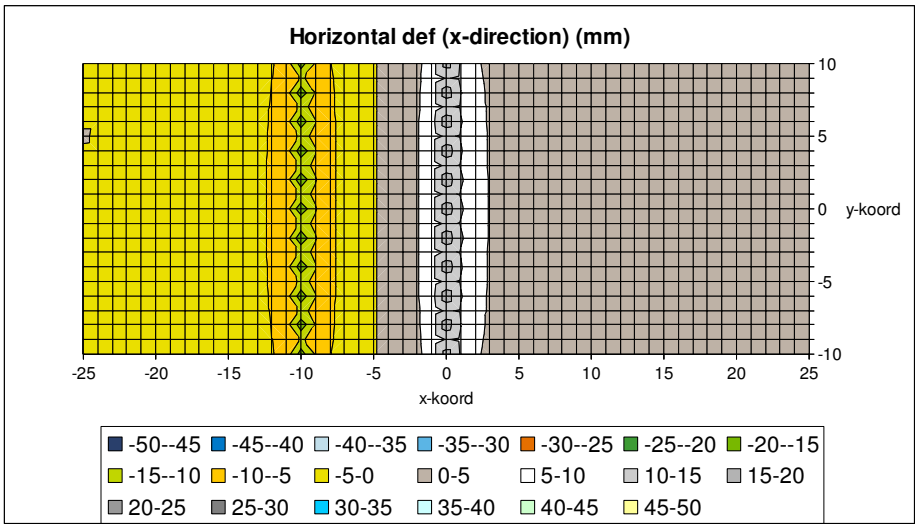

(c)

Horizontal displacement after installation of perpendicular plates (short columns), at a distance ≥∞ m in y-direction from the inclinometer.

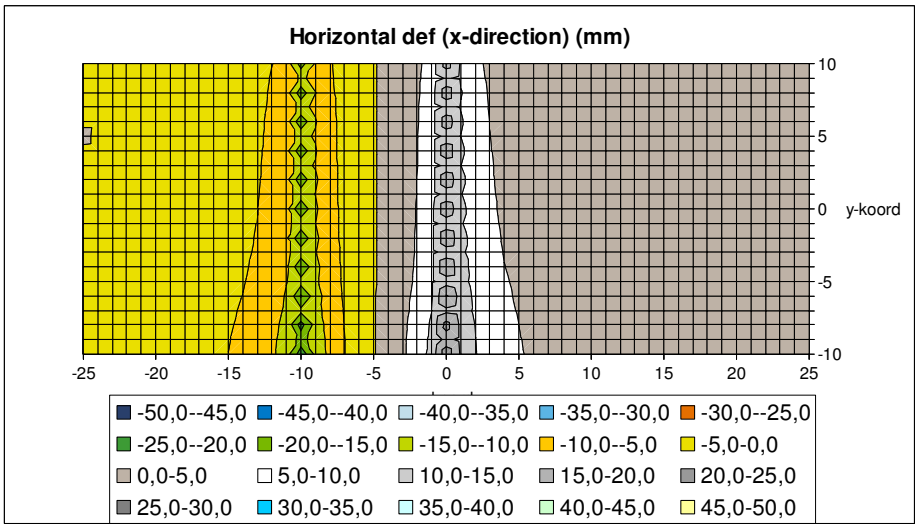

(d)

Horizontal displacement after installation of singular columns (long columns), at a distance ≥8 m in y-direction from the inclinometer.

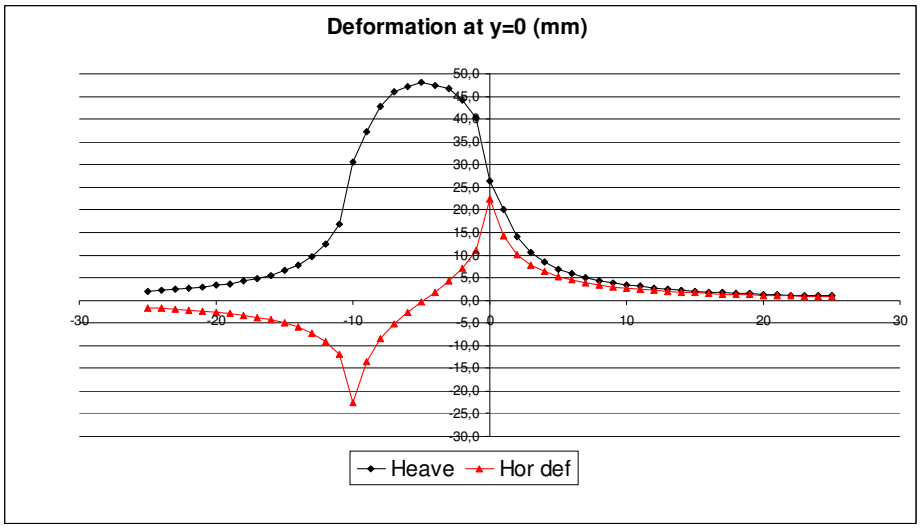

(e)

Horizontal displacement after installation of singular columns (long columns), at a distance ≥0 m in y-direction from the inclinometer.

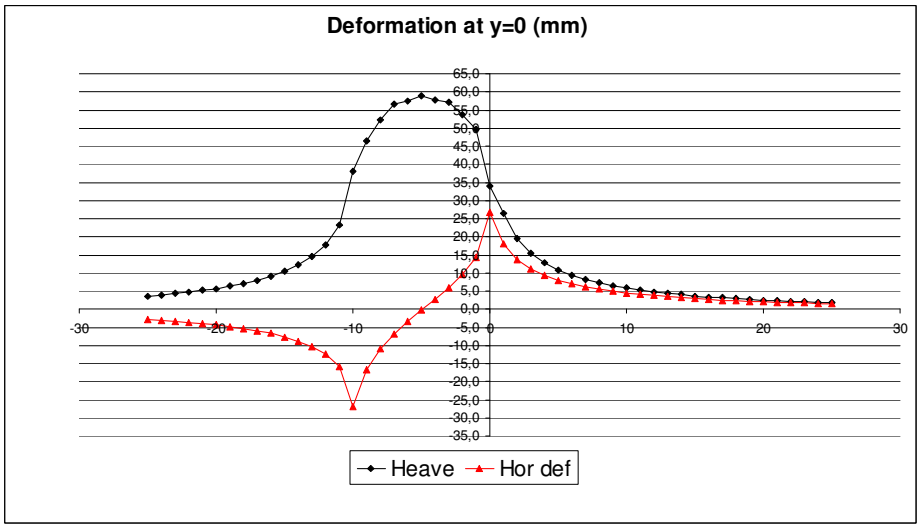

(f)

Horizontal displacement after installation of singular columns (long columns), at a distance ≥∞ m in y-direction from the inclinometer.

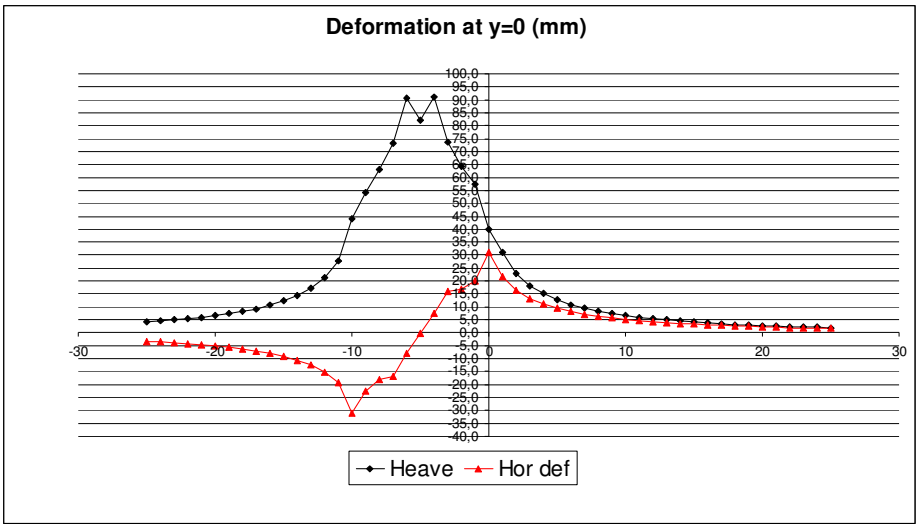

(g)

Horizontal displacement after installation of parallel plates (dynamic columns), at a distance ≥7 m in x-direction from the inclinometer.

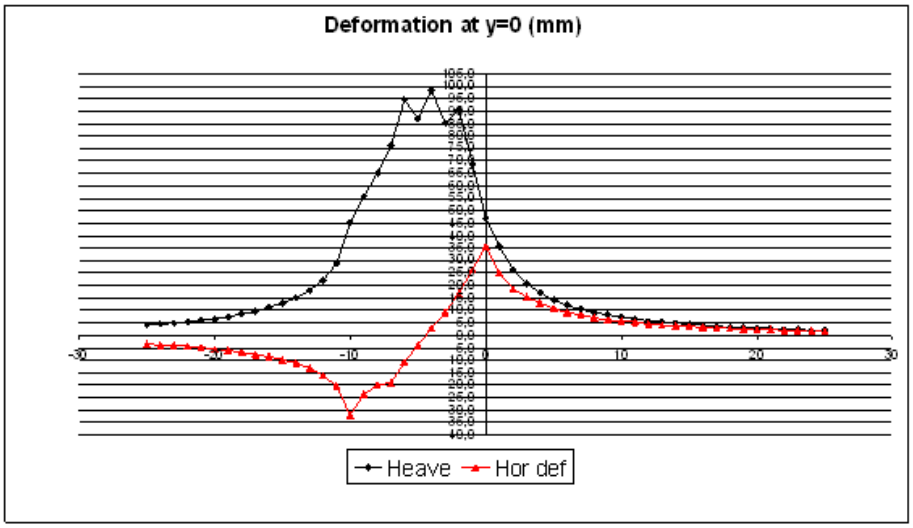

(h)

Horizontal displacement after installation of parallel plates (dynamic columns), at a distance ≥5 m in x-direction from the inclinometer.

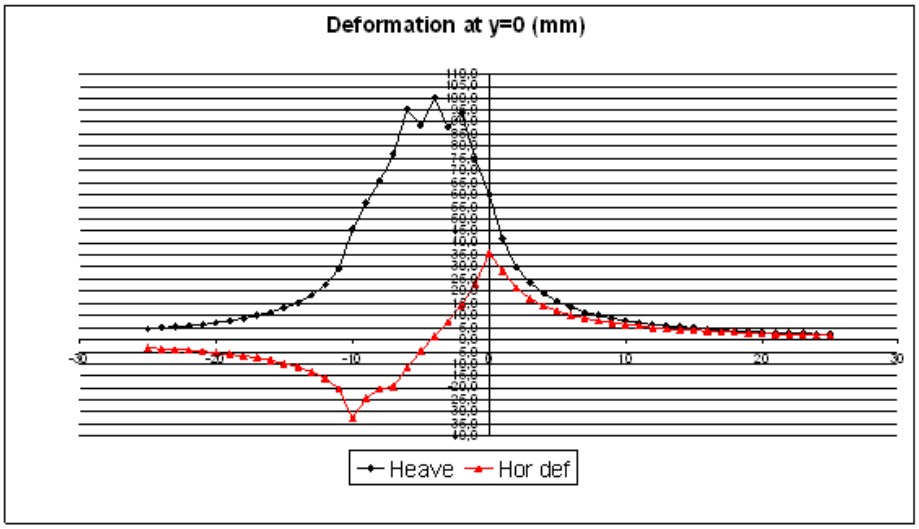

(i)

Horizontal displacement after installation of parallel plates (dynamic columns), at a distance ≥4 m in x-direction from the inclinometer.

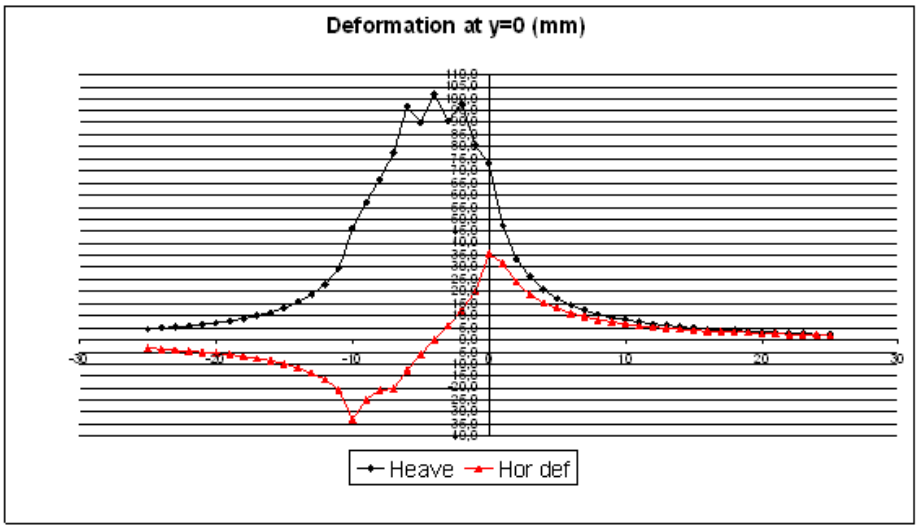

(j)

Horizontal displacement after all columns are installed.

Drawings

Section 459+400-600	Drawing 1
Section 459+700-900	Drawing 2
Section 459+490-780	Drawing 3

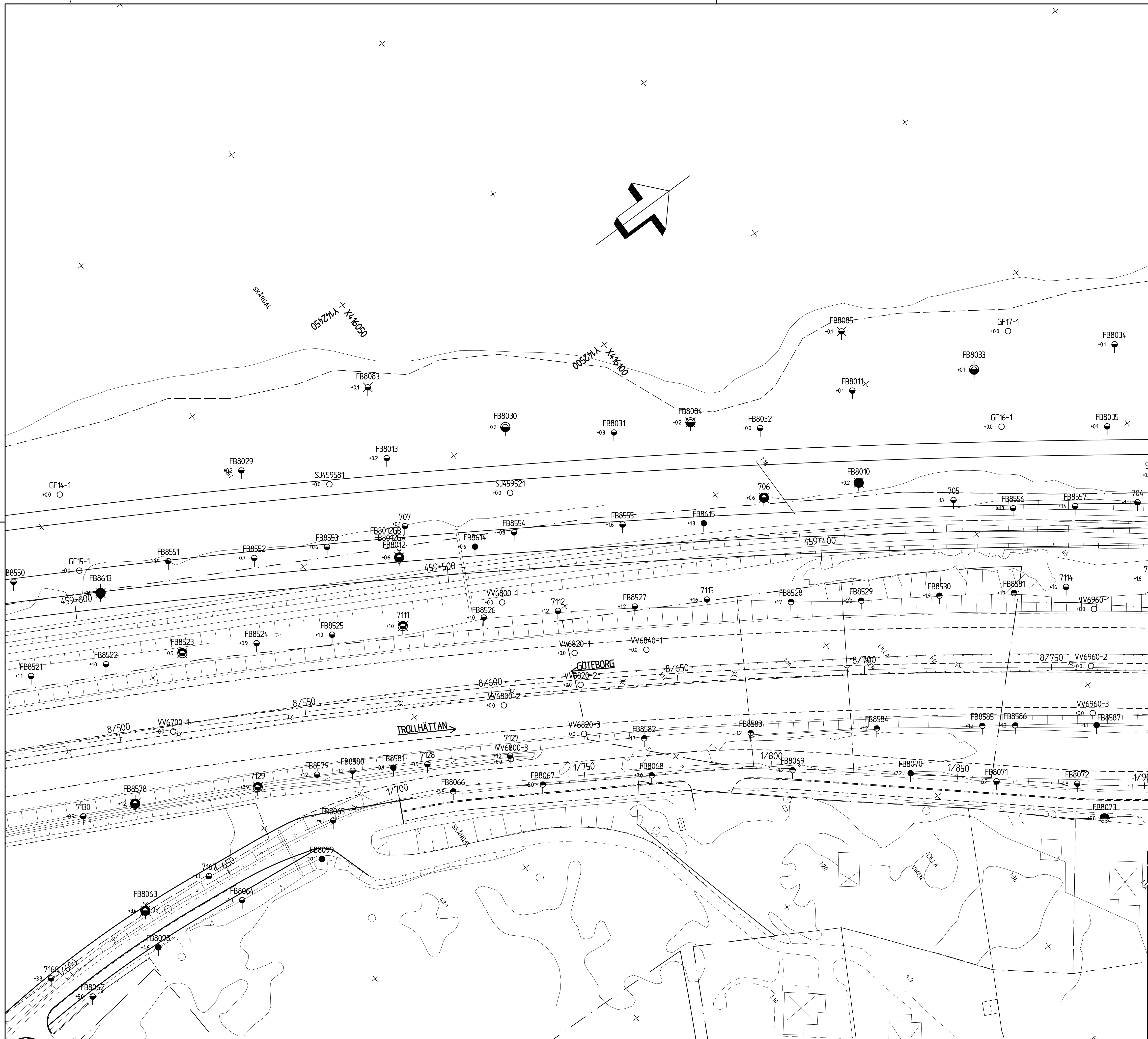

BETECKNINGAR

GEOTEKNISKA BETECKNINGAR ENLIGT
SGF:S BETECKNINGSSYSTEM, SE www.sgf.net

KOORDINATSYSTEM RT 90 7.5 gon V 60:-1
HÖJDSYSTEM RHB 70

REV	ANT	ÄNDRINGEN AVSER	GODK.	DATUM	VV DATUM	VV DIARIENUMMER

BYGGHANDLING

Vägverket
BANVERKET
FLYGFÄLTSBYRÅN

FB Engineering AB
Box 12076, 402 41 GÖTEBORG
Tel: 031-775 10 00
Fax: 031-12 20 63

BanaVäg i Väst

E 45 - NORGE-VÄNERBANAN
DELEN BOHUS - NÖDINGE

ENTREPRENAD E32

GEOTEKNISK UNDERSÖKNING
KM 459+400 - 459+600
LOKALVÄG 233 KM 1/600 - 1/900
PLAN

UPPDRAGSANSVARIG	UPPDRAGSNUMMER	KONSTRUKTIONSNR	FORMAT	SKALA	REV
A BERGHOLTZ	161289		A1	1:500	
KONSTR: MP	GRANSK: CHJU	OBJEKT NR: 542764/4530	RITNINGSNR: 200G0206		
GÖTEBORG	2008-02-20				

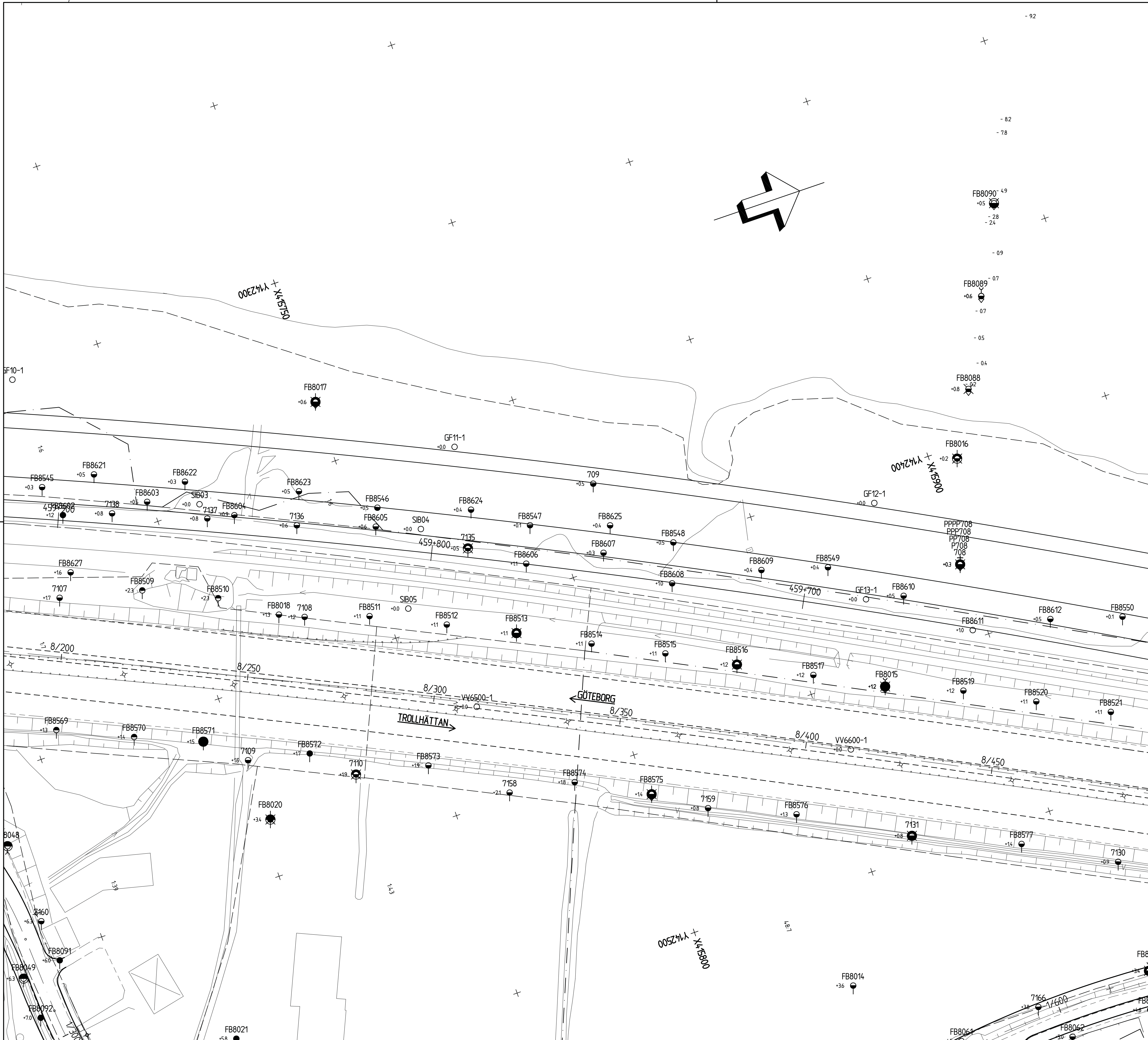

BETECKNINGAR

GEOTEKNISKA BETECKNINGAR ENLIGT
SGF:S BETECKNINGSSYSTEM, SE www.sgf.net

KOORDINATSYSTEM RT 90 7.5 gon V 60:-1
HÖJDSYSTEM RHB 70

REV	ANT	ÄNDRINGEN AVSER	GODK.	DATUM	VV DATUM	VV DIARIENUMMER

BYGGHANDLING

Vägverket
BANVERKET

BANAVÄG I VÄST

E 45 - NORGE-VÄNERBANAN
DELEN BOHUS - NÖDINGE

FLYGFÄLTSBYRÅN
FB Engineering AB
Box 12076, 402 41 GÖTEBORG
Tel: 031-775 10 00
Fax: 031-12 20 63

ENTREPRENAD E32

GEOTEKNISK UNDERSÖKNING

KM 459+700 - 459+900
PLAN

UPPDRAGSANSVARIG: A BERGHOLTZ	UPPDRAGSNUMMER: 161289				
KONSTR: MP	GRANSK: CHJU	KONSTRUKTIONSNR:	FORMAT: A1	SKALA: 1:500	
GÖTEBORG	2008-02-20	OBJEKT NR: 542764/4530	RITNINGSNR: 200G0205		REV:

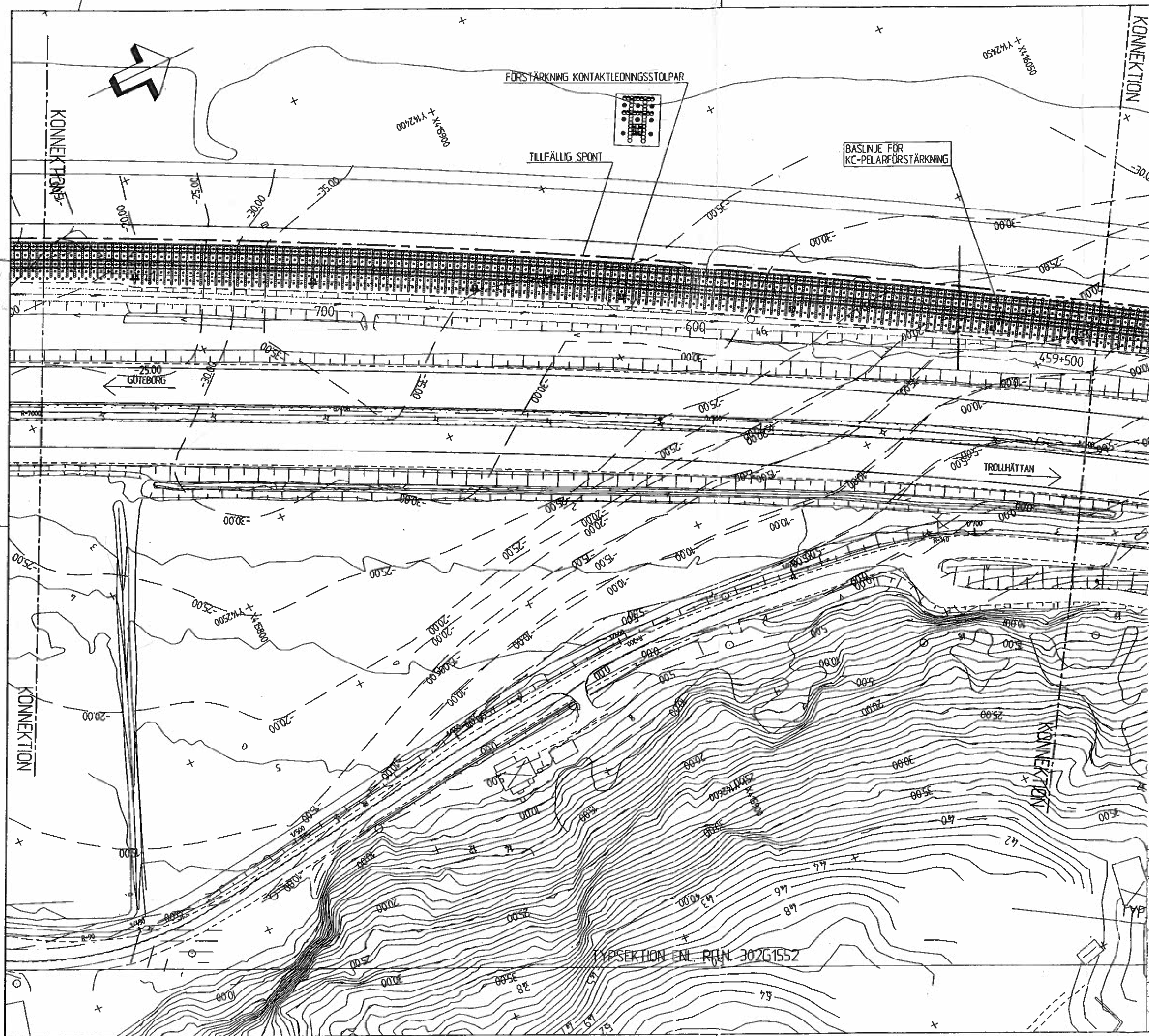

ANMÄRKNINGAR:

KOORDINATSYSTEM: RT 90 7.5 gon V. 60:-1
HÖJDSYSTEM: RH8 70

HÄNVISNINGAR

INSTALLATION AV KALKCEMENTPELARE UTFÖRES ENLIGT RITNING 300G1541 (FÖRESKRIFTER KALKCEMENTPELARE), 302G1551 - 302G1580 (ARBETSORDNING OCH TYPSEKTIONER) OCH 302G1531 - 302G1541 (LÄNGDSEKTION).

LEDNINGSPLAN, SE RITNING 300W5101-300W5126.

FÖRKLARINGAR

+5.00 BEDÖMD BERGNIVÅ
-15.00 BEDÖMD NIVÅ UNDERKANT LERA
UNDERKANT SCHAKT
TILLFÄLLIG SPONT

KC-PELARE

○ TILL NIVÅ -3,5
◑ TILL NIVÅ -6,5
⊗ TILL NIVÅ -12,0
◐ TILL NIVÅ -15,0
● TILL NIVÅ -21,5

URGRÄVNING

BERGSCHAKT

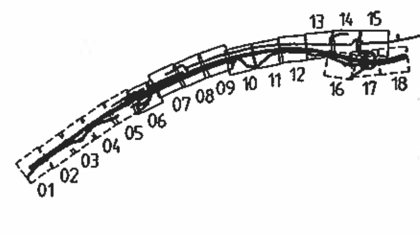

REV	ANT	ÄNDRINGEN AVSER	GODK	DATUM	VV DATUM	VV DIARIENUMMER

BYGGHANDLING

Vägverket
BANVERKET

BANAVÄG I VÄST

E45 NORGE/VÄNERBANAN
DELEN BOHUS - NÖDINGE

FB FLYGFÄLTSBYRÅN
FB Engineering AB Box 12076, 402 41 GÖTEBORG Tel 031-776 10 00 Fax 031-12 20 63

ENTREPRENAD E33

FÖRSTÄRKNINGSÅTGÄRDER JÄRNVÄG

KM 459+780 - 459+490
PLAN

UPPDRAGSANSVARIG: A BERGHOLTZ	UPPDRAGSNUMMER: 161289	KONSTRUKTIONSNR	FORMAT: A1	SKALA: 1:500	
KONSTR: VHO	GRANSK: MISCH				
GÖTEBORG A BERGHOLTZ	2009-01-12	OBJEKT NR: 542764/4530	RITNINGSNR: 302G1511		REV